

UNIVERSITA' DEGLI STUDI DI PARMA

Dottorato di ricerca in Progettazione e Sintesi di
Composti Biologicamente Attivi

Ciclo XXV

**SMALL-MOLECULE MODULATORS OF
RECEPTOR TYROSINE KINASES AS POTENTIAL
ANTITUMOR AGENTS**

Coordinatore:

Chiar.mo Prof. Marco Mor

Tutor:

Chiar.mo Prof. Marco Mor

Dottoranda:

Simonetta Russo

TABLE OF CONTENTS

1. Inhibition strategies of receptor tyrosine kinases	1
Introduction	1
Aim of the work	6
References	8
2. Epidermal growth factor receptor (EGFR)	11
Introduction	11
Irreversible inhibition of EGFR activity by 3-Aminopropanamides	17
Results and discussion	20
<i>Kinase and cellular inhibitory activities</i>	20
<i>Activity on gefinitib-resistant H1975 cells</i>	22
<i>Reactivity studies</i>	23
<i>Evidence for irreversible binding to EGFR</i>	28
Conclusions	29
Chemistry	31
<i>General synthesis of compounds 4-9 (series A)</i>	31
<i>General synthesis of compounds 10-13 (series B)</i>	32
<i>General synthesis of compounds 14-21 (series C and D)</i>	34
Materials and methods	35
Experimental section	36
References	46
3. Eph receptors and ephrins	53
Introduction	53
Lithocholic acid (LCA) is a competitive and reversible Eph receptor ligand	57
Structure activity relationships of a first selected set of LCA derivatives	61
Amino acid derivatives of LCA as novel antagonists of the EphA2 receptor	65
Results and discussion	67
<i>Molecular design and characterization of LCA conjugates</i>	67

<i>Structure activity relationships (SAR) analysis of LCA derivatives</i>	69
<i>Effects on EphA2 phosphorylation in intact cells</i>	72
Conclusions	73
Chemistry	75
<i>General synthesis of compounds 2, 4-7, 12-21</i>	75
<i>General synthesis of compounds 8-9</i>	77
<i>General synthesis of compounds 10-11</i>	79
Materials and methods	81
Experimental section	82
References	116

INHIBITION STRATEGIES FOR RECEPTOR TYROSINE KINASES

Introduction

Protein kinases (PKs) are a large family of ATP-dependent phosphotransferases, that catalyze the transfer of the terminal γ -phosphate from ATP to the hydroxyl group on the side chains of serine, threonine or tyrosine residues of the substrate proteins. The reversible hydroxyl-phosphorylation of proteins represents a major post-translational signaling mechanism and regulatory pathway that controls a diverse set of cellular processes.¹

The protein kinases are classified as serine/threonine or tyrosine kinases based on the receiving aminoacid of their substrates. The human genome encodes for 518 protein kinases, of which approximately 100 are tyrosine kinases (TKs).² These kinases have been divided into two major groups: receptor TKs, characterized by membrane localization, and non-receptor TKs, mainly located in the cell cytoplasm as components of the signaling cascades triggered by cell-surface receptors.

Tyrosine kinase receptors (RTKs) are cell-surface localized, therefore they are predisposed to recognize extracellular signals, triggered by endogenous ligands, such as growth factors. The structure of RTKs is composed of an extracellular region, containing the ligand-binding domain, a single transmembrane segment and a cytoplasmic tyrosine kinase catalytic domain. Ligand binding to the extracellular domain leads to the activation of the intracellular kinase domain, giving rise to signal transduction pathways that affect many key processes, including cell growth and survival.

In normal cells, RTK activity is strictly regulated; but dysregulation or constitutive activation of RTK has been shown to correlate with the

development and progression of numerous human cancers. Aberrant kinase activity can disrupt the normal control of cellular phosphorylation pathways, causing significant alterations in many important cellular functions, such as transcription, proliferation, differentiation, angiogenesis, and inhibition of apoptosis. Since RTKs have been implicated in many aspects of malignant phenotypes, they have become attractive therapeutic targets.³

There are two main approaches that could be used to effectively block signaling from RTK. One way is to prevent receptor-ligand interaction, using agents directed against the extracellular domain of the receptor. The alternative strategy is to inhibit the enzymatic activity of the receptor, targeting intracellular sites on the kinase domain.

Two main classes of anticancer agents, that reflect the two aforementioned distinct strategies of RTKs blockage, have been successfully tested in clinical trials and achieved regulatory approval for the treatment of cancer. These are monoclonal antibodies (mAbs) directed against the extracellular domain of the receptor and small molecule ATP-competitive inhibitors of the receptor tyrosine kinase.

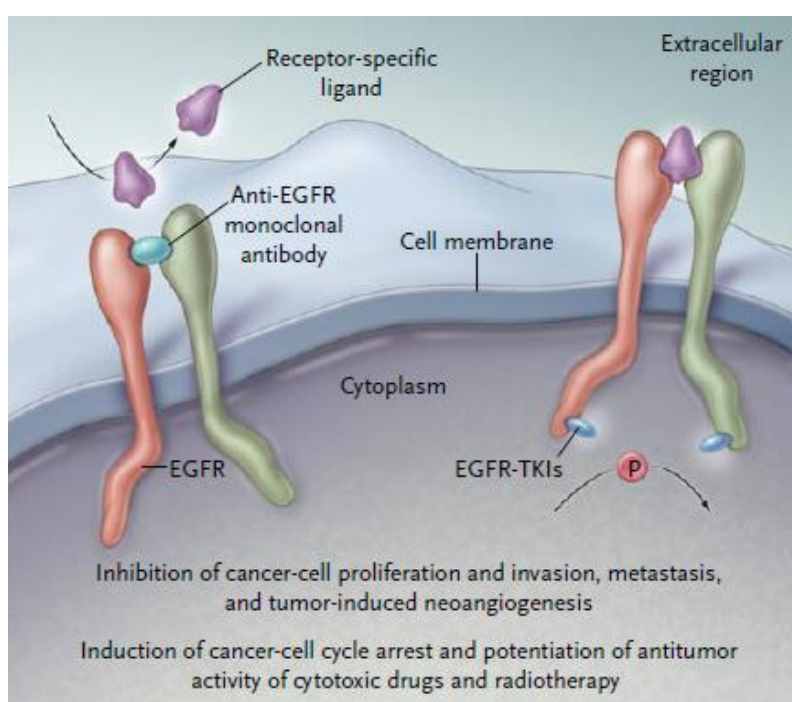


Figure 1. Mechanism of action of anti-RTK drugs in cancer cells (EGFR is a typical example of tyrosine kinase receptor). [Image from Ref 5].

Therapeutic monoclonal antibodies, that have received marketing approval, include: *trastuzumab* (Herceptin[®]), developed against Erb2 or HER2, approved for the treatment of breast cancer; *cetuximab*⁴ (Erbix[®]), a chimeric mAb, and *panitumumab*⁴ (Vectibix[®]), a humanized mAb, both directed against EGFR and approved for the treatment of metastatic colorectal cancer. All these antibodies selectively and specifically bind to the extracellular portion of the corresponding receptor and compete for receptor binding, by occluding the ligand-binding region. MAbs block the ligand-induced receptor tyrosine kinase activation and cause receptor internalization, without stimulating receptor phosphorylation. Furthermore, in the case of cetuximab, the antitumor efficacy also results from the promotion of the host immune response (antibody-dependent cellular cytotoxicity).⁵

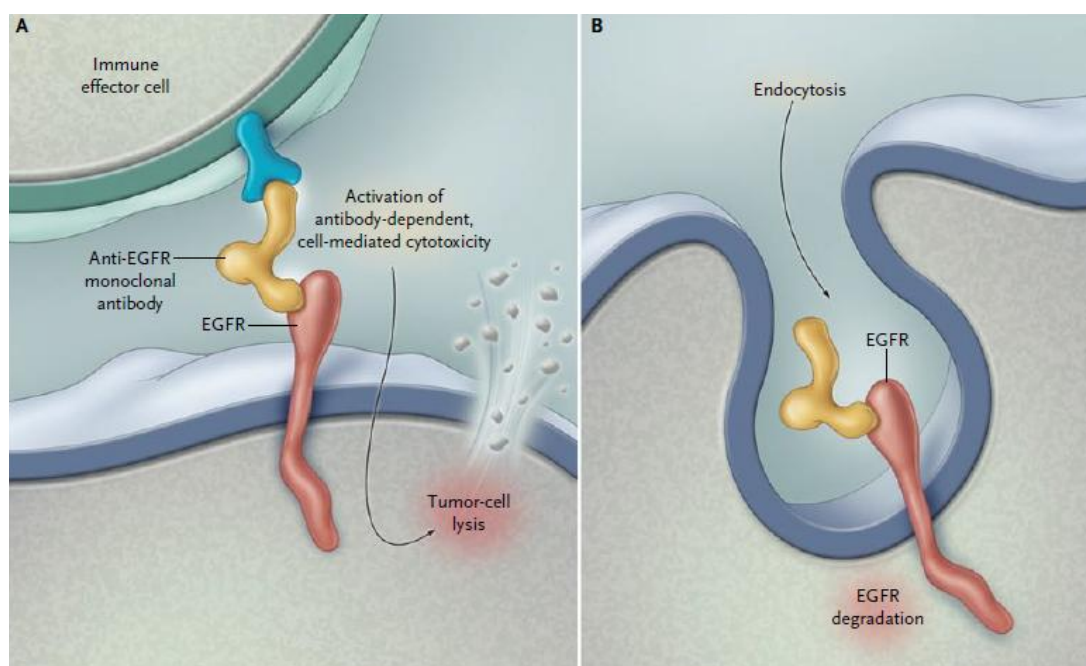


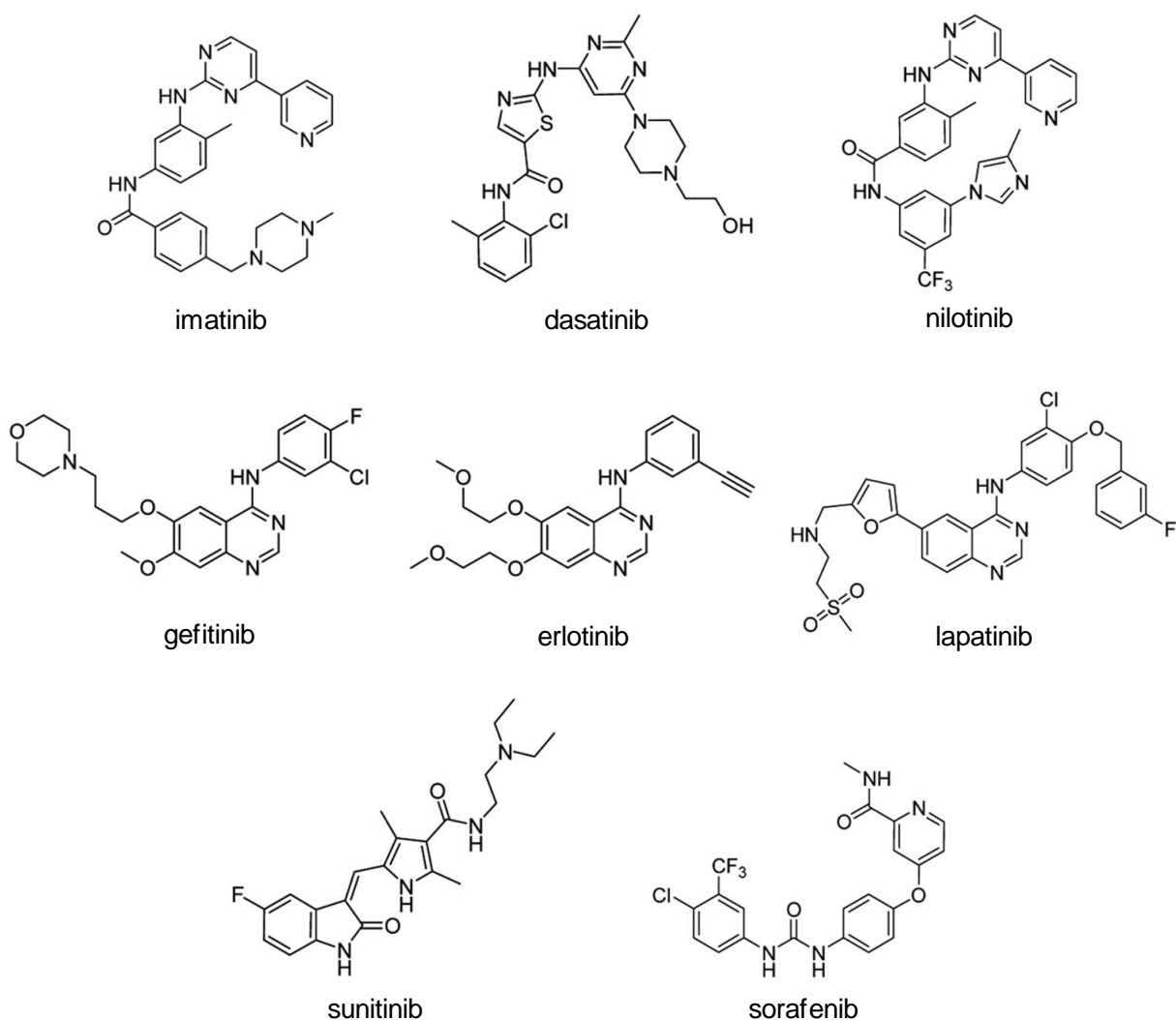
Figure 2. Mechanism of action of anti-RTK monoclonal antibodies in cancer cells (EGFR is a typical example of tyrosine kinase receptor). [Image from Ref 5].

Bevacizumab (Avastin[®]) is a mAb in clinical use as well, approved for the treatment of metastatic colorectal cancer. Unlike the above-mentioned antibodies that are directed against a RTK, bevacizumab specifically targets a growth factor, VEGF.

To date, fourteen small-molecule protein kinase inhibitors have been approved by FDA for therapeutic use in oncological diseases.⁶ These compounds can be generally classified depending on the protein kinase that they mainly target:⁷ the Bcr-

Abl fusion protein kinase; the human epidermal growth factor receptor tyrosine kinases EGFR/HER1 or ErbB2/HER2; the vascular endothelial growth factor receptor tyrosine kinase VEGFR; the anaplastic lymphoma kinase ALK; the janus kinases JAK. *Imatinib* (Gleevec[®]), *dasatinib* (Sprycel[®]), *nilotinib* (Tasigna[®]) and *vemurafinib* (Zelboraf[®]) are inhibitors of Bcr-Abl fusion protein kinase, an oncoprotein for chronic myeloid leukemia (CML). *Gefitinib* (Iressa[®]), *erlotinib* (Tarceva[®]) and *lapatinib* (Tykerb[®]) are inhibitors of EGFR family members and blocks tumorigenic effects of these RTKs. *Sunitinib* (Sutent[®]), *sorafenib* (Nexavar[®]), *pazopanib* (Votrient[®]), *vandetanib* (Caprelsa[®]) and *axitinib* (Inlyta[®]) inhibit VEGFR and other protein kinases involved in tumor angiogenesis. *Crizotinib* (Xalkori[®]) inhibits ALK and MET kinases. *Ruxolitinib* (Jakafi[®]) inhibits JAK1/2 kinases.^{6,7}

Figure 3. Chemical structure of the first eight FDA approved protein kinase inhibitors.



All these marketed compounds are ATP-competitive inhibitors. They inhibit protein catalytic activity in a reversible manner, by occluding the ATP binding site on the kinase domain of the corresponding targets. Some of these compounds also inhibit other kinases in addition to those described above, due to the high structural homology between the ATP-binding site of PKs.

Table 1. Targeted molecular cancer therapeutics received marketing approval.^{6,7}

Drug type	Drug	Company	Disease indication	Primary molecular target
Antabody	Trastuzumab (Herceptin)	Roche	Breast cancer	HER2
	Bevacizumab (Avastin)	Genetech, OSI	Colorectal cancer	VEGF
	Cetuximab (Erbix)	ImClone	Colorectal cancer	EGFR
	Panitumumab (Vectibix)	Amgen	Colorectal cancer	EGFR
Small molecule	Imatinib (Gleevec)	Novartis	CML	Bcr-Abl, c-Kit, PDGFR
	Gefitinib (Iressa)	AstraZeneca	NSCLC	EGFR
	Erlotinib (Tarceva)	Genetech, OSI	NSCLC, pancreatic cancer	EGFR
	Sorafenib (Nexavar)	Bayer, Onyx	Hepatocellular carcinoma, renal cell carcinoma (RCC)	VEGFR, c-Raf, PDGFR
	Sunitinib (Sutent)	Pfizer	Gastrointestinal stromal tumor (GIST), RCC	VEGFR, c-Kit, PDGFR
	Dasatinib (Sprycel)	Bristol-Meyers Squibb	CML	Bcr-Abl, Src, c-Kit, PDGFR, Eph receptors
	Nilotinib (Tasigna)	Novartis	CML	Bcr-Abl, Src, c-Kit, PDGFR
	Lapatinib (Tykerb)	GlaxoSmithKline	Breast cancer	HER2, EGFR
	Pazopanib (Votrient)	GlaxoSmithKline	RCC	VEGFR, c-Kit, PDGFR
	Vandetanib (Caprelsa)	AstraZeneca	Thyroid cancer	VEGFR, EGFR, RET
	Vemurafinib (Zelboraf)	Roche, Plexxikon	CML	Bcr-Abl, Src, c-Kit, PDGFR, Eph receptors
	Crizotinib (Xalkori)	Pfizer	NSCLC	ALK, MET
	Ruxolitinib (Jakafi)	Incyte	myelofibrosis	JAK1/2
	Axitinib (Inlyta)	Pfizer	RCC	VEGFR, c-Kit, PDGFR

Besides the previously described approaches to block the activation of kinase proteins, some novel strategies have been proposed, such as the use of substrate competitive inhibitors or compounds targeting allosteric sites that stabilized inactive conformations.

Aim of the work

The present PhD research project focuses on the synthesis of novel small-molecule modulators of receptor tyrosine kinases as potential antitumor agents which could be addressed against both the intracellular ATP-binding domain or the extracellular ligand-binding domain. In particular, in the following chapters it will be reported the synthesis of novel irreversible inhibitors targeting the kinase domain of the epidermal growth factor receptor (EGFR) and the synthesis of new compounds able to block the Eph receptor activation by occupying the ephrin-binding domain.

EGFR is a well-known and validated anticancer drug target.⁸ As referred in the introduction, there are EGFR inhibitors that have already reached the market for anticancer therapy and many others are in clinical development. All the marketed small molecule drugs targeting EGFR are reversible ATP-competitive inhibitors and are often liable to lack of efficacy because of development of acquired resistance.⁹ On the other hand, the irreversible inhibitors of EGFR under clinical studies have been proved to overcome resistance, but suffer from high reactivity, that could lead to high off-target toxicity.⁶ In this context, the design of not only potent but also low-reactive EGFR inhibitors is a challenge. In the first chapter of the present work, it will be described the strategy adopted to reduce the reactivity of the irreversible inhibitors preserving, at the same time, their ability to covalently interact with the target and thus to guarantee a long-lasting effect. As a strategy to optimize a well-known class of EGFR inhibitors, in this study the design and the synthesis of 3-aminopropanamide derivatives will be described.¹⁰

Eph receptors are the largest family of RTKs. This family of TK-receptors has gained a progressively increasing attention during the two last decades, by virtue of the recent findings regarding the involvement of these receptors and their ligands (ephrins) in tumorigenicity and tumor angiogenesis.¹¹ Although the role of the Eph-ephrin system in cancer is not completely clear,¹² this system is emerging as a novel target for the development of anticancer and anti-angiogenic therapies. To date, numerous examples of Eph receptor inhibitors targeting the intracellular kinase domain have been reported in literature;¹³ above all, dasatinib is a potent EphA2 inhibitor, that blocks the catalytic activity of the kinase by occupying the ATP-binding site.^{14,15} Nevertheless, considering that the ATP-binding pocket is highly conserved

among protein kinases, especially among the members of the same family of protein kinases, these kind of inhibitors generally suffer from lack of selectivity,¹⁶ which limits their use as pharmacological tools in vivo. Conversely, compounds acting on the extracellular ligand binding domain of the Eph receptors have some advantages with respect to standard tyrosine kinase inhibitors because they can block Eph receptor activity without having to penetrate inside the cell and because they could ensure greater selectivity than the ATP-mimicking agents. To date, several inhibitors have been reported in literature that generally include antibodies, soluble form of Eph receptors or ephrins, and peptides.¹³ Only recently few classes of small molecules able to impede the interaction between two macromolecules, like the Eph receptor and the ephrin protein, have been discovered. These include: *i*) salicylic-acid derivatives [4-(2,5-dimethyl-1H-pyrrol-1-yl)-2-hydroxybenzoic acid];^{17,18} *ii*) doxazosin;¹⁹ and *iii*) some polyphenols and polyphenol metabolites.^{20,21,22} However, their usefulness as biological tools appears to be limited by important pharmacological and chemical issues. For instance, the marketed doxazosin (Cardura™) binds the EphA2 receptor with micromolar affinity but also has a well known inhibitory activity on the α 1-adrenergic receptor.¹⁹ The EphA2/EphA4 salicylic acid antagonists have been recently indicated to suffer from poor chemical stability and their pharmacological activity is probably due to degradation products.^{18,23} In the second chapter of the present work, the design and the synthesis of novel low-weight molecules as Eph receptor antagonists will be reported. These compounds, that target the ephrin-binding domain, were obtained starting from the recently identified Eph-receptor inhibitor, lithocholic acid. This study is aimed at achieving new biological tools that could help to elucidate the role of the Eph-ephrin system in cancer and to assess Eph receptors as novel anti-angiogenic drug targets.

References

-
- ¹ Johnson L.N. Protein kinase inhibitors: contribution from structure to clinical compounds. *Q. Rev. Biophys.* **2009**; 19: 1-40.
- ² Manning G., Whyte D.B., Martinez R., Hunter T., Sudarsanam S. The protein kinase complement of the human genome. *Science.* **2002**; 298: 1912-1934.
- ³ Takeuchi K., Ito F. Receptor tyrosine kinases and targeted cancer therapeutics. *Biol. Pharm. Bull.* **2011**; 34: 1774-1780.
- ⁴ Capdevila J., Elez E., Macarulla T., Ramos F.J., Ruiz-Echarri M. Anti-epidermal growth factor receptor monoclonal antibodies in cancer treatment. *Cancer Treatment Reviews.* **2009**; 35: 354-363.
- ⁵ Ciardiello F., Tortora G. EGFR antagonists in cancer treatment. *N. Engl. J. Med.* **2008**; 358: 1160-1174.
- ⁶ Barf T., Kaptein A. Irreversible protein kinase inhibitors: balancing the benefits and risks. *J. Med. Chem.* **2012**; 55: 6243-6262.
- ⁷ Grant S.K. Therapeutic protein kinase inhibitors. *Cell. Mol. Life Sci.* **2009**; 66: 1163-1177.
- ⁸ Bianco R., Gherlaldi T., Damiano V., Ciardiello F., Tortora G. Rational bases for the development of EGFR inhibitors for cancer treatment. *The International Journal of Biochemistry & Cell Biology.* **2007**; 39: 1416-1431.
- ⁹ Engelman J. A., Janne P. A. Mechanisms of acquired resistance to epidermal growth factor receptor tyrosine kinase inhibitors in non-small cell lung cancer. *Clin. Cancer Res.* **2008**; 14: 2895-2899.
- ¹⁰ Carmi C., Galvani E., Vacondio F., Rivara S., Lodola A., Russo S., Aiello S, Bordi F., Costantino C., Cavazzoni A., Alfieri R. R., Ardizzoni A., Petronini P., Mor M. Irreversible inhibition of epidermal growth factor receptor activity by 3-aminopropanamides. *J Med Chem.* **2012**; 55: 2251-64.
- ¹¹ Surawska H., Ma P. C., Salgia R. The role of ephrins and Eph receptors in cancer. *Cytokine & Growth Factor Review.* **2004**; 15: 419-433.
- ¹² Pasquale E. B. Eph receptors and ephrins in cancer: bidirectional signaling and beyond. *Nat Rev Cancer.* **2010**; 10: 165-180.

-
- ¹³ Noberini R., Lamberto I., Pasquale E. B. Targeting Eph receptors with peptides and small molecules: progress and challenges. *Seminars in cell & developmental biology*. **2012**; 23: 51-57.
- ¹⁴ Chang Q, Jorgensen C., Pawson T., Hedley D. W. Effects of dasatinib on EphA2 receptor tyrosine kinase activity and downstream signaling in pancreatic cancer. *Br. J. Cancer*. **2008**; 99: 1074-1082.
- ¹⁵ Farenc C., Celie P. H. N., Tensen C. P., de Esch I. J. P., Siegal G. Crystal structure of EphA4 protein tyrosine kinase domain in the apo- and dasatinib-bound state. *FEBS letters*. **2011**; 585: 3593-3599.
- ¹⁶ Karaman M. W., Herrgard S., Treiber D. K., Gallant P., Atteridge C. E., Campbell B. T., Chan K. W., Ciceri P., Davis M. I., Edeen P. T., Faraoni R., Floyd M., Hunt J. P., Lockhart D. J., Milanov Z. V., Morrison M. J., Pallares G., Patel H. K., Pritchard S., Wodicka L. M. & Zarrinkar P. P. A quantitative analysis of kinase inhibitor selectivity. *Nature Biotechnology*. **2008**; 26: 127-132.
- ¹⁷ Noberini R., Koolpe M., Peddibhotla S., Dahl R., Su Y., Cosford N. D., Roth G. P., Pasquale E. B. Small Molecules Can Selectively Inhibit Ephrin Binding to the EphA4 and EphA2 Receptors. *J Biol Chem*. **2008**; 283: 29461-29472.
- ¹⁸ Noberini R., De S. K., Zhang Z., Wu B., Raveendra-Panickar D., Chen V., Vazquez J., Qin H., Song J., Cosford N. D., Pellecchia M., Pasquale E. B. A disalicylic acid-furanyl derivative inhibits ephrin binding to a subset of Eph receptors. *Chem Biol Drug Des*. **2011**; 78: 667-678.
- ¹⁹ Petty A., Myshkin E., Qin H., Guo H., Miao H., Tochtrop G. P., Hsieh J. T., Page P., Liu L., Lindner D. J., Acharya C., Mackerell A. D. Jr., Ficker E., Song J., Wang B. A small molecule agonist of EphA2 receptor tyrosine kinase inhibits tumor cell migration in vitro and prostate cancer metastasis in vivo. *PLoS One*. **2012**; 7(8): e42120.
- ²⁰ Mohamed I. H., Giorgio C., Bruni R., Flammini L., Barocelli E., Rossi D., Domenichini G., Poli F., Tognolini M. Polyphenol rich botanicals used as food supplements interfere with EphA2-ephrinA1 system. *Pharmacol Res*. **2011**; 64(5): 464-470.
- ²¹ Noberini R., Koolpe M., Lamberto I., Pasquale E. B. Inhibition of Eph receptor-ephrin ligand interaction by tea polyphenols. *Pharmacol Res*. **2012**, 66(4): 363-373.
- ²² Tognolini M., Giorgio C., Hassan Mohamed I., Barocelli E., Calani L., Reynaud E., Dangles O., Borges G., Crozier A., Brighenti F., Del Rio D. Perturbation of the EphA2-ephrinA1

system in human prostate cancer cells by colonic (poly)phenol catabolites. *J Agric Food Chem.* **2012**; 60(36): 8877-8884.

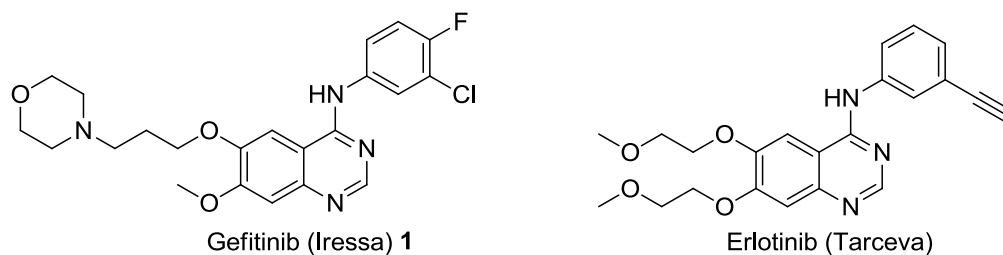
²³ Baell J. B., Holloway G. A. New substructure filters for removal of pan assay interference compounds (PAINS) from screening libraries and for their exclusion in bioassay. *J Med Chem.* **2010**; 53(7): 2719-2740.

EPIDERMAL GROWTH FACTOR RECEPTOR

Introduction

The epidermal growth factor receptor (erbB1/EGFR) is a transmembrane receptor tyrosine kinase (RTK) belonging to the erbB family, which also includes erbB2/HER2, erbB3/HER3 and erbB4/HER4.^{1,2} Upon ligand binding, EGFR undergoes homo- or heterodimerization and autophosphorylation of specific tyrosine residues within the intracellular domain. The autophosphorylated receptor activates a series of downstream signals that promote cell growth, proliferation, differentiation and migration.^{3,4} Deregulation of EGFR signaling has been observed in many human cancers, including lung, head and neck, colorectal, ovarian, breast and bladder cancers,^{5,6} and it has been associated with more aggressive disease and poorer clinical outcome.⁷ Therefore, inhibitors targeting the EGFR have been extensively investigated and employed as anti-tumor agents.

Hyperactivation of EGFR can be produced by gene amplification, receptor overexpression, activating mutations, overexpression of receptor ligands and/or loss of regulatory controls.⁸ Several oncogenic mutations in EGFR have been related to the development of cancer, particularly non-small cell lung cancer (NSCLC).^{9,10} Deletions in exon 19 (del19), a substitution mutation in the exon 21 (L858R), and less common mutations (e.g. G719S) enable constitutive activation of the kinase function, stabilizing the active conformation of the kinase domain in the absence of ligand-induced stimulation.^{11,12} Two selective EGFR inhibitors, gefitinib¹³ (Iressa[®], AstraZeneca) and erlotinib¹⁴ (Tarceva[®], OSI Pharmaceuticals), have higher potency against these mutant kinases than the wild-type enzyme¹⁵ and are approved for the treatment of NSCLC in patients having the activating mutations of EGFR. These tyrosine kinase inhibitors, belonging to the chemical class of 4-anilinoquinazolines, compete with ATP in a reversible manner, binding to the kinase domain of the target through weak interactions (hydrogen-bonds, van der Waals and hydrophobic interactions).

Figure 1. Reversible EGFR-TKIs in clinical therapy.

Although gefitinib is effective in the NSCLC treatment in patients having activating mutations within the EGFR tyrosine kinase domain, accumulating clinical experience indicates that most patients develop resistance after repeated treatments.¹⁰ In approximately half of NSCLC cases that show an initial response to reversible EGFR tyrosine kinase inhibitors and that subsequently progress, resistance is associated with the emergence of a secondary acquired mutation in the catalytic domain of EGFR: substitution of the gatekeeper residue threonine 790 with methionine (T790M).^{10,16,17} The bulkier side chain of the mutated methionine residue is thought to sterically impede binding of these reversible inhibitors and disrupt the formation of a crucial water-mediated hydrogen bond between the inhibitor (N3 of the quinazoline core) and T790 of wild type EGFR.¹⁸

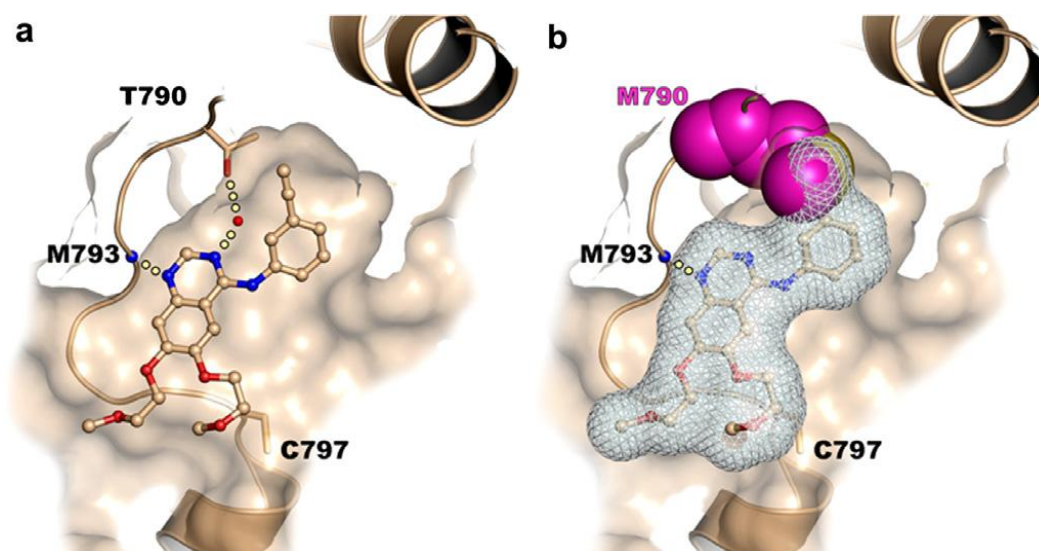


Figure 2. **a)** Crystal structure of wild type EGFR complexed with the reversible ATP competitive drug erlotinib. **b)** Drug resistance mutation T790M is modeled and highlights the steric clash with the acetylene moiety of erlotinib. [Image from Ref 18].

The need to overcome acquired resistance¹⁹ has prompted to the development of a second-generation of EGFR inhibitors, able to irreversibly inhibit their target protein, by alkylation of a cysteine residue (Cys797), positioned at the entrance of the ATP binding site of EGFR.²⁰

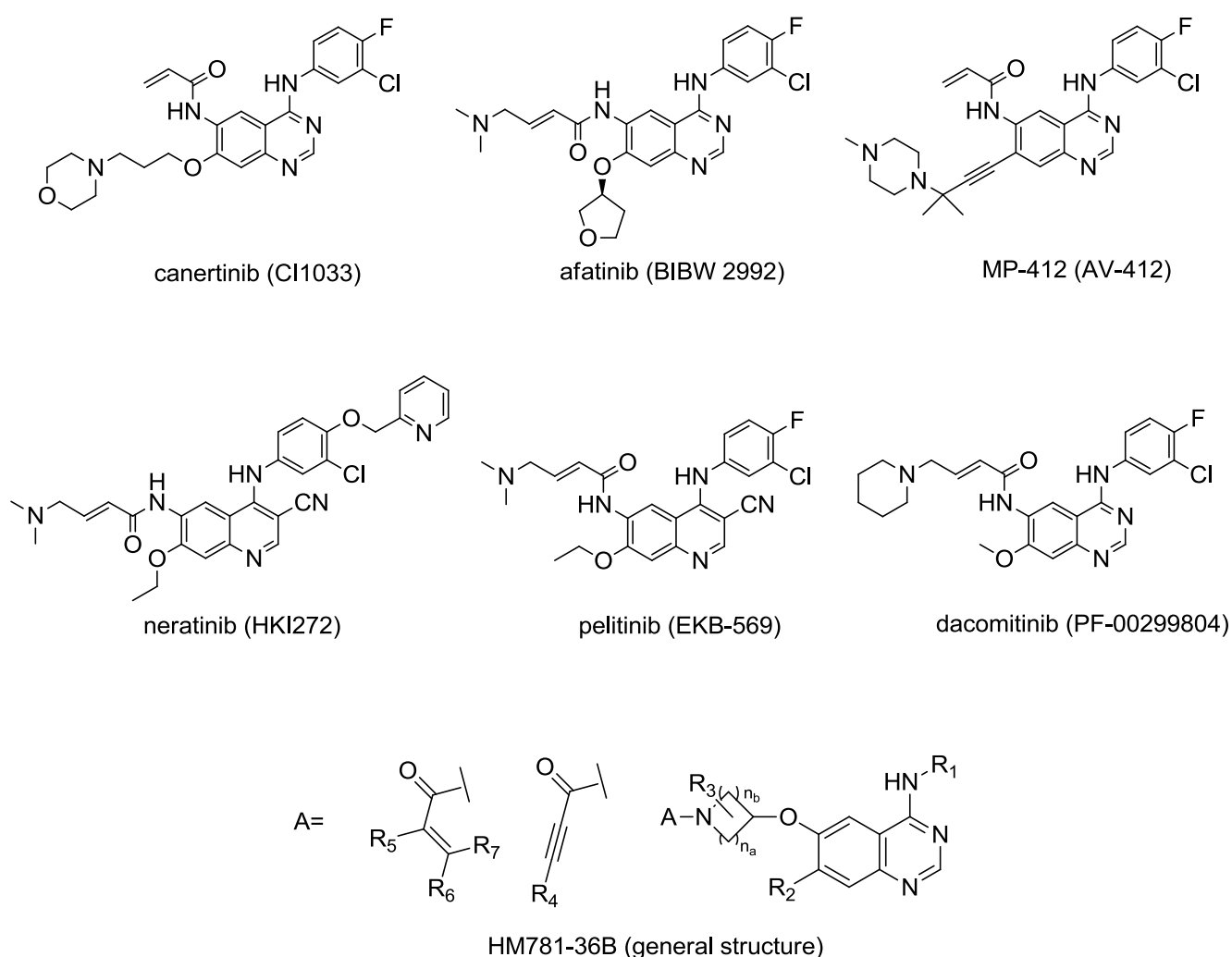
Currently, seven inhibitors of this class are under clinical investigation as anticancer agents (Table 1 and figure 3).²¹

Table 1. Irreversible EGFR-TKIs in clinical development. [Table from ref. 21]

Drug	Target kinase(s)	Company	Cancer	Development Phase
Canertinib (CI-1033)	EGFR, HER2-4	Pfizer	NSCLC	Phase II (no ongoing trials)
			Breast cancer	Phase II (no ongoing trials)
Pelitinib (EKB-569)	EGFR, HER2	Wyeth/ Pfizer	NSCLC	Phase II (no ongoing trials)
			Colorectal cancer	Phase II (no ongoing trials)
Neratinib (HKI-272)	EGFR, HER2	Wyeth/ Pfizer	NSCLC	Phase II (no ongoing trials)
			Breast cancer	Phase III
			Solid tumors	Phase II
Dacomitinib (PF00299804)	EGFR, HER2-4	Pfizer	NSCLC	Phase III
			Gastric cancer	Phase I/II
			Head and neck cancer	Phase I/II
			Glioblastoma	Phase I/II
Afatinib (BIBW2992)	EGFR, HER2	Boehringer Ingelheim	NSCLC	Phase III
			Breast cancer	Phase III
			Head and neck cancer	Phase III
			Prostate cancer	Phase II
			Esophagogastric cancer	Phase II
			Colorectal cancer	Phase II
			Glioma	Phase II
			Glioblastoma	Phase I
HM781-36B	EGFR, HER2	Hanmi Pharmaceutical Co., Ltd	Solid tumors	Phase I
AV-412/MP-412	EGFR	AVEO Pharmaceuticals, Inc.	Solid tumors	Phase I

EGFR irreversible covalent inhibitors are characterized by a heterocyclic core structure (driving portion), generally resembling that of reversible inhibitors (4-anilinoquinazoline or a 4-anilino-3-cyanoquinoline), carrying at a proper position an electrophilic “warhead” (acrylamide, substituted acrylamide, or propargylamide), that covalently interacts with the specific cysteine residue in the target protein.^{22, 23}

Figure 3. Chemical structure of irreversible EGFR-TKIs in clinical development.



Alkylation of the thiol group of Cys797 in the ATP binding pocket of EGFR was demonstrated for the 6-acrylamido-4-anilinoquinazoline PD168393 (Figure 4) by mass spectroscopy and site-directed mutagenesis.²⁴ Co-crystallization of PD168393 within the kinase domain of human EGFR showed that the inhibitor is covalently bound to Cys797 (Figure 4) and adopts an accommodation similar to that observed for several reversible quinazoline inhibitors in complex with kinases.²⁵

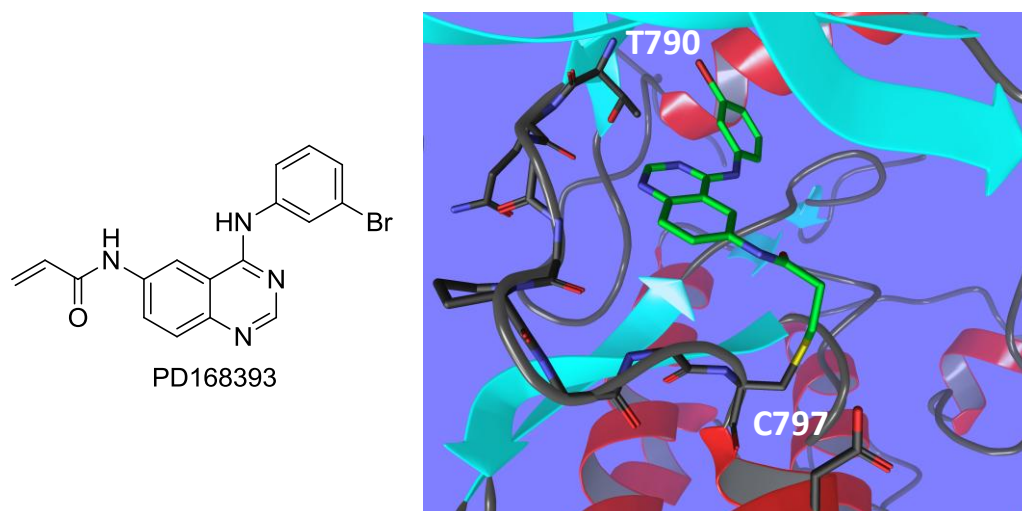
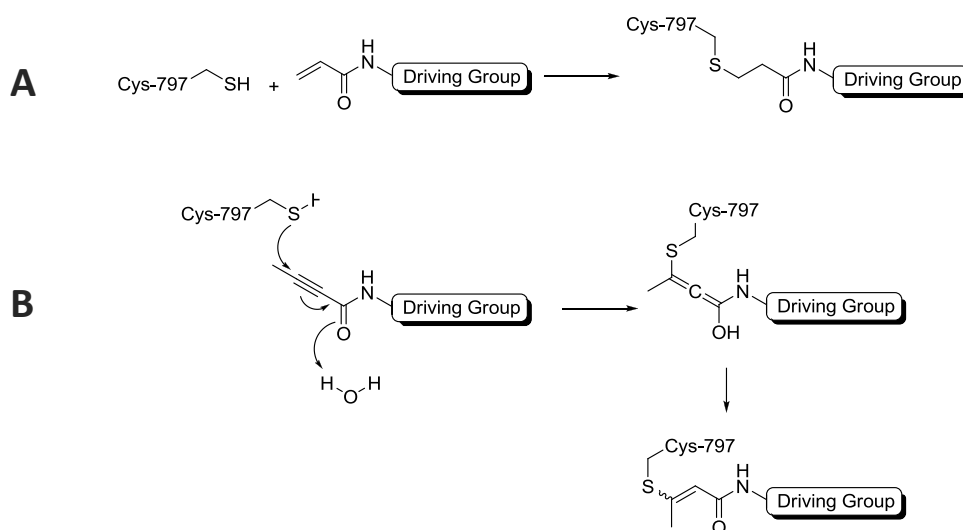


Figure 4. Co-crystal structure of the 6-acrylamide-4-anilinoquinazoline PD168393 within the catalytic site of EGFR.

The covalent bond is formed between the β -carbon atom of the acrylamide (which behaves as a Michael acceptor) on PD168393 and the sulfur atom of Cys797. Moreover, N1 and N3 on the quinazoline driving portion are involved in two crucial hydrogen bonds, one with the backbone nitrogen of Met793 and the other with the side chain of Thr790, through a conserved water molecule. The 4-aniline substituent points toward the hydrophobic pocket beyond the gatekeeper Thr790 (Figure 4).²⁴ Like acrylamides, also propargylamides provide irreversible inhibitors when inserted on a suitable scaffold, able to recognize the EGFR kinase domain.^{26,27} The alkynamide warhead can react with nucleophiles, including thiols of cysteines, giving Michael-type addition product (Figure 5B).

Figure 5. Reaction mechanism of acrylamides (A) and propargylamides (B) toward cys-797. [Image from ref. 23].



There are several potential advantages for irreversible inhibitors over conventional ATP-competitive ones. An irreversible inhibitor would be expected to have prolonged pharmacologic effects relative to systemic exposure. In fact, when the target enzyme is deactivated by covalent bond, the biological effect should persist even after the inhibitor has left the circulation. Furthermore, covalent bond formation can circumvent competition with high intracellular ATP concentrations.²¹ Moreover, considering that the targeted cysteine residue is conserved within the erbB-family kinase domains (Cys797 in EGFR, Cys805 in erbB2, and Cys803 in erbB4), and that only a limited group of kinases has a cysteine at the corresponding position,²⁸ irreversible inhibitors with an electrophilic group in the proper position are expected to be rather selective for erbB-family tyrosine kinases.

On the other hand, the intrinsic reactivity of cysteine-reactive groups leads to non-selective reactions with cellular thiols like glutathione and cysteines in off-target proteins, giving rise to increased toxicity and lack of target specificity.^{29, 30}

However, higher selectivity against off-targets can be achieved by combining a low intrinsic reactivity of the electrophilic warhead with a suitable arrangement of the driving portion, so that the reaction with the thiol can only occur when preceded by specific non-covalent binding of the inhibitor, presenting the reactive counterpart at a favorable distance and orientation. So, in order to identify new drug-like leads for the development of irreversible inhibitors of the erbB family kinases as potential candidates for cancer therapy, it is important that: the driving portion should assure both high target affinity, by containing the structural elements required for covalent interaction with the ATP-binding site of EGFR, and target selectivity, by carrying the electrophilic functionality at the proper position with a geometry that is compatible with the formation of the critical bond; the intrinsic reactivity of cysteine-reactive groups should be sufficiently low to avoid indiscriminate reaction with non-target-related proteins.

Irreversible inhibition of EGFR activity by 3-Aminopropanamides

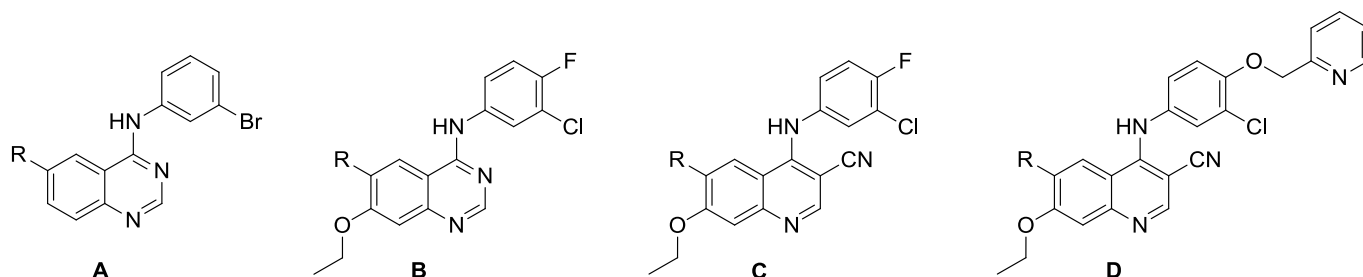
The present PhD work makes part of a research project aimed at the identification of new irreversible inhibitors of EGFR with optimized reactivity/toxicity ratios.

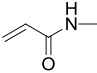
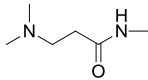
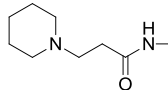
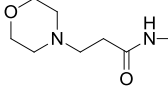
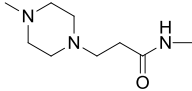
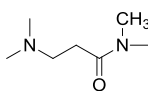
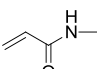
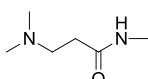
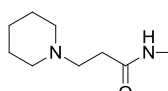
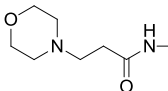
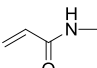
The strategy adopted for this purpose was to substitute the highly electrophilic Michael acceptor groups with less reactive groups that preserve the ability to covalently interact with the nucleophile within the target protein. The low-reactive chemical entities proposed in this study as functional groups able to covalently interact with cysteine residue of EGFR are β -aminocarbonyl groups. In particular, it was explored a series of 3-aminopropanamides, inserted on appropriate driving portions, synthesizing a series of Mannich base derivatives as new EGFR-TK inhibitors, endowed with low non-specific reactivity.

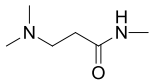
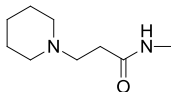
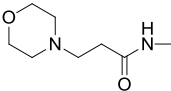
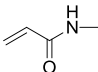
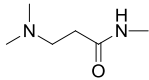
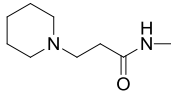
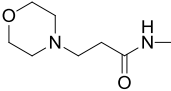
Aryl β -aminoethyl ketones (Mannich bases) have already been described in literature as irreversible inhibitors of enzymes having a crucial cysteine residue in the active site or at regulatory positions.^{31,32,33} These compounds possess a particular profile of reactivity, being non-reactive directly, but able to covalently modify their biological target after bioconversion via β -elimination to the corresponding α,β -unsaturated carbonyl compound.

In the present study, the synthesis and biological evaluation of new EGFR-TK inhibitors containing a 3-aminopropanamide side chain linked to a 4-anilinoquinazoline (**5-9** A-series, and **11-13** B-series in Table 1) or 4-anilinoquinoline-3-carbonitrile (**15-17**, and **19-21**, C- and D-series, respectively, in Table 1) driving portion is described. Reference acrylamide derivatives for each series were also prepared (**3**, **10**, **14**, and **18**, Table 2).³⁴

Table 2. EGFR tyrosine kinase and autophosphorylation inhibition in A549 cells. Viability inhibition of H1975 gefitinib-resistant cell line.



Compd	Series	R	kinase assay ^a	autophosphorylation assay (A549) ^b		H1975 cell line ^c
			IC ₅₀ (nM)	% inhibition 1 μM		IC ₅₀ (μM)
				1 h	8 h	
3	A		1.69 ± 0.16 ^d	98 ± 1.8	86 ± 0.4	0.61 ± 0.05 ^d
4	A	H ₂ N-	n.d.	91 ± 5.9	0.0 ± 0.1	19.5 ± 2.46 ^d
5	A		0.28 ± 0.07	97 ± 1.4	89 ± 1.0	3.69 ± 1.10
6	A		0.27 ± 0.04	95 ± 2.6	93 ± 4.0	6.67 ± 0.75
7	A		0.51 ± 0.06	98 ± 1.8	91 ± 5.4	> 20
8	A		0.23 ± 0.07	99 ± 0.5	79 ± 11	14.3 ± 2.23
9	A		17.4 ± 1.62	47 ± 8.8	10 ± 3.3	13.6 ± 1.66
10	B		0.18 ± 0.04	96 ± 4.0	99 ± 0.6	1.62 ± 0.45
11	B		0.27 ± 0.05	98 ± 1.1	100 ± 0.3	2.21 ± 0.69
12	B		0.51 ± 0.06	98 ± 1.6	92 ± 3.7	1.61 ± 0.07
13	B		0.29 ± 0.06	97 ± 2.3	97 ± 0.4	2.11 ± 0.63
14	C		1.46 ± 0.37	92 ± 4.4	33 ± 11	3.57 ± 1.04

15	C		0.68 ± 0.11	88 ± 2.8	67 ± 8.6	2.37 ± 0.15
16	C		2.21 ± 0.37	96 ± 5.8	82 ± 3.6	2.73 ± 0.28
17	C		2.02 ± 0.44	86 ± 5.2	48 ± 7.4	3.93 ± 0.95
18	D		50.7 ± 1.33	100 ± 0.3	83 ± 7.9	0.63 ± 0.13
19	D		12.5 ± 0.88	61 ± 5.2	59 ± 11	2.03 ± 0.42
20	D		24.8 ± 3.88	71 ± 2.1	58 ± 3.2	0.71 ± 0.14
21	D		37.5 ± 8.99	48 ± 3.3	39 ± 9.5	2.76 ± 0.41

^a Concentration to inhibit by 50% EGFR-wt tyrosine kinase activity. IC_{50} values were measured by the phosphorylation of a peptide substrate using time-resolved fluorometry. Mean values of three independent experiments \pm SEM are reported. ^b Inhibition of EGFR autophosphorylation was measured in A549 intact cells by Western blot analysis. Percent inhibition at 1 μ M concentration was measured immediately after and 8 h after removal of the compound from the medium (1 h incubation). Mean values of at least two independent experiments \pm SEM are reported. ^c Concentration to inhibit by 0% the proliferation of NSCLC H1975. The cell proliferation was determined by the MTT assay, after 72 h of incubation with compounds (0.1–20 μ M). Mean values of three independent experiments \pm SEM are reported. ^d [Data from Ref. 35]

The new compounds were tested as EGFR tyrosine kinase inhibitors in enzyme-based and cell-based assays. Antiproliferative activity of the new compounds was also investigated in the gefitinib-resistant H1975 NSCLC cell line, harboring the T790M mutation. It was hypothesized that the observed long-lasting effect on EGFR autophosphorylation was the result of an irreversible covalent interaction between the 3-aminopropanamide side chain and Cys797 within the active site of the enzyme. The reactivity of the synthesized compounds was tested by a series of in vitro chemical stability assays, including reactivity studies in the presence of thiol nucleophiles and reactivity studies toward EGFR tyrosine kinase. Pharmacological data and reactivity study results were combined and evaluated in order to identify

new irreversible EGFR inhibitors with lower intrinsic reactivity and optimized efficacy/toxicity profile compared to those of the other cysteine-reactive species described to date.

Results and discussion

Kinase and cellular inhibitory activities

Compounds **3-21** (Table 2) were evaluated in enzyme-based and cell-based assays for their ability to inhibit EGFR tyrosine-kinase activity. Their inhibitor potency on human EGFR in a cell-free environment was measured on the phosphorylation of a peptide substrate, using time-resolved fluorometry. In these conditions, the reference compound **3** had an IC_{50} of 1.7 nM.³⁵ Within the series of quinazoline derivatives with the same driving portion as **3** (series A in Table 2), substitution of the acrylamide warhead with a substituted 3-aminopropanamide (**5-8**) produced a generalized increase in inhibitor potency, with IC_{50} values in the subnanomolar range. These values likely result from a complex inhibition mechanism, including reversible competition with ATP and covalent interaction with EGFR in different proportions for different compounds. Methylation of the amide nitrogen of **5** to the tertiary amide **9** notably reduced EGFR-TK inhibition potency (IC_{50} 17 nM). B-series quinazoline compounds **10-13**, carrying 4-(4-fluoro-3-chloroanilino) and 7-ethoxy substituents, did not show significant changes in kinase inhibition potencies when the electrophilic warhead (**10**) was replaced with 3-dimethylaminopropanamide in **11**, 3-piperidinopropanamide in **12** or 3-morpholinopropanamide in **13**, all compounds having subnanomolar IC_{50} values. Considering the two series of quinoline-3-carbonitriles C and D, compounds **14-17** (C-series) were only slightly less potent in inhibiting EGFR-TK compared to the parent B-series quinazoline derivatives, while compounds **17-21** (D-series), carrying a 3-chloro-4-(pyridin-2-ylmethoxy)anilino substituent at position 4, were up to 60-fold less potent than the A- and B-series quinazolines.

The ability of the compounds to inhibit EGFR autophosphorylation was investigated in the A549 human lung cancer cell line by Western blotting. Percent inhibitions at 1 μ M concentration are reported in Table 2. Results were compared to those observed for the reference compounds **3** and **4**, recognized as irreversible and reversible

EGFR inhibitors, respectively. A549 cells, which express gefitinib-sensitive EGFR, were treated for 1 h with inhibitor and then washed with drug-free medium. The degree of EGFR autophosphorylation was measured either immediately after or 8 h after removal of the inhibitor.³⁶ As previously reported,³⁷ 80% or greater EGFR inhibition 8 h after removal of the inhibitor from the medium were considered a sign of irreversible inhibition. Within the A-series of 4-anilinoquinazolines, the irreversible acrylamide **3** showed 86% inhibition after the 8 h washout. Substitution of the reactive acrylamide warhead with 3-dimethylaminopropanamide in **5**, 3-piperidinopropanamide in **6** or 3-morpholinopropanamide in **7** gave similar results on EGFR autophosphorylation, both immediately after and 8 h after washout, with inhibition of EGFR autophosphorylation over 95% and in the range 89-93% at 1 h and 8 h, respectively. The 4-methylpiperazine analogue **8** strongly inhibited EGFR autophosphorylation after 1 h (> 99% inhibition), while it showed a slightly decrease in inhibitory activity 8 h after removal from the medium (79% inhibition). The tertiary amide **9** poorly inhibited EGFR (47% inhibition at 1 h) with only 10% residual inhibition 8 h after treatment, probably because of reduced affinity at the recognition site. As expected, the 6-amino derivative **4** completely inhibited EGFR activity after 1 h treatment and did not show any inhibitory effect 8 h after its removal from the medium.

The 3-aminopropanamido fragment was further introduced on quinazoline or quinoline-3-carbonitrile scaffolds with 3-chloro-4-fluoro substitution on the 4-aniline ring and a 7-ethoxy group on the heterocyclic nucleus (B- and C-series, Table 2) since previous work had suggested that this substitution pattern led to optimal activity.^{22,26} The acrylamide derivative **10**, belonging to the B-series of quinazolines, completely inhibited EGFR autophosphorylation 1 h and 8 h after treatment at 1 μ M concentration (96% and 99% inhibition, respectively). Substitution of the electrophilic warhead of **10** with a 3-aminopropanamide side chain led to compounds **11** (dimethylamino), **12** (piperidino), and **13** (morpholino), which gave EGFR percents inhibition at 1 h and 8 h after removal from the medium between 92 and 100%. In the C-series of compounds, the acrylamide **14** proved efficient in inhibiting EGFR at 1 μ M concentration after 1 h treatment (92% inhibition), but produced only partial inhibition 8 h after washout (33% inhibition). This unexpected behavior may be due to the reduced solubility of compound **14** in the reaction medium (data not shown). In fact,

among 3-aminopropanamides **15-17**, only the piperidino derivative **16** gave complete and irreversible EGFR inhibition (92% and 82% inhibition 1 h and 8 h after removal from the medium, respectively), while dimethylamino (**15**) and morpholino (**17**) compounds inhibited EGFR at 1 h, but produced only a partial, yet significant, irreversible inhibition 8 h after treatment, as demonstrated by 67% and 48% inhibition of autophosphorylation, respectively.

Partial inhibition of EGFR autophosphorylation in A549 cells was also shown by the other series of quinoline-3-carbonitrile derivatives (D-series, **19-21**). In this series, the acrylamide **18** was quite effective as an irreversible inhibitor of EGFR (100% and 83% inhibition at 1 h and 8 h after treatment, respectively), while 3-dimethylamino- (**19**), 3-piperidino- (**20**) and 3-morpholinopropanamide (**21**) produced incomplete EGFR inhibition after 1 h treatment at 1 μM concentration (inhibitions between 48% and 71%) with only partial inhibition 8 h after removal from the medium (**19**, 59% inhibition; **20**, 58% inhibition; and **21**, 39% inhibition at 8 h).

Activity on gefitinib-resistant H1975 cells

Compounds **5-21** were evaluated for their ability to inhibit the growth of the gefitinib-resistant H1975 NSCLC cell line harboring the T790M mutation, by MTT assay. Results were compared with those of the reference compounds **1** (gefitinib), **3** and **4** in the same assay. As reported in Table 2, the 3-dimethylaminopropanamide **5** showed the best antiproliferative activity on H1975 cells within the A-series of quinazoline compounds with IC_{50} of 3.7 μM , being times more potent than **1** (IC_{50} of 8.3 μM)³⁵ and 5-fold more active than **4** (IC_{50} of 19.5 μM).³⁵ Substitution of the dimethylamino group with a piperidine made compound **6** equally potent to **1** (IC_{50} of 6.7 μM), while 3-morpholinopropanamide **7**, 3-(4-methylpiperazino)propanamide **8**, and 3-(dimethylamino)-*N*-methylpropanamide **9** gave IC_{50} values over 13 μM . B-series 3-aminoamides **11-13** proved 3-4 times more effective than **1** in inhibiting H1975 proliferation and showed IC_{50} values between 1.6 and 2.2 μM , in the same range of the corresponding irreversible acrylamide **10** (IC_{50} of 1.6 μM). Compounds characterized by a quinoline-3-carbonitrile driving portion (C- and D-series) were more potent than **1** in inhibiting H1975 cell proliferation. In particular, 3-aminopropanamides **15-17** (C-series) showed IC_{50} values between 2.4 and 4.0 μM

comparable to that of the corresponding acrylamide derivative **14**. Finally, D-series quinoline-3-carbonitrile **19-21** gave similar results, with the compounds displaying IC₅₀ values in the low micromolar or submicromolar range. The 3-piperidinopropanamide derivative **20** showed the most potent antiproliferative effect on H1975 cells within the all series of 3-aminopropanamide derivatives (IC₅₀ of 0.7 μM), 11 times more potent than **1** in the same test.

Reactivity studies

Compound **5**, carrying a 3-dimethylaminopropanamidic side chain at position 6 on a 4-(3-bromoanilino)quinazoline nucleus, was chosen as the prototype of the new series and tested for its chemical (buffered solutions at pH 7.4 and pH 9.0) and biological (80% v/v rat plasma) stability, as well as for its reactivity against low-molecular weight thiol nucleophiles. Results were compared to those obtained for the acrylamide **3** (Tables 3 and 4).

Table 3. In vitro stability studies on compounds **3** and **5**.

Conditions	% Remaining compound (1 μM, 24 h) ^a	
	3	5
pH 7.4	102.3 ± 3.1	97.5 ± 0.1
pH 9.0	105.2 ± 3.7	77.0 ± 0.8
80% v/v rat plasma	21.8 ± 7.4	98.7 ± 4.6

^a Percentage of parent compound detected by LC-UV and LC-ESI-MS after incubation for the indicated time at 37 °C. Mean ± SD, n = 3.

Table 4. In vitro reactivity studies on compounds **3** and **5**.

Conditions	% Remaining Compound (1 μM, 1 h) ^a	
	3	5
DTT	100.0 ± 2.3	99.2 ± 8.1

Conditions	% Remaining Compound (1 μ M, 1 h) ^a	
	3	5
GSH	63.8 \pm 1.9	101.4 \pm 2.8
NAC	85.6 \pm 3.1	100.4 \pm 2.1
cysteamine	20.1 \pm 0.4	100.0 \pm 1.1

^a Percentage of parent compound detected by LC-UV and LC-ESI-MS after incubation in the presence of LMW thiols (2 mM) for the indicated time at pH 7.4, 37 °C. Mean \pm SD, n = 3.

Both compounds **3** and **5** were stable at pH 7.4, with percentages of remaining compound over 97% after 24 h incubation at 37 °C in buffer (Table 3). Under alkaline pH conditions (pH 9.0), while **3** was stable over the entire incubation time, 77% of intact 3-aminopropanamide **5** was recovered, with acrylamide **3** (19%) and amine **4** (4%) as the major degradation products (Figure 6). Thus, in alkaline conditions the dialkylamino-propanamide fragments undergoes retro-Michael degradation with formation of a significant amount of acrylamide.

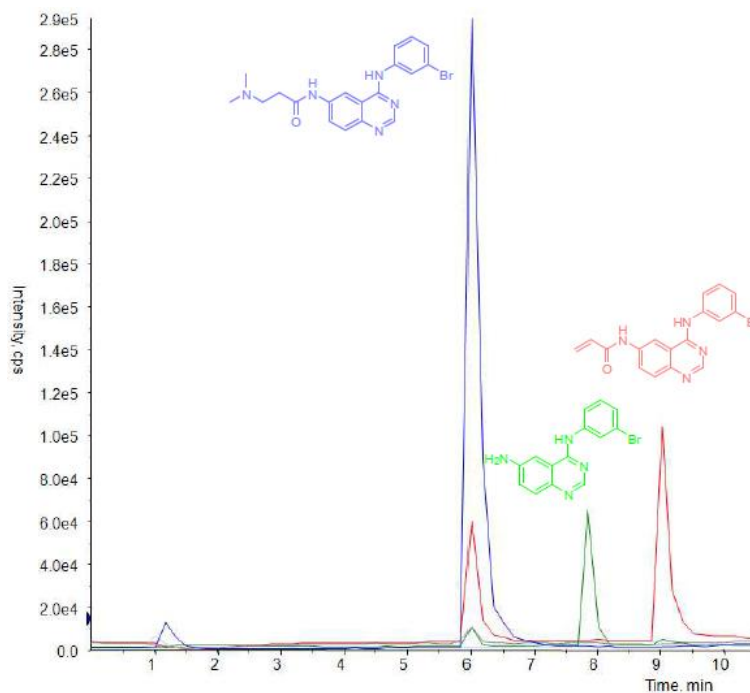


Figure 6. HPLC-MS chromatogram of compound **5** (UPR1157) after 24 h incubation under alkaline conditions (pH 9.0) at 37 °C. Mass balance studies revealed 77% of **5**

(blue) recovered after 24 h, with acrylamide **3** (19%, in red) and amine **4** (4%, in green) as degradation products.

On the other hand, in the presence of rat plasma compound **5** showed high stability, while only 22% of acrylamide **3** was detected after 24 h incubation (table3). This was the first evidence of higher stability of the aminopropanamide fragment in biological environments, compared to acrylamide.

The reactivity of compounds **3** and **5** against thiol nucleophiles was evaluated according to literature procedures.^{38,39} While for the acrylamide derivative **3** significant formation of conjugates was detected in the presence of cysteamine, glutathione (GSH), and *N*-acetylcysteine (NAC) (Table 4 and Figure 7), compound **5** gave no measurable adducts with thiol derivatives up to 24 h of incubation.

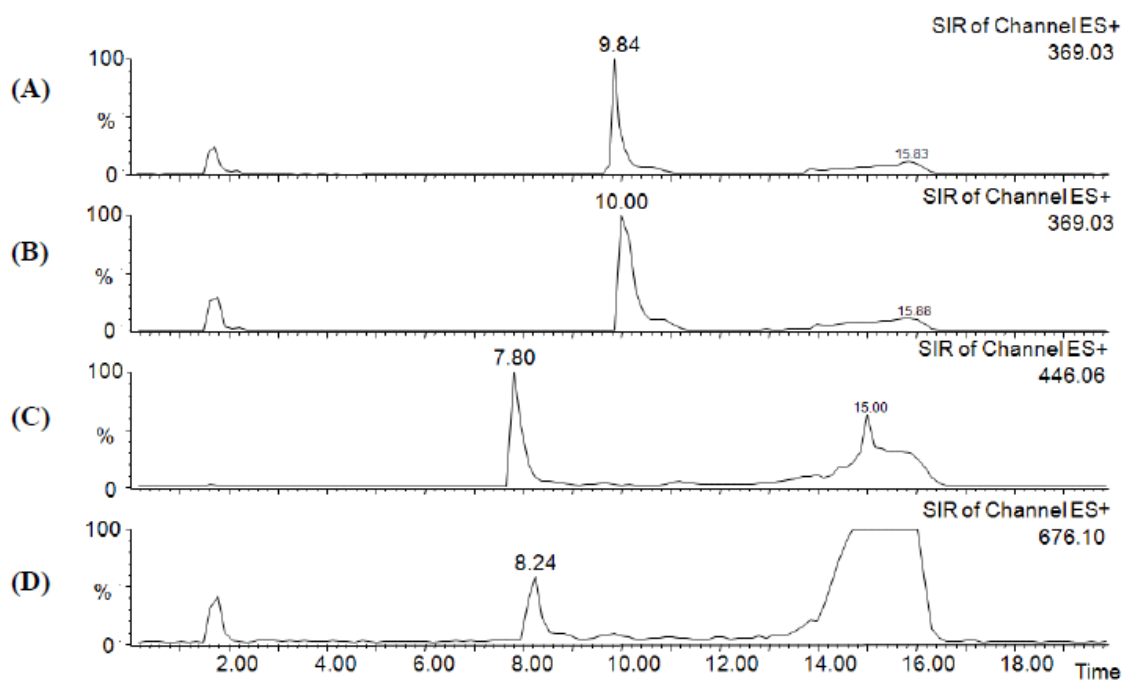


Figure 7. HPLC-MS chromatograms of compound **3** incubated in the presence of LMW thiols cysteamine and GSH. As a title of example, reported in Figure 7 are LC/MS traces corresponding to the formation of GSH- ($m/z = 676.10$) and cysteamine- ($m/z = 446.06$) conjugates by compound **3** ($m/z = 369.03$) after 1 h incubation at 37 °C. **(A)** Acrylamide **3** incubated in the presence of cysteamine ($t = 0$, $m/z = 369.03$); **(B)** Acrylamide **3** incubated in the presence of GSH ($t = 0$, $m/z = 369.03$); **(C)** Acrylamide **3** incubated in the presence of cysteamine ($t = 1$ h, $m/z = 446.06$); **(D)** Acrylamide **3** incubated in the presence of GSH ($t = 1$ h, $m/z = 676.10$).

The reactivity of **5** was also tested in the presence of purified EGFR-TK by a fluorescence-based assay for evaluation of irreversible kinase inhibition.^{40,41} Fluorescent molecules are very sensitive to solvent polarity and dipolar perturbation from their environments.^{42,43} Moreover, reversible interactions,⁴⁴ such as solvation, hydrogen bonding, charge transfer and redox, as well as irreversible interactions,⁴⁵ such as Michael addition of thiols to electron-deficient alkenes, significantly influence fluorescent spectra of fluorophores. In particular, quinazoline and quinoline fluorophores had been shown to significantly enhance fluorescence emission after covalent reaction with Cys797 of EGFR-TK.⁴⁰ Thus, the 3-aminopropanamide **5** was added to a buffered solution containing EGFR-TK (Figure 8A), samples were excited at 390 nm and fluorescence emission at 420 nm was monitored over time. Results were compared to those of the irreversible **3** and the reversible *N*-(4-(3-bromoanilino)quinazolin-6-yl)acetamide⁴⁶ **46** (Figure 8B).

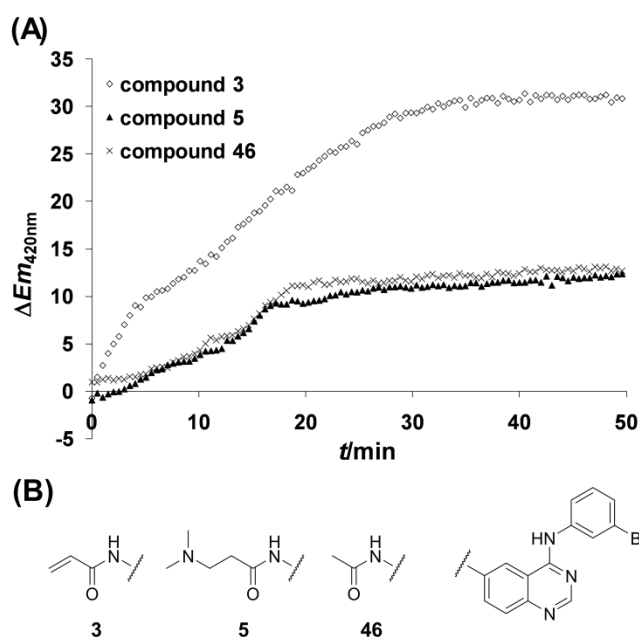


Figure 8. Fluorescence-based assay for irreversible kinase inhibition. **(A)** Compounds **3**, **5**, and **46** (1 μ M) were added to purified EGFR-TK (0.5 μ M) in the presence of ATP (1 mM) and fluorescence emission was monitored at 420 nm in real time over 50 min (excitation 390 nm); $\Delta Em_{420nm} = Em_{Compd+EGFR\ solution} - Em_{Compd\ solution} - Em_{EGFR\ solution}$. **(B)** Chemical structures of compounds **3**, **5**, and **46**.

Upon addition of **3** to EGFR-TK, covalent bond formation with cysteine sulfhydryl group resulted in a time-dependent saturable increase in emission intensity at 420 nm, whereas a significantly lower fluorescence change was observed over 50 min when the reversible 6-acetyl compound **46** or the 3-aminopropanamide **5** were added to EGFR-TK. This result shows that **5** behaves more like the acetamide derivative than like the acrylamide one, suggesting that the 3-aminopropanamide fragment does not alkylate directly EGFR under these experimental conditions.

Finally, compounds **5** and **3** were tested for their reactivity in A549 cell lysate. The formation of conjugates with cysteine added in molar excess (2 mM) was evaluated in cell lysate by LC-HR-MS employing a LTQ-Orbitrap mass analyzer.⁴⁷ Compound **3** quickly reacted with the thiol derivative to form the corresponding cysteine conjugate (data not shown). When compound **5** was added to the cell lysate containing cysteine, a peak corresponding to the acrylamide derivative **3** was detected after 1 h ($[M + H]^+ = 369.03$, $t_R = 8.87$; Figure 9A), as well as a peak corresponding to the adduct of cysteine to the acrylamide fragment ($[M + H]^+ = 490.05$, $t_R = 6.61$ min; Figure 9B).

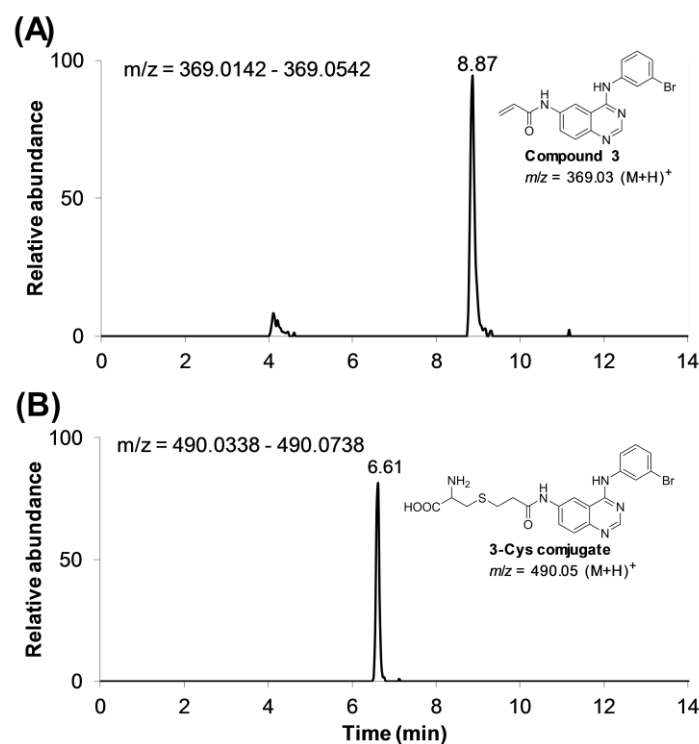


Figure 9. HPLC-HRMS extracted ion chromatograms of A549 cell lysate after 1 h incubation in the presence of compound **5** (10 μ M) and cysteine (2 mM).

(A) The formed acrylamide derivative ($m/z = 369.03$ (M+H)⁺; $t_R = 8.81$ min).

(B) The acrylamide-cysteine conjugate ($m/z = 490.03$ (M+H)⁺; $t_R = 6.61$ min).

After 1 h of incubation, 25.5% of starting acrylamide **3** had been converted to the corresponding cysteine conjugate, compared to a 1.1% conversion observed for **5**. The concentration of cysteine conjugate doubled for both **3** and **5** at the second time point ($t = 4$ h), being 54.4% (**3**) and 2.0% (**5**) of starting concentrations, respectively.

Evidence for irreversible binding to EGFR

Mannich bases are versatile synthetic intermediates used in various transformations to prepare Michael acceptors via elimination of the amino moiety.⁴⁸ As reported in the literature, aryl β -aminoethyl ketones can irreversibly inhibit enzymes by covalent interaction with cysteine residues^{31,32,33} after bioconversion to the corresponding α,β -unsaturated carbonyl compound. The new 3-aminopropanamides, characterized by a quinazoline (**5-7** and **11-13**) or quinoline-3-carbonitrile (**15-17** and **19-21**) driving portion, showed inhibition of EGFR autophosphorylation in A549 cells after 1 h incubation at 1 μ M concentration and the effect generally persisted up to 8 h after removal of the compounds from the reaction medium (Table 2). In principle, the long-lasting effect observed on EGFR autophosphorylation could be ascribed to different phenomena: (i) accumulation of the inhibitor in cells, as previously demonstrated for some reversible quinazolines;⁴⁹ (ii) conversion of the competitive inhibitor into an irreversible one at the active site of the enzyme (mechanism-based inhibition), as described for other β -aminocarbonyl compounds;³¹ (iii) generation of the corresponding reactive acrylamide, as described for aryl β -aminoethyl ketones that have potential application as prodrugs of unsaturated ketones.⁵⁰

Data from fluorescence-based assay for irreversible enzyme inhibition (Figure 8) ruled out direct interaction between the 3-aminopropanamide **5** and purified EGFR-TK in the chosen time period. The reactivity studies on **5** indicated that the compound regenerated significant amounts of the acrylamide **3** only in the presence of cell lysate (Figure 9) while it did not under cell-free conditions (Tables 3 and 4). The results demonstrate that **5** can act as prodrug of **3** releasing the acrylamide fragment in the intracellular environment of A549 cells.

In principle, activation of 3-aminopropanamides to acrylamides in the intracellular environment could be affected by the nature of the heterocyclic nucleus (i.e. quinazoline or quinoline-3-carbonitrile), since a specific enzymatic transformation is likely to occur. However, the similar behavior of quinazolines (A- and B-series) and quinoline-3-carbonitriles (C- and D-series) on EGFR autophosphorylation at 8 h, as well as previous data on in vivo activity of Mannich bases, suggest that activation of the β -aminocarbonyl fragment to a Michael acceptor is a rather general process. In this context, masking the electrophilic warhead may provide some improvements in the pharmacokinetic or pharmacodynamic profile of antiproliferative agents. Although not a conclusive evidence of specific advantages, the observation that some 3-aminopropanamide derivatives in the quinazoline and quinoline-3-carbonitrile series showed inhibition potencies on H1975 cell lines close to those of the corresponding acrylamides encourages further evaluation of the biological properties of these compounds.

Conclusions

In the present work it was reported a new series of EGFR inhibitors containing a 3-aminopropanamide linked to a 4-anilinoquinazoline (**5-7** and **11-13**) or 4-anilinoquinoline-3-carbonitrile (**15-17** and **19-21**) nucleus. The newly synthesized 3-aminopropanamides proved efficient in inhibiting EGFR-TK activity, showing a long-lasting effect on the enzyme autophosphorylation in A549 lung cancer cells. Notably, several 3-aminopropanamides suppressed proliferation of gefitinib-resistant NSCLC cells (H1975) at significantly lower concentration than **1**.

Finally, a combined approach, based on (i) in vitro chemical stability assays, (ii) reactivity studies in the presence of thiol nucleophiles, and (iii) reactivity studies toward EGFR tyrosine kinase and in the presence of cell lysate, showed that 3-dimethylaminopropanamide **5** acts as prodrug, releasing the acrylamide derivative **3** in the intracellular environment, although it is stable in other conditions.

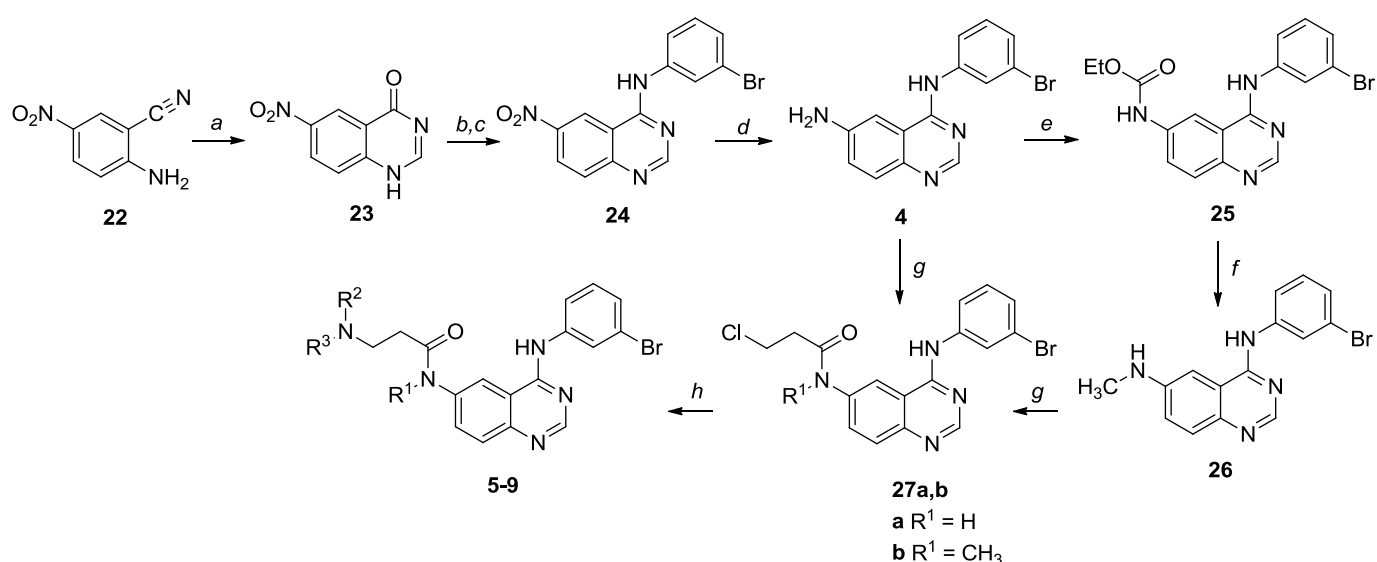
In conclusion, these findings expand the chemical diversity of irreversible inhibitors of EGFR, and similar strategies might be applied to the design of compounds able to form a covalent bond with a peripheral cysteine residue within a biological target.

Notably, preliminary results of in vivo studies showed that a 3-aminopropanamide derivative (**12**), at the oral dose of 25 mg/kg, inhibited the growth of NSCLC xenografts in nude mice; at the same dose, gefitinib did not inhibit tumor growth and an acrylamide derivative, now in the clinical phases, was more toxic. The chemical strategy here devised looks therefore promising for the development of novel antitumor drugs addressed at the kinase domain and interacting with the target by selective covalent addition.

Chemistry

General synthesis of compounds 4-9 (series A)

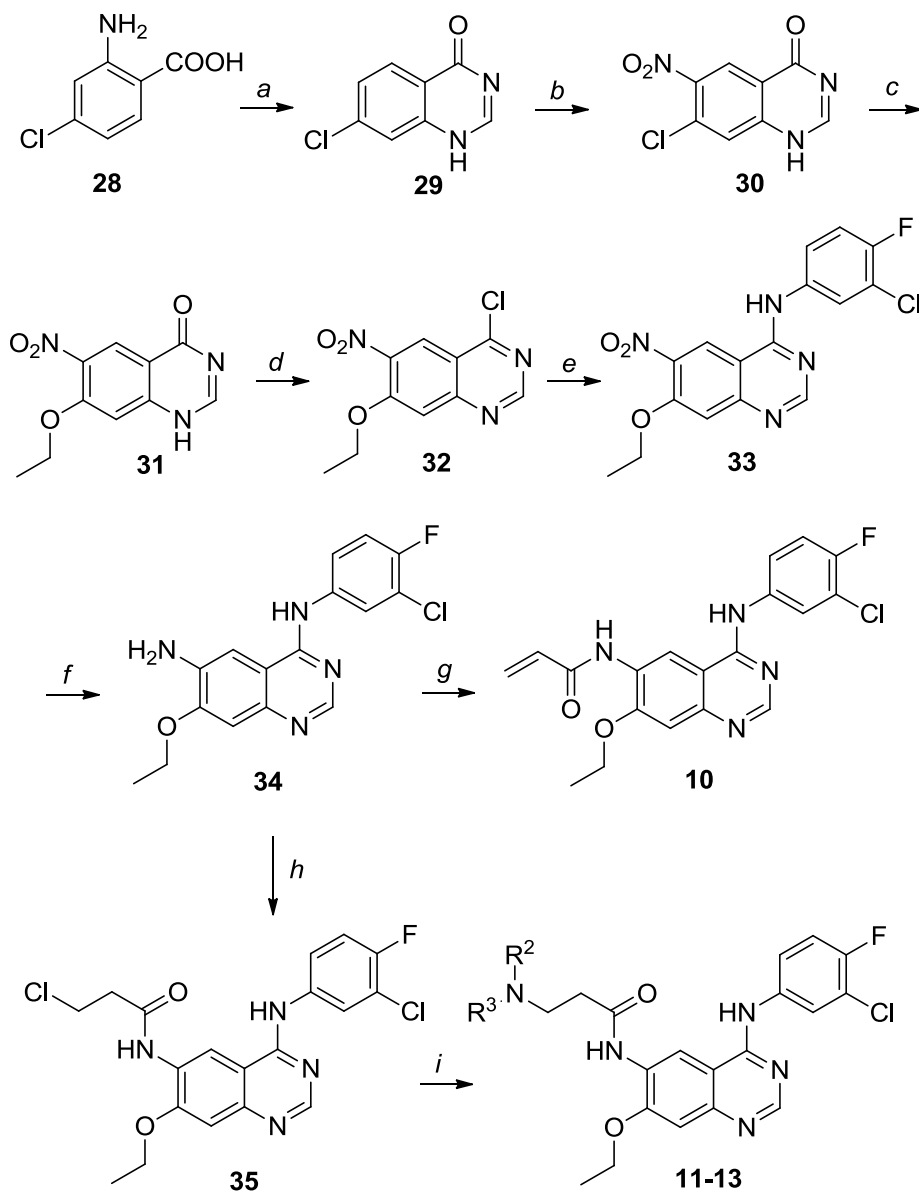
Compounds of series A (**5-9**) of Table 2 were synthesized by coupling their precursor amines (**4** or **26**) with the proper carboxylic acid and substituting the terminal chlorine with various amines, as described in Scheme 1. The 6-amino-4-(3-bromoanilino)quinazoline **4** was prepared in three steps from 5-nitroanthranilonitrile **22**, following known procedures (Scheme 1).^{51,52} Condensation of **4** with 3-chloropropionyl chloride gave the 3-chloropropionamide intermediate **27a**, which underwent substitution with the proper amine to obtain the secondary 3-aminopropionamides **5-8**. Alternatively, 6-aminoquinazoline **4** was converted to its *N*-methyl analogue **26**⁵³ by carbamoylation with ethyl chloroformate in pyridine followed by reduction of the resulting carbamate **25** with sodium bis(2-methoxyethoxy)aluminum hydride (Red-Al). The *N*-methylaminoquinazoline **26** thus generated was first condensed with 3-chloropropionyl chloride to **27b**, and then substituted with dimethylamine to obtain the tertiary 3-aminopropionamide derivative **9** (Scheme 1).

Scheme 1^a

^a (a) H_2SO_4 , formic acid, reflux; (b) SOCl_2 , dioxane, reflux; (c) 3-bromoaniline, *i*-PrOH, 60 °C; (d) Fe, AcOH, EtOH/ H_2O , reflux; (e) ClCOOEt , anhydrous pyridine, 0 °C to rt; (f) Red-Al, THF, rt; (g) $\text{ClCH}_2\text{CH}_2\text{COCl}$, THF, 50 °C; (h) $\text{R}^2\text{R}^3\text{NH}$, KI, abs EtOH, reflux.

General synthesis of compounds 10-13 (series B)

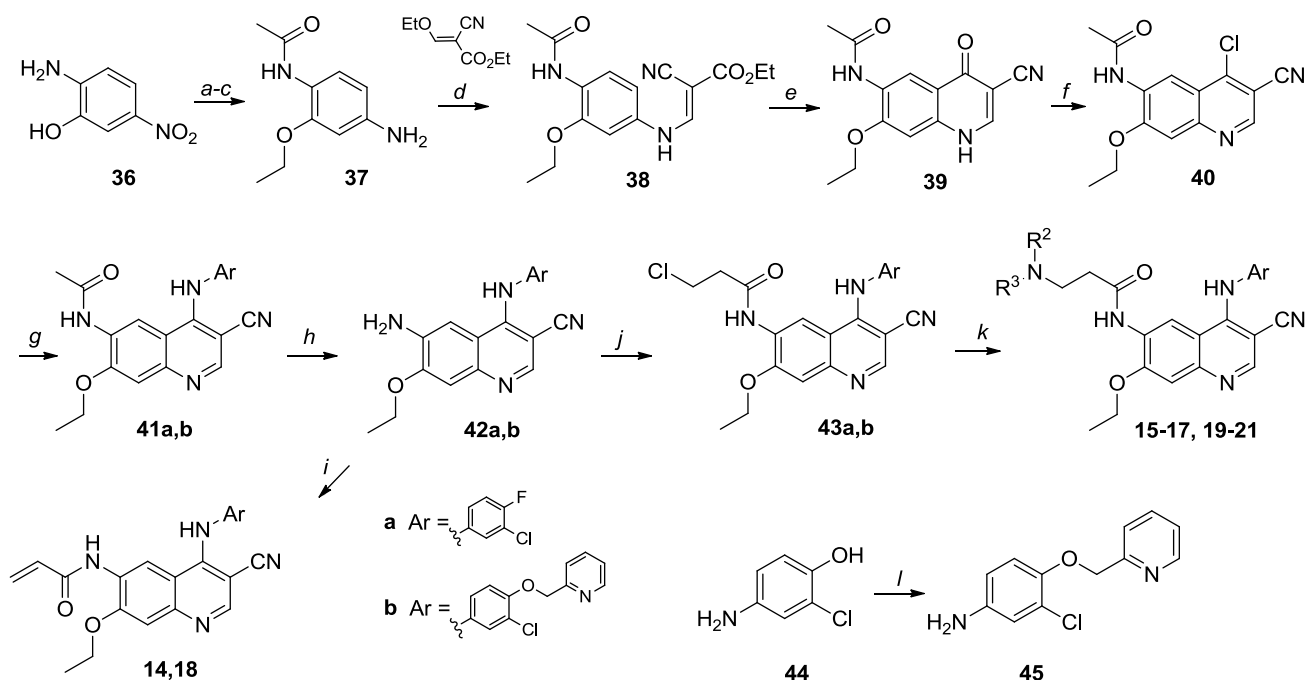
4-(3-Chloro-4-fluoroanilino)-7-ethoxyquinazolino compounds of series B (**10-13**) of Table 2 were synthesized as described in Scheme 2. 6-Aminoquinazoline intermediate **34**⁵⁴ was obtained, following a procedure that has been slightly modified from a described one,⁵⁵ from 4-chloroanthranilic acid **28**. Briefly, cyclization of **28** with formamidine acetate followed by nitration gave a mixture of isomers from which pure **30** was obtained after recrystallization from acetic acid. The 7-chlorine group was substituted with sodium ethoxide and the resulting 7-ethoxy derivative **31** was first chlorinated by heating in phosphorus oxychloride, then substituted with 3-chloro-4-fluoroaniline to obtain the intermediate **33**. Reduction of the nitro group of **33** with iron and acetic acid gave the 6-aminoquinazoline **34**. The 6-acrylamide derivative **10** was then obtained from **34** with acryloyl chloride in the presence of *N,N*-diisopropylethylamine (DIPEA). Finally, 3-aminopropanamides **11-13** were synthesized from **34** by reaction with 3-chloropropionyl chloride to **35** and then substituting the chlorine with the proper secondary amine (Scheme 2).

Scheme 2^a

^a (a) Formamidinium acetate, 2-methoxyethanol, 130 °C; (b) H₂SO₄, HNO₃, 100 °C; (c) NaOEt, anhydrous EtOH, reflux; (d) POCl₃, reflux; (e) 3-chloro-4-fluoroaniline, *i*-PrOH, reflux; (f) Fe, AcOH, EtOH/H₂O, reflux; (g) acryloyl chloride, DIPEA, DMF, 0 °C to 50 °C; (h) ClCH₂CH₂COCl, 50 °C; (i) R²R³NH, KI, abs EtOH, reflux.

General synthesis of compounds 14-21 (series C and D)

4-Anilinoquinoline-3-carbonitriles of series C and D (**14-17** and **18-21**, respectively) of Table 2 were synthesized as described in Scheme 3. The key *N*-(4-chloro-3-cyano-7-ethoxyquinolin-6-yl)acetamide intermediate **40** was synthesized in 6 steps from 2-amino-5-nitrophenol **36**, as described in the literature.⁵⁶ The quinoline intermediate **40** was reacted with the proper aniline (to **41a** and **41b**) and deacetylated in aqueous hydrochloric acid to amines **42a**⁵⁷ and **42b**.⁵⁸ Aniline derivative **45** was synthesized by reaction of 4-amino-2-chlorophenol **44** and picolyl chloride in the presence of benzaldehyde as described in Scheme 3.⁵⁹ The acrylamides **14** and **18** were subsequently synthesized from amine precursors, **42a** and **42b** respectively, with acryloyl chloride in the presence of a base (DIPEA). The 3-aminopropanamides **15-17** and **19-21** were synthesized in two steps from amines **42** by condensation with 3-chloropropionyl chloride and substitution with a secondary amine (Scheme 3).

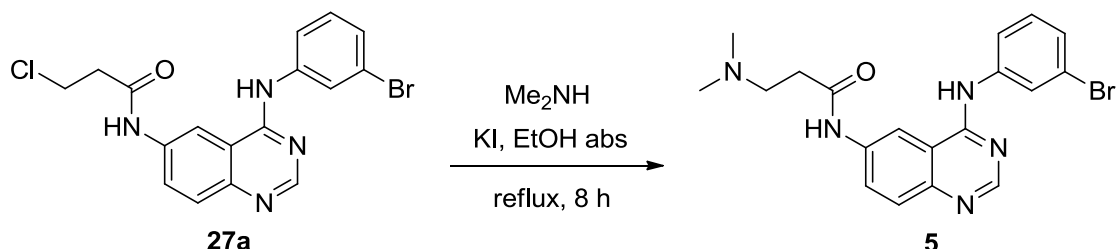
Scheme 3^a

^a (a) Ac₂O, AcOH, 60 °C; (b) EtBr, DMF, K₂CO₃, 60 °C; (c) H₂, Pd/C, THF, rt; (d) toluene, 90 °C; (e) Dowterm, 250 °C; (f) POCl₃, diglyme, 100 °C; (g) 3-chloro-4-fluoroaniline or **45**, pyridine hydrochloride, *i*-PrOH, reflux; (h) HCl, reflux; (i) acryloyl chloride, DIPEA, DMF, 0 °C to 50 °C; (j) ClCH₂CH₂COCl, THF, 50 °C; (k) R²R³NH, KI, abs EtOH, reflux; (l) PhCHO, K₂CO₃, picolyl chloride hydrochloride, DMF, 50 °C.

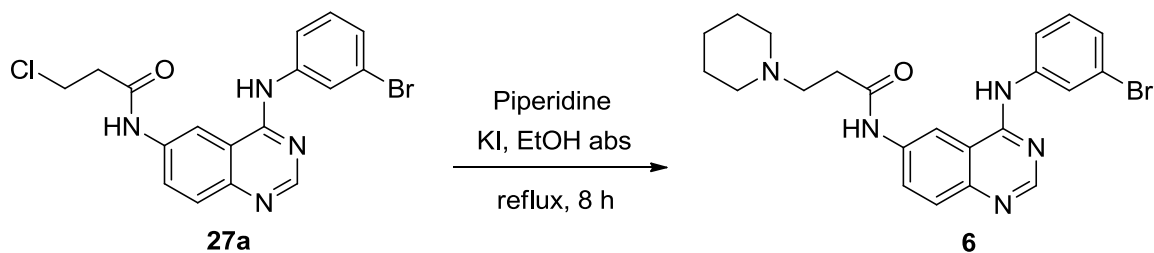
Materials and methods

Reagents were obtained from commercial suppliers and used without further purification. Reactions were monitored by TLC, on Kieselgel 60 F₂₅₄ (DC-Alufolien, Merck). Final compounds and intermediates were purified by flash chromatography (SiO₂ 60, 40-63 μm). Microwave reactions were conducted using a CEM Discover Synthesis Unit (CEM Corp., Matthews, NC). Solvents were purified and stored according to standard procedures. Anhydrous reactions were conducted under a positive pressure of dry N₂. Melting points were determined with a Gallenkamp melting point apparatus and were not corrected. The ¹H NMR spectra were recorded on a Bruker 300 MHz Avance or on a Bruker 400 MHz Avance spectrometer; chemical shifts (δ scale) are reported in parts per million (ppm) relative to the central peak of the solvent. ¹H NMR spectra are reported in the following order: multiplicity, approximate coupling constant (*J* value) in Hertz (Hz) and number of protons; signals were characterized as s (singlet), d (doublet), dd (doublet of doublets), t (triplet), dt (doublet of triplets), q (quartet), m (multiplet) br s (broad signal). Mass spectra were recorded using an API 150 EX instrument (AB/SCIEX, Toronto, Canada). The final compounds were analyzed on ThermoQuest (Italia) FlashEA 1112 Elemental Analyzer, for C, H and N. Analyses were within $\pm 0.4\%$ of the theoretical values. All tested compounds were $> 95\%$ pure by elemental analysis. Compounds **1**,⁶⁰ **3**,³⁷ and **4**⁶¹ were synthesized according to literature methods.

Experimental section

***N*-4-(3-Bromoanilino)quinazolin-6-yl)-3-(dimethylamino)propanamide (5).**

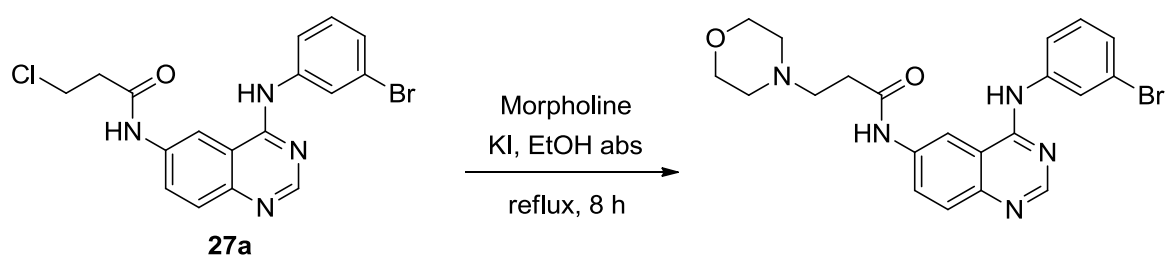
A 33% v/v solution of dimethylamine in absolute EtOH (0.8 mL, 4.46 mmol) was added over 15 min to a stirred suspension of 3-chloropropanamide **27a** (145 mg, 0.36 mmol) and KI (42 mg, 0.25 mmol) in absolute EtOH (10 mL) and the resulting mixture was refluxed for 8 h. After cooling to 0 °C, the mixture was basified with KOH pellets (0.74 g) and stirred for 1 h at 0 °C. The solvent was evaporated under reduced pressure and the solid residue was dissolved with EtOAc and washed with brine. The organic phase was dried, the solvent evaporated, and the residue purified by silica gel chromatography (CH₂Cl₂/MeOH, 99:1 to 70:30) to give **5** as pale yellow solid (86%): mp (EtOAc/*n*-hexane) 170-172 °C; ¹H NMR (CD₃OD, 300 MHz) δ 2.35 (s, 6H), 2.65 (t, *J* = 6.5 Hz, 2H), 2.78 (t, *J* = 6.5 Hz, 2H), 7.29-7.31 (m, 2H), 7.74 (m, 3H), 8.12 (br s, 1H), 8.53 (s, 1H), 8.66 (br s, 1H); MS (APCI) *m/z* 414.4, 416.4; Anal. calc for C₁₉H₂₀BrN₅O: C, 55.08; H, 4.87; N, 16.90; found: C, 54.69; H, 4.89; N, 16.53.

***N*-4-(3-Bromoanilino)quinazolin-6-yl)-3-piperidin-1-ylpropanamide (6).**

N-4-(3-Bromoanilino)quinazolin-6-yl)-3-chloropropanamide **27a** was reacted with anhydrous piperidine according to the procedure described for compound **5**. The

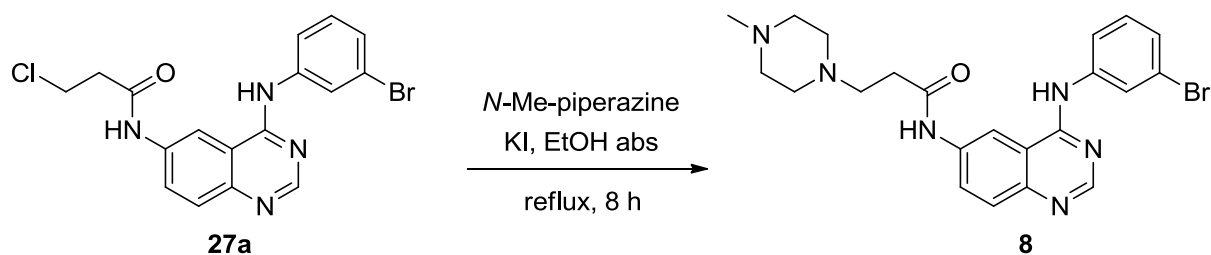
product was purified by silica gel chromatography (CH₂Cl₂/MeOH, 95:5) to give **6** as a white solid (78%): mp (Et₂O) 184-186 °C; ¹H NMR (DMSO-*d*₆, 300 MHz) δ 1.61 (m, 2H), 1.74-1.82 (m, 10H), 2.68-2.73 (m, 2H), 7.18-7.32 (m, 3H), 7.67 (d, *J* = 6.8 Hz, 1H), 7.83 (d, *J* = 8.8 Hz, 1H), 7.97 (s, 1H), 8.08 (s, 1H), 8.71 (s, 1H), 8.89 (s, 1H), 12.04 (s, 1H); MS (APCI) *m/z* 454.1, 456.2; Anal. calc for C₂₂H₂₄BrN₅O·3/4H₂O: C, 56.47; H, 5.49; N, 14.96; found: C, 56.46; H, 5.43; N, 14.77.

***N*-(4-(3-Bromoanilino)quinazolin-6-yl)-3-morpholino-1-ylpropanamide (7).**



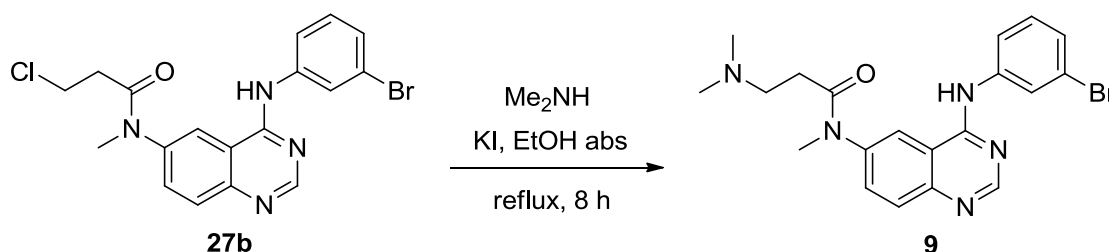
N-(4-(3-Bromoanilino)quinazolin-6-yl)-3-chloropropanamide **27a** was reacted with morpholine according to the procedure described for compound **5**. The product was purified by silica gel chromatography (CH₂Cl₂/MeOH, 95:5) to give **7** as a yellow solid (70%): mp (Et₂O/*n*-hexane) 196-198 °C; ¹H NMR (CDCl₃, 300 MHz) δ 2.59-2.77 (m, 8H), 3.89 (m, 4H), 7.17-7.25 (m, 3H), 7.62 (d, *J* = 7.4 Hz, 1H), 7.76 (d, *J* = 8.9 Hz, 1H), 7.90 (s, 1H), 8.16 (bs, 1H), 8.67 (s, 1H), 8.93 (d, *J* = 1.9 Hz, 1H), 11.40 (s, 1H); MS (APCI) *m/z* 456.2, 458.4; Anal. calc for C₂₁H₂₂BrN₅O₂·1/3H₂O: C, 54.56; H, 4.94; N, 15.15; found: C, 54.75; H, 4.99; N, 14.88.

***N*-(4-(3-Bromoanilino)quinazolin-6-yl)-3-(4-methylpiperazin-1-yl)propanamide (8).**



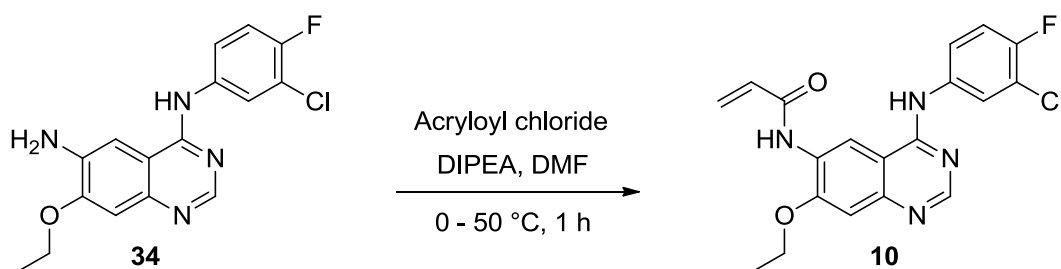
N-(4-(3-Bromoanilino)quinazolin-6-yl)-3-chloropropanamide **27a** was reacted with *N*-methylpiperazine according to the procedure described for compound **5**. The product was purified by silica gel chromatography (CH₂Cl₂/MeOH, 95:5) to give **8** as a white solid (77%): mp (Et₂O) 196 °C; ¹H NMR (CDCl₃, 300 MHz) δ 2.33 (s, 3H), 2.42-2.49 (m, 12H), 6.94-7.07 (m, 3H), 7.44-7.51 (m, 2H), 7.58 (s, 1H), 8.50 (s, 1H), 8.68 (m, 1H), 8.88 (s, 1H), 11.55 (s, 1H); MS (APCI) *m/z* 469.3, 471.3; Anal. calc for C₂₂H₂₅BrN₆O·1/2H₂O: C, 55.23; H, 5.48; N, 17.57; found: C, 55.22; H, 5.54; N, 17.28.

***N*-(4-(3-Bromophenylamino)quinazolin-6-yl)-3-(dimethylamino)-*N*-methylpropanamide (9).**



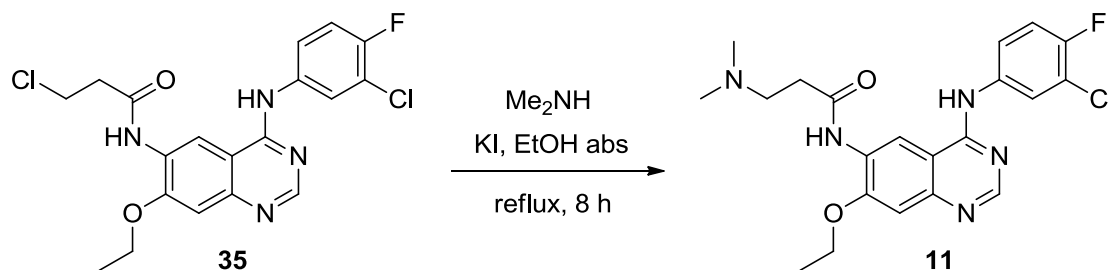
N-(4-(3-Bromophenylamino)quinazolin-6-yl)-3-chloro-*N*-methylpropanamide **27b** was reacted with dimethylamine according to the procedure described for compound **5**. Silica gel chromatography purification (CH₂Cl₂/MeOH, 98:2 to 90:10) afforded **9** as a white solid (68%): mp (CH₂Cl₂/*n*-hexane) 169-172 °C; ¹H NMR (CD₃OD, 300 MHz) δ 2.14 (s, 6H), 2.39 (br s, 2H), 2.67 (br s, 2H), 3.40 (s, 3H), 7.34 (m, 2H), 7.79 (m, 1H), 7.85 (dd, *J* = 8.6, 2.3 Hz, 1H), 7.93 (d, *J* = 8.0 Hz, 1H), 8.17 (s, 1H), 8.42 (s, 1H), 8.66 (s, 1H); MS (APCI) *m/z* 430.4, 431.4, 432.4; Anal. calc for C₂₀H₂₂BrN₅O: C, 56.08; H, 5.18; N, 16.35; found: C, 56.48; H, 5.15; N, 16.13.

***N*-(4-(3-Chloro-4-fluoroanilino)-7-ethoxyquinazolin-6-yl)acrylamide (10).**



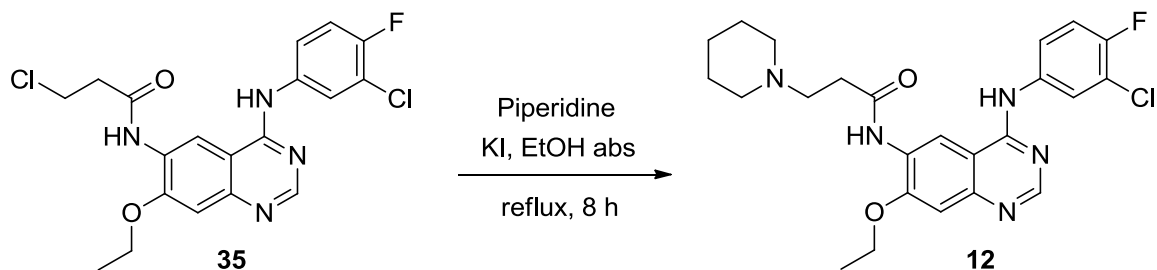
Acryloyl chloride (25 μ L, 0.3 mmol) in anhydrous THF (0.5 mL) was added dropwise to a solution of 6-aminoquinazoline **34** (100 mg, 0.3 mmol) and *N,N*-diisopropylethylamine (DIPEA) (52 μ L, 0.3 mmol) in anhydrous DMF (2.5 mL) at 0 °C. The reaction mixture was stirred for 1 h, then the solvent was removed under reduced pressure and the residue was purified by silica gel chromatography ($\text{CH}_2\text{Cl}_2/\text{MeOH}$, 95:5) to afford **10** as a white solid (25%): mp (EtOH/ H_2O) 228.5-230 °C; ^1H NMR (Acetone- d_6 , 400 MHz) δ 1.52 (t, J = 6.9 Hz, 3H), 4.35 (q, J = 6.9 Hz, 2H), 5.83 (dd, J = 10.1, 1.7 Hz, 1H), 6.45 (dd, J = 16.8, 1.7 Hz, 1H), 6.70 (dd, J = 16.8, 10.1 Hz, 1H), 7.29 (s, 1H), 7.32 (t, J = 9.0 Hz, 1H), 7.86 (ddd, J = 9.0, 4.1, 2.8 Hz, 1H), 8.25 (dd, J = 6.8, 2.6 Hz, 1H), 8.57 (s, 1H), 9.04 (s, 1H); MS (APCI) m/z 387.3, 389.3; Anal. calc for $\text{C}_{19}\text{H}_{16}\text{ClFN}_4\text{O}_2 \cdot 2/3\text{CH}_3\text{CH}_2\text{OH}$: C, 58.49; H, 4.83; N, 13.42; found: C, 58.31; H, 4.75; N, 13.09.

***N*-(4-(3-Chloro-4-fluoroanilino)-7-ethoxyquinazolin-6-yl)-3-(dimethylamino)propanamide (11).**



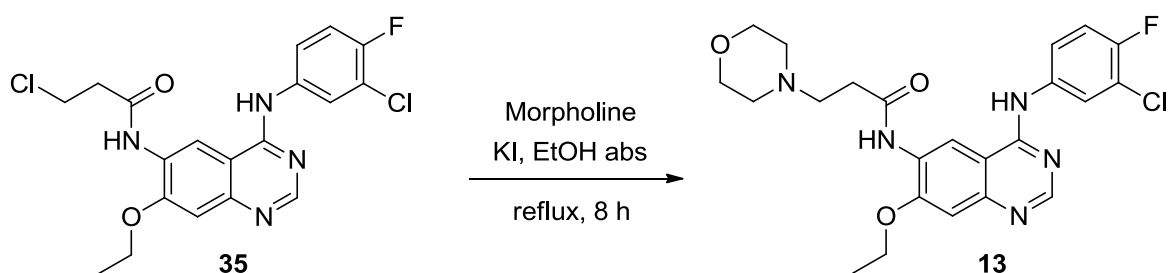
3-Chloropropanamide **35** was reacted with dimethylamine according to the procedure described for compound **5**. The product was purified by silica gel chromatography (AcOEt/MeOH, 99:1 to 85:15) to obtain **11** as a white solid (85%): mp (EtOH/ H_2O) 182-183 °C; ^1H NMR (CD_3OD , 300 MHz) δ 1.54 (t, J = 7.0 Hz, 3H), 2.37 (s, 6H), 2.69 (m, 4H), 4.26 (q, J = 7.0 Hz, 2H), 7.11 (s, 1H), 7.21 (t, J = 9.0 Hz, 1H), 7.62 (ddd, J = 9.0, 4.1, 2.7 Hz, 1H), 7.95 (dd, J = 6.7, 2.6 Hz, 1H), 8.41 (s, 1H), 8.83 (s, 1H); MS (APCI) m/z 432.5, 434.3; Anal. calc for $\text{C}_{21}\text{H}_{23}\text{ClFN}_5\text{O}_2 \cdot 2/3\text{H}_2\text{O}$: C, 56.81; H, 5.53; N, 15.78; found: C, 56.92; H, 5.58; N, 15.47.

***N*-4-(3-Chloro-4-fluoroanilino)-7-ethoxyquinazolin-6-yl)-3-(piperidin-1-yl)propanamide (12).**



3-Chloropropanamide **35** was reacted with anhydrous piperidine according to the procedure described for compound **5**. The product was purified by silica gel chromatography (AcOEt/MeOH, 99:1 to 93:7) to give **12** as a white solid (60%): mp (EtOH/H₂O) 106.5-108 °C; ¹H NMR (DMSO-*d*₆, 400 MHz) δ 1.54 (t, *J* = 6.9 Hz, 5H), 1.68 (4H, m), 2.56 (s, 4H), 2.75 (m, 4H), 4.38 (q, *J* = 6.9 Hz, 2H), 7.22 (s, 1H), 7.25 (t, *J* = 8.9 Hz, 1H), 7.65 (ddd, *J* = 9.0, 3.7, 2.8 Hz, 1H), 7.99 (dd, *J* = 6.6, 2.5 Hz, 1H), 8.47 (s, 1H), 8.83 (s, 1H); MS (APCI) *m/z* 472.2, 474.2; Anal. calc for C₂₄H₂₇ClFN₅O₂·1H₂O: C, 58.83; H, 5.97; N, 14.29; found: C, 59.20; H, 5.97; N, 14.08.

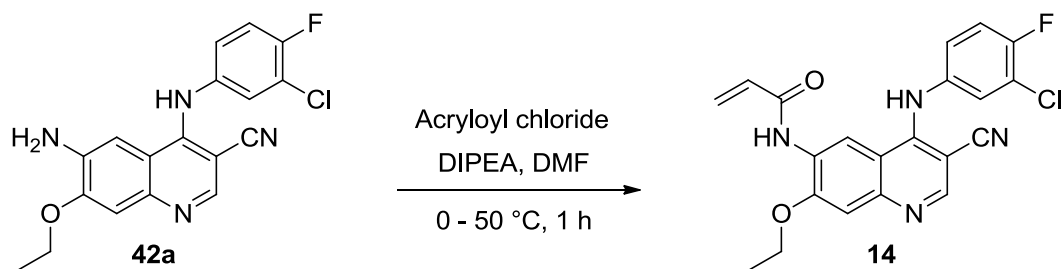
***N*-4-(3-Chloro-4-fluorophenylamino)-7-ethoxyquinazolin-6-yl)-3-morpholinopropanamide (13).**



3-Chloropropanamide **35** was reacted with morpholine according to the procedure described for compound **5**. The product was purified by silica gel chromatography (AcOEt/MeOH, 99:1 to 96:4) to obtain **13** as a light yellow solid (96%): mp (EtOH/H₂O) 108-110 °C; ¹H NMR (DMSO-*d*₆, 400 MHz) δ 1.54 (t, *J* = 7.0 Hz, 3H), 2.60 (m, 4H), 2.74 (t, *J* = 6.0, 2H), 2.81 (t, *J* = 5.8 Hz, 2H), 3.77 (t, *J* = 4.6 Hz, 4H),

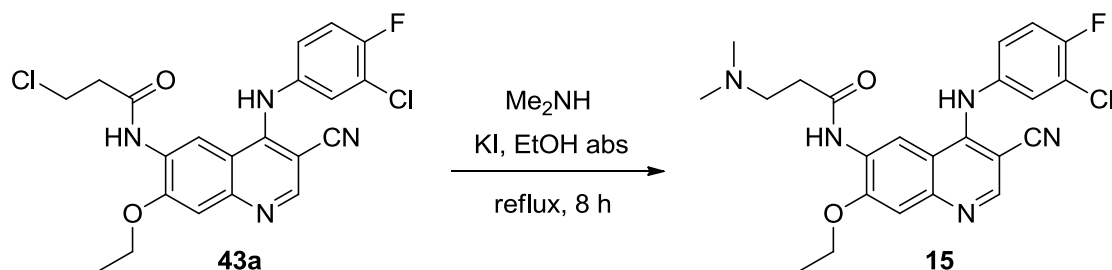
4.37-4.41 (m, 2H), 7.18-7.26 (m, 2H), 7.63-7.65 (m, 1H), 7.97-7.99 (m, 1H), 8.46 (d, $J = 2.9$ Hz, 1H), 8.83 (d, $J = 4.7$ Hz, 1H); MS (APCI) 474.0, 476.3 °C; Anal. calc for $C_{23}H_{25}ClFN_5O_3 \cdot 2/3H_2O$: C, 56.85; H, 5.46; N, 14.41; found: C, 57.22; H, 5.44; N, 14.09.

***N*-(4-(3-Chloro-4-fluoroanilino)-3-cyano-7-ethoxyquinolin-6-yl)acrylamide (14).**



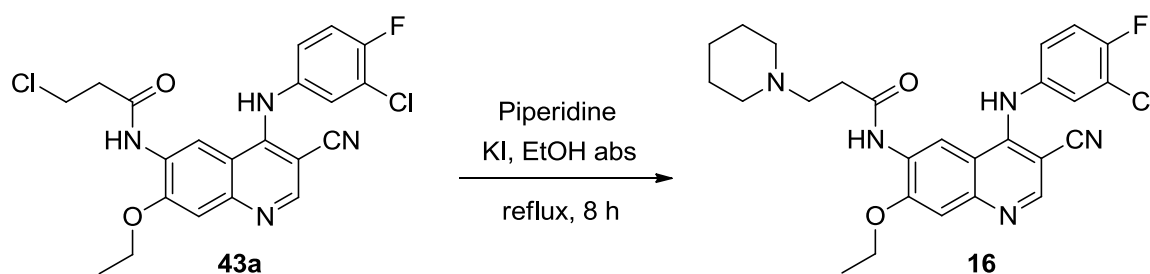
The product was obtained by coupling the amino intermediate **42a** with acryloyl chloride as described for compound **10**. Silica gel chromatography purification (EtOAc/*n*-hexane, 60:40) afforded **14** (40%) as a white solid: mp (EtOH/H₂O) > 230 °C; ¹H NMR (DMSO-*d*₆, 300MHz) δ 1.48 (t, $J = 6.9$ Hz, 3H), 4.33 (q, $J = 6.9$ Hz, 2H), 5.81 (d, $J = 10.7$ Hz, 1H), 6.29 (d, $J = 16.5$ Hz, 1H), 6.77 (dd, $J = 16.5, 9.7$ Hz, 1H), 7.25 (m, 1H), 7.41 (m, 3H), 8.53 (s, 1H), 8.98 (s, 1H), 9.60 (s, 1H), 9.75 (br s, 1H); MS (APCI) *m/z* 411.0; Anal. calc for $C_{21}H_{16}ClFN_4O_2 \cdot 1/2H_2O$: C, 60.07; H, 4.08; N, 13.35; found: C, 60.09; H, 3.95; N, 13.15.

***N*-(4-(3-Chloro-4-fluoroanilino)-3-cyano-7-ethoxyquinolin-6-yl)-3-(dimethylamino)propanamide (15).**



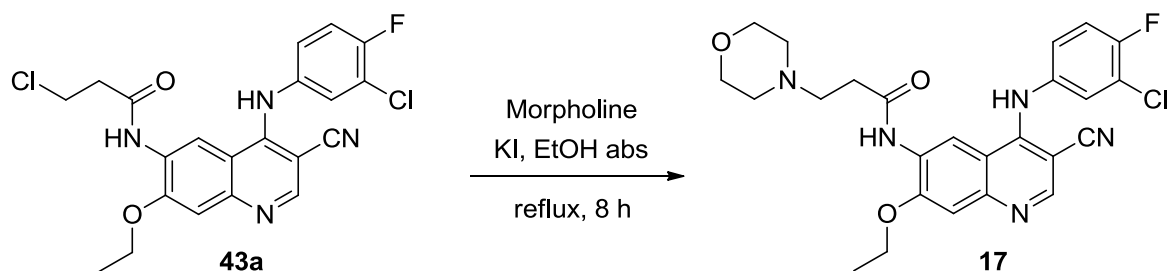
3-Chloropropanamide **43a** was reacted with dimethylamine according to the procedure described for compound **5**. Silica gel chromatography (CH₂Cl₂/MeOH, 99:1 to 97:3) gave **15** as a light yellow solid (69%): mp (EtOH) 168-171 °C; ¹H NMR (DMSO-*d*₆, 300 MHz) δ 1.48 (t, *J* = 7.0 Hz, 3H), 2.29 (s, 6H), 2.57 (m, 4H), 4.32 (q, *J* = 7.0 Hz, 2H), 7.19 (m, 1H), 7.40 (m, 3H), 8.54 (s, 1H), 9.06 (s, 1H), 9.68 (br s, 1H), 10.98 (s, 1H); MS (APCI) *m/z* 545.4, 547.3; Anal. calc for C₂₃H₂₃ClFN₅O₂·1H₂O: C, 58.29; H, 5.35; N, 14.78; found: C, 57.93; H, 5.32; N, 14.69.

***N*-4-(3-Chloro-4-fluoroanilino)-3-cyano-7-ethoxyquinolin-6-yl)-3-(piperidin-1-yl)propanamide (16).**



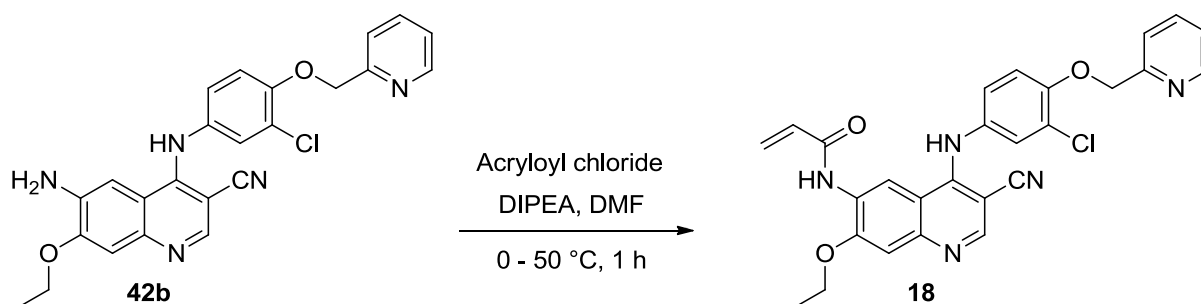
3-Chloropropanamide **43a** was reacted with piperidine according to the procedure described for compound **5**. Silica gel chromatography (CH₂Cl₂/MeOH, 96:4) gave **16** as a white solid (45%): mp (EtOH) 180-184 °C; ¹H NMR (DMSO-*d*₆, 400 MHz) δ 1.46 (t, *J* = 7.0 Hz, 3H); 1.49 (m, 2H), 1.56 (m, 4H), 2.44 (m, 4H), 2.60 (s, 4H), 4.39 (t, *J* = 7.0 Hz, 2H), 7.22 (m, 1H), 7.41 (m, 3H), 8.54 (s, 1H), 8.97 (s, 1H), 9.68 (br s, 1H), 10.24 (s, 1H); MS (APCI) *m/z* 496.4, 497.3, 499.4; Anal. calc for C₂₆H₂₇ClFN₅O₂·1/2CH₃CH₂OH: C, 62.48; H, 5.83; N, 13.50; found: C, 62.15; H, 5.58; N, 13.82.

***N*-4-(3-Chloro-4-fluoroanilino)-3-cyano-7-ethoxyquinolin-6-yl)-3-morpholinopropanamide (17).**



3-Chloropropanamide **43a** was reacted with morpholine according to the procedure described for compound **5**. Silica gel chromatography (CH₂Cl₂/MeOH, 98:2) afforded **17** as a white solid (52%): mp (EtOH/H₂O) 195-198 °C; ¹H NMR (DMSO-*d*₆, 400 MHz) δ 1.45 (t, *J* = 7.0 Hz, 3H), 2.46 (m, 4H), 2.63 (m, 4H), 3.62 (t, *J* = 4.2 Hz, 4H), 4.36 (q, *J* = 7.1 Hz, 2H), 7.20 (br s, 1H), 7.39 (m, 3H), 8.53 (br s, 1H), 8.94 (s, 1H), 9.69 (br s, 1H), 9.89 (s, 1H); MS (APCI) *m/z* 498.3, 499.2, 500.3; Anal. calc for C₂₅H₂₅ClFN₅O₃·1/2CH₃CH₂OH: C, 59.94; H, 5.42; N, 13.44; found: C, 60.22; H, 5.47; N, 13.23.

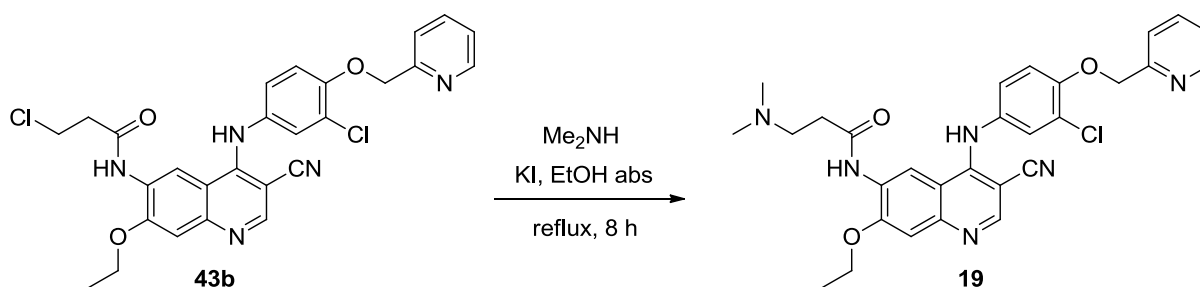
***N*-(4-(3-Chloro-4-(pyridin-2-ylmethoxy)anilino)-3-cyano-7-ethoxyquinolin-6-yl)acrylamide (18).**



The product was obtained by coupling the amino intermediate **42b** with acrylic acid as described for compound **10**. Silica gel chromatography purification (CH₂Cl₂/MeOH, 98:2) gave **18** as a white solid (35%): mp (EtOH/H₂O) > 230 °C; ¹H NMR (DMSO-*d*₆, 300MHz) δ 1.53 (t, *J* = 6.9 Hz, 3H), 4.39 (q, *J* = 6.9 Hz, 2H), 5.32 (s, 2H); 5.79 (dd, *J* = 10.1, 1.9 Hz, 1H), 6.39 (dd, *J* = 16.9, 1.9 Hz, 1H), 6.68 (dd, *J* = 16.9, 10.1 Hz, 1H), 7.30 (m, 3H), 7.41 (s, 1H), 7.48 (d, *J* = 2.3 Hz, 1H), 7.68 (d, *J* = 7.8 Hz, 1H), 7.87 (td, *J* = 7.8, 1.8 Hz, 1H), 8.50 (s, 1H), 8.60 (d, *J* = 4.5 Hz, 1H), 9.05

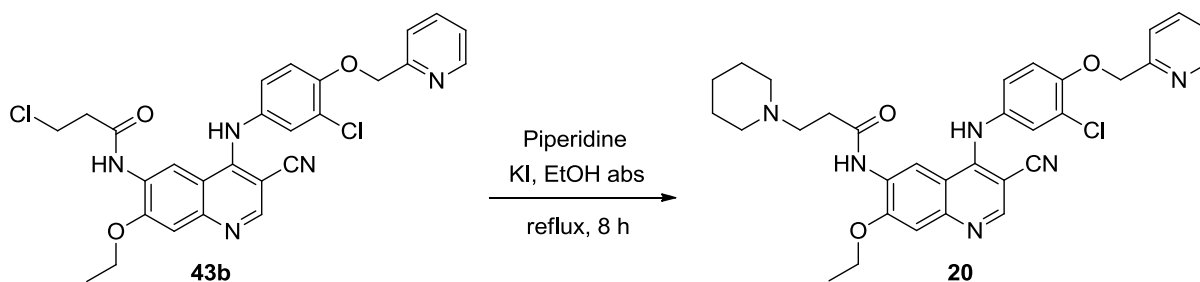
(s, 2H), 9.16 (s, 1H); MS (APCI) m/z 500.1; Anal. calc for $C_{27}H_{22}ClN_5O_3 \cdot 2/3CH_3OH$: C, 63.74; H, 4.99; N, 13.42; found: C, 64.04; H, 4.76; N, 13.04.

***N*-(4-(3-Chloro-4-(pyridin-2-ylmethoxy)anilino)-3-cyano-7-ethoxyquinolin-6-yl)-3-(dimethylamino)propanamide (19).**



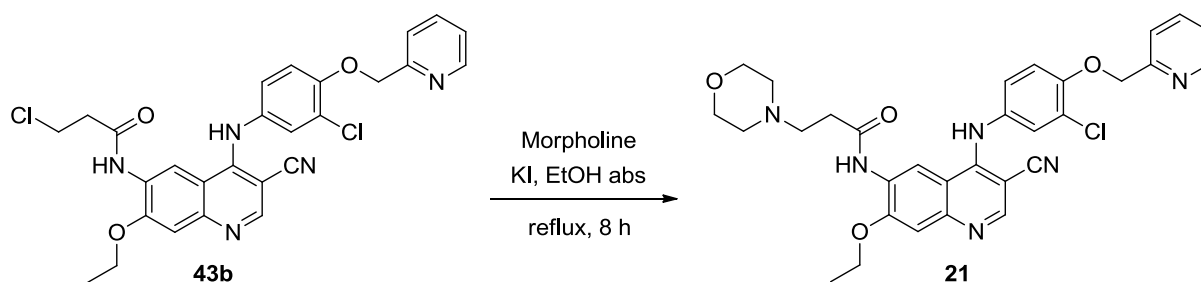
3-Chloropropanamide **43b** was reacted with dimethylamine according to the procedure described for compound **5**. Silica gel chromatography ($CH_2Cl_2/MeOH$, 99:1 to 90:10) gave **19** as a white solid (73%): mp (EtOH) 235-237 °C; 1H NMR (DMSO- d_6 , 300 MHz) δ 2.29 (s, 6H), 2.54-2.61 (m, 4H), 4.31 (q, $J = 7.0$ Hz, 2H), 5.28 (s, 2H), 7.17 (dd, $J = 7.7, 1.7$ Hz, 1H), 7.25 (d, $J = 8.8$ Hz, 1H), 7.38-7.40 (m, 3H), 7.59 (d, $J = 7.9$ Hz, 1H), 7.88 (dt, $J = 7.7, 1.7$ Hz, 1H), 8.47 (s, 1H), 8.60 (d, $J = 4.0$ Hz, 1H), 9.06 (s, 1H), 9.58 (br s, 1H), 10.92 (br s, 1H); MS (APCI) m/z 545.4, 547.3, 502.7, 500.2; Anal. calc for $C_{29}H_{29}ClN_6O_3 \cdot 1/2H_2O$: C, 62.81; H, 5.23; N, 15.41; found: C, 62.81; H, 5.40; N, 15.10.

***N*-(4-(3-Chloro-4-(pyridin-2-ylmethoxy)anilino)-3-cyano-7-ethoxyquinolin-6-yl)-3-(piperidin-1-yl)propanamide (20).**



3-Chloropropanamide **43b** was reacted with piperidine according to the procedure described for compound **5**. Silica gel chromatography (CH₂Cl₂/MeOH, 97:3 to 95:5) gave **20** as a light yellow solid (69%): mp (EtOH) 190-193 °C; ¹H NMR (DMSO-*d*₆, 400 MHz) δ 1.45 (t, *J* = 6.8 Hz, 3H), 1.50 (m, 2H), 1.56 (m, 4H), 2.44 (m, 4H), 2.60 (s, 4H), 4.36 (q, *J* = 7.0 Hz, 2H), 5.28 (s, 2H), 7.18 (d, *J* = 8.2 Hz, 1H), 7.25 (d, *J* = 8.4 Hz, 1H), 7.39 (m, 3H), 7.58 (d, *J* = 7.2 Hz, 1H), 7.88 (t, *J* = 7.3 Hz, 1H), 8.47 (s, 1H), 8.60 (d, *J* = 4.3 Hz, 1H), 8.95 (s, 1H), 9.59 (s, 1H), 10.21 (s, 1H); MS (APCI) *m/z* 585.2, 587.5, 588.5; Anal. calc for C₃₂H₃₃ClN₆O₃·3/2H₂O: C, 62.79; H, 5.93; N, 13.73; found: C, 63.08; H, 6.12; N, 13.35.

***N*-(4-(3-Chloro-4-(pyridin-2-ylmethoxy)anilino)-3-cyano-7-ethoxyquinolin-6-yl)-3-morpholinopropanamide (21).**



3-Chloropropanamide **43b** was reacted with morpholine according to the procedure described for compound **5**. Silica gel chromatography (CH₂Cl₂/MeOH, 99:1 to 97:3) gave **21** as a light yellow solid (74%): mp (EtOH) 224-228 °C; ¹H NMR (CDCl₃, 400 MHz) δ 1.49 (t, *J* = 6.9 Hz, 3H), 2.55 (m, 4H), 2.67 (m, 4H), 3.77 (s, 4H), 4.30 (q, *J* = 6.8 Hz, 2H), 5.19 (s, 2H), 6.72 (s, 2H), 7.61 (d, *J* = 7.8 Hz, 2H), 7.75 (t, *J* = 7.7 Hz, 1H), 8.16 (s, 1H), 8.32 (s, 1H), 8.58 (d, *J* = 4.4 Hz, 1H), 9.19 (s, 1H), 10.08 (s, 1H); MS (APCI) *m/z* 587.3, 589.5; Anal. calc for C₃₁H₃₁ClN₆O₄: C, 63.42; H, 5.32; N, 14.32; found: C, 63.08; H, 6.48; N, 13.92.

References

-
- ¹Yarden, Y.; Sliwkowski, M.X. Untangling the ErbB signaling network. *Nat. Rev. Mol. Cell Biol.*, **2001**, 2(2), 127-137.
- ² Hynes, N.E.; Lane, H.A. ErbB receptors and cancer: the complexity of targeted inhibitors. *Nat. Rev. Cancer*, **2005**, 5(5), 341-354.
- ³ Schlessinger, J. Cell signaling by receptor tyrosine kinases. *Cell.*, **2000**, 103, 211-225.
- ⁴ Olayioye, M.A.; Neve, R.M.; Lane, H.A.; Hynes, N.E. The ErbB signaling network: receptor heterodimerization in development and cancer. *EMBO J.*, **2000**, 19(13), 3159-3167.
- ⁵ Mendelson, J.; Balsega, J. Epidermal growth factor receptor targeting in cancer. *Semin. Oncol.*, **2006**, 33(4), 369-385.
- ⁶ Salomon, D.S.; Brandt, R.; Ciardello, F.; Normanno, N. Epidermal growth factor-related peptides and their receptors in human malignancies. *Crit. Rev. Oncol. Hematol.*, **1995**, 19(3), 183-232.
- ⁷ Teman, S.; Kawaguchi, H.; El-Naggar, A.K.; Jelinek, J.; Tang, H.; Liu, D.D.; Lang, W.; Issa, J.P.; Lee, J.J.; Mao, L. Epidermal growth factor receptor copy number alterations correlate with poor clinical outcome in patients with head and neck squamous cancer. *J. Clin. Oncol.*, **2007**, 25, 2164–2170.
- ⁸ Baselga, J.; Arteaga, C.L. Critical update and emerging trends in epidermal growth factor receptor targeting in cancer. *J. Clin. Oncol.*, **2005**, 23(11), 2445–2459.
- ⁹ Johnson, B.E.; Janne, P.A. Epidermal growth factor receptor mutations in patients with non-small-cell lung cancer. *Cancer Res.*, **2005**, 65, 7525-7529.
- ¹⁰ Kobayashi, S.; Boggon, T.J.; Dayaram, T.; Janne, P.A.; Kocher, O.; Meyerson, M.; Johnson, B.E.; Eck, M.J.; Tenen, D.G.; Halmos, B. EGFR mutation and resistance of non-small-cell lung cancer to gefitinib. *N. Engl. J. Med.*, **2005**, 352, 786–792.
- ¹¹ Chan, S.K.; Gullick, W.J.; Hill, M.E. Mutations of the epidermal growth factor receptor in non-small cell lung cancer – search and destroy. *Eur. J. Cancer*, **2006**, 42, 17-23.

-
- ¹² Yun, C.H.; Boggon, T.J.; Li, Y.; Woo, M.S.; Greulich, H.; Meyerson, M.; Eck, M.J. Structures of lung cancer-derived mutants and inhibitor complexes: mechanism of activation and insights into differential inhibitor sensitivity. *Cancer Cell.*, **2007**, *11*, 217-227.
- ¹³ Barker, A.J.; Gibson, K.H.; Grundy, W.; Godfrey, A.A; Barlow, J.J.; Healy, M.P.; Woodburn, J.R.; Ashton, S.E.; Curry, B.J.; Sarlett, L.; Henthorn, L.; Richards, L.; Studies leading to the identification of ZD1839 (Iressa): an orally active, selective epidermal growth factor receptor tyrosine kinase inhibitor targeted to the treatment of cancer. *Bioorg. Med. Chem. Lett.*, **2001**, *11*, 1911–1914
- ¹⁴ Moyer, J.D.; Barbacci, E.G.; Iwata, K.K.; Arnold, L.; Boman, B.; Cunningham, A.; Di Orio, C.; Doty, J.; Morin, M. J.; Moyer, M. P.; Neveu, M.; Pollack, V.A.; Pustilnick, L.R.; Reynolds, M.M.; Sloan, D.; Theleman, A.; Miller, P.; Induction of apoptosis and cell cycle arrest by CP-358,774, an inhibitor of epidermal growth factor receptor tyrosine kinase. *Cancer Res.*, **1997**, *57*, 4838–4848.
- ¹⁵ Lynch, T.J.; Bell, D.W.; Sordella, R.; Gurubhagavatula, S.; Okimoto, R.A.; Brannigan, B.W.; Harris, P.L.; Haserlat, S.M.; Supko, J G.; Haluska, F.G.; Louis, D.N.; Christiani, D.C.; Settleman, J.; Haber, D.A. Activating mutations in the epidermal growth factor receptor underlying responsiveness of non-small-cell lung cancer to gefitinib. *N. Engl. J. Med.*, **2004**, *350*, 2129–2139.
- ¹⁶ Pao, W.; Miller, V.A.; Politi, K.A.; Riely, G.J.; Somwar, R.; Zakowski, M.F.; Heelan, R.T.; Kris, M.G.; Varmus, H.E. *KRAS* mutations and primary resistance of lung adenocarcinomas to gefitinib or erlotinib. *PLoS Med*, **2005**, *2*, e17.
- ¹⁷ Engelman, J.A.; Janne, P.A. Mechanisms of acquired resistance to epidermal growth factor receptor tyrosine kinase inhibitors in non-small cell lung cancer. *Clin. Cancer Res.*, **2008**, *14*, 2895–2899.
- ¹⁸ Michalcyk, A.; Kluter, S.; Rode, H. B.; Simard, J. R.; Grutter, C.; Rabiller, M; Rauh D. Structural insights into how irreversible inhibitors can overcome drug resistance in EGFR. *Bioorg. Med. Chem.* **2008**, *16*, 3482-3488.
- ¹⁹ Kwak, E.L.; Sordella, R.; Bell, D.W.; Godin-Heymann, N.; Okimoto, R.A.; Brannigan, B.W.; Harria, P.L.; Driscoli, D.R.; Fidias, P.; Lynch, T.J.; Rabindran, S.K.; McGinnis, J.P.; Sharma, S.V.; Isselbacher, K.J.; Settleman, J.; Haber, D.A. Irreversible inhibitors of the EGF

receptor may circumvent acquired resistance to gefitinib. *Proc. Natl. Acad. Sci. U.S.A.*, **2005**, *102*, 7665–7670.

²⁰ Fry, D.W.; Bridges, A.J.; Denny, W.A.; Doherty, A.; Greis, K.D.; Hicks, J.L.; Hook, K.E.; Keller, P.R.; Leopold, W.R.; Loo, J.A.; McNamara, D.J.; Nelson, J.M.; Sherwood, V.; Smaill, J.B.; Trumpp-Kallmeyer, S.; Dobrusin, E.M. Specific, irreversible inactivation of the epidermal growth factor receptor and erbB2, by a new class of tyrosine kinase inhibitor. *Proc. Natl. Acad. Sci. U.S.A.*, **1998**, *95*, 12022–12027.

²¹ Carmi, C.; Mor, M.; Petronini, P.; Alfieri, R.R. Clinical perspectives for irreversible tyrosine kinase inhibitors in cancer. *Biochemical Pharmacology*. **2012**. *84*, 1388-1399.

²² Tsou, H.-R.; Mamuya, N.; Johnson, B. D.; Reich, M. F.; Gruber, B. C.; Ye, F.; Nilakantan, R.; Shen, R.; Discafani, C.; DeBlanc, R.; Davis, R.; Koehn, F. E.; Greenberger, L. M.; Wang, Y.-F.; Wissner, A. 6-Substituted-4-(3-bromophenylamino)quinazolines as putative irreversible inhibitors of the epidermal growth factor receptor (EGFR) and human epidermal growth factor receptor (HER-2) tyrosine kinases with enhanced antitumor activity. *J. Med. Chem.* **2001**, *44*, 2719–2734.

²³ Carmi, C.; Lodola, A.; Rivara, S.; Vacondio, F.; Cavazzoni, A.; Alfieri, R. R.; Ardizzoni, A.; Petronini, P. G.; Mor, M. Epidermal growth factor receptor irreversible inhibitors: Chemical exploration of the cysteine-trap portion. *Mini Rev. Med. Chem.* **2011**, *11*, 1019–1030.

²⁴ Blair, J.A.; Rauh, D.; Kung, C.; Yun, C.-H.; Fan, Q.-W.; Rode, H.; Zhang, C.; Eck, M.J.; Weiss, W.A.; Shokat, K. M. Structure-guided development of affinity probes for tyrosine kinases using chemical genetics. *Nature Chem. Biol.*, **2007**, *3*(4), 229-238.

²⁵ Stamos, J.; Sliwkowski, M.X.; Eigenbrot, C. Structure of the epidermal growth factor receptor kinase domain alone and in complex with a 4-anilinoquinazoline inhibitor. *J. Biol. Chem.*, **2002**, *277*, 46265–46272.

²⁶ Wissner, A.; Tsou, H.-R.; Johnson, B.D.; Hamann, P.R.; Zhang, N. Substituted quinazoline derivatives and their use as tyrosine kinase inhibitors. World Pat. Appl. 9909016, February 1999.

²⁷ Discafani, C.M.; Carroll, M.L.; Floyd Jr., M.B.; Hollander, I.J.; Husain, Z.; Johnson, B.D.; Kitchen, D.; May, M.K.; Malo, M.S.; Minnick Jr., A.A.; Nilakantan, R.; Shen, R.; Wang, Y.-F.; Wissner, A.; Greenberger, L.M. Irreversible inhibition of epidermal growth factor receptor

tyrosine kinase with in vivo activity by *N*-[4-[(3-bromophenyl)amino]-6-quinazoliny]-2-butynamide (CL-387,785). *Biochem. Pharmacol.*, **1999**, *57*(8), 917-925.

²⁸ Singh, J.; Petter, R.C.; Kluge, A.F. Targeted covalent drugs of the kinase family. *Curr. Opinion Chem. Biol.*, **2010**, *14*, 475-480.

²⁹ Jänne, P. A.; von Pawel, J.; Cohen, R. B.; Crino, L.; Butts, C. A.; Olson, S. S.; Eiseman, I. A.; Chiappori, A. A.; Yeap, B. Y.; Lenehan, P. F.; Dasse, K.; Sheeran, M.; Bonomi, P. D. Multicenter, randomized, phase II trial of CI-1033, an irreversible pan-ERBB inhibitor, for previously treated advanced non small-cell lung cancer. *J. Clin. Oncol.* **2007**, *25*, 3936–3944.

³⁰ Besse, B.; Eaton, K. D.; Soria, J. C.; Lynch, T. J.; Miller, V.; Wong, K. K.; Powell, C.; Quinn, S.; Zacharchuk, C.; Sequist, L. V. Neratinib (HKI-272), an irreversible pan-ErbB receptor tyrosine kinase inhibitor: preliminary results of a phase 2 trial in patients with advanced non-small cell lung cancer. *Eur. J. Cancer* **2008**, *Suppl. 6*, 64.

³¹ Maresso, A. W.; Wu, R.; Kern, J. W.; Zhang, R.; Janik, D.; Misiakas, D. M.; Duban, M.-E.; Joachimiak, A.; Schneewind, O. Activation of inhibitors of sortase triggers irreversible modification of the active site. *J. Biol. Chem.* **2007**, *282*, 23129–23139.

³² Wenzel, N. I.; Chavain, N.; Wang, Y.; Friebolin, W.; Maes, L.; Pradines, B.; Lanzer, M.; Yardley, V.; Brun, R.; Herold-Mende, C.; Biot, C.; Tóth, K.; Davioud-Charvet, E. Antimalarial versus cytotoxic properties of dual drugs derived from 4-aminoquinolines and Mannich bases: Interaction with DNA. *J. Med. Chem.* **2010**, *53*, 3214–3226.

³³ Hwang, J. Y.; Arnold, L. A.; Zhu, F.; Kosinski, A.; Mangano, T. J.; Setola, V.; Roth, B. L.; Guy, R. K. Improvement of pharmacological properties of irreversible thyroid receptor coactivator binding inhibitors. *J. Med. Chem.* **2009**, *52*, 3892–3901.

³⁴ Carmi, C.; Galvani, E.; Vacondio, F.; Rivara, S.; Lodola, A.; Russo, S.; Aiello, S.; Bordi, F.; Costantino, C.; Cavazzoni, A.; Alfieri, R. R.; Ardizzoni, A.; Petronini, P.; Mor, M. Irreversible inhibition of epidermal growth factor receptor activity by 3-aminopropanamides. *J Med Chem.* **2012**; *55*, 2251-64.

³⁵ Carmi, C.; Cavazzoni, A.; Vezzosi, S.; Bordi, F.; Vacondio, F.; Silva, C.; Rivara, S.; Lodola, A.; Alfieri, R. R.; La Monica, S.; Galetti, M.; Ardizzoni, A.; Petronini, P. G.; Mor, M. Novel irreversible epidermal growth factor receptor inhibitors by chemical modulation of the cysteine-trap portion. *J. Med. Chem.* **2010**, *53*, 2038–2050.

³⁶ Fry, D. W.; Bridges, A. J.; Denny, W. A.; Doherty, A.; Greis, K. D.; Hicks, J. L.; Hook, K. E.; Keller, P. R.; Leopold, W. R.; Loo, J. A.; McNamara, D. J.; Nelson, J. M.; Sherwood, V.; Smail, J. B.; Trumpp-Kallmeyer, S.; Dobrusin, E. M. Specific, irreversible inactivation of the epidermal growth factor receptor and erbB2, by a new class of tyrosine kinase inhibitor. *Proc. Natl. Acad. Sci. U.S.A.* **1998**, *95*, 12022–12027.

³⁷ Smail, J. B.; Palmer, B. D.; Rewcastle, G. W.; Denny, V. A.; McNamara, D. J.; Dobrusin, E. M.; Bridges, A. J.; Zhou, H.; Showalter, H. D. H.; Winters, R. T.; Leopold, V. R.; Fry, D. V.; Nelson, J. M.; Slintak, V.; Elliot, V. L.; Roberts, B. J.; Vincent, P. W.; Patmore, S. J. Tyrosine kinase inhibitors. 15. 4-(Phenylamino)quinazoline and 4-(phenylamino)pyrido[d]pyrimidine acrylamides as irreversible inhibitors of the ATP binding site of the Epidermal Growth Factor Receptor. *J. Med. Chem.* **1999**, *42*, 1803–1815.

³⁸ Böhme, A.; Thaens, D.; Paschke, A.; Schüürmann, G. Kinetic glutathione chemoassay to quantify thiol reactivity of organic electrophiles: application to alpha,beta-unsaturated ketones, acrylates, and propiolates. *Chem Res Toxicol.* **2009**, *22*, 742–750.

³⁹ Oballa, R. M; Truchon, J. F; Bayly, C. I.; Chauret, N.; Day, S.; Crane, S.; Berthelette, C. A generally applicable method for assessing the electrophilicity and reactivity of diverse nitrile-containing compounds. *Bioorg. Med. Chem. Lett.* **2007**, *17*, 998–1002.

⁴⁰ Külter, S.; Simard, J. R.; Rode, H. B.; Grütter, C.; Pawar, V.; Raaijmakers, H. C. A.; Barf, T. A.; Rabiller, M.; van Otterlo, W. A. L.; Rauh, D. characterization of irreversible kinase inhibitors by direct detecting covalent bond formation: A tool for dissecting kinase drug resistance. *ChemBioChem* **2010**, *11*, 2557–2566.

⁴¹ Sos, M. L.; Rode, H. B.; Heynck, S.; Peifer, M.; Fischer, F.; Klüter, S.; Pawar, V. G.; Reuter, C.; Heuckmann, J. M.; Weiss, J.; Ruddigkeit, L.; Rabiller, M.; Koker, M.; Simard, J. R.; Getlik, M.; Yuza, Y.; Chen, T. H.; Greulich, H.; Thomas, R. K.; Rauh, D. Chemogenomic profiling provides insights into the limited activity of irreversible EGFR inhibitors in tumor cells expressing the T790M EGFR resistance mutation. *Cancer Res.* **2010**, *70*, 868–874.

⁴² Prendergast, F. G.; Meyer, M.; Carlson, G. L.; Iida, S.; Potter, D. Synthesis, spectral properties, and use of 6-acryloyl-2-dimethylaminonaphthalene (Acrylodan). A thiol-selective, polarity-sensitive fluorescent probe. *J. Biol. Chem.* **1983**, *258*, 7541–7544.

⁴³ Weber, G.; Farris, F. J. Synthesis and spectral properties of a hydrophobic fluorescent probe: 6-propionyl-2-(dimethylamino)naphthalene. *Biochemistry* **1979**, *18*, 3075–3078.

- ⁴⁴ De Silva, A. P.; Gunaratne, H. Q. N.; Gunnlaugsson, T.; Huxley, A. J. M.; McCoy, C. P.; Rademacher, J. T.; Rice, T. E. Signaling recognition events with fluorescent sensors and switches. *Chem. Rev.* **1997**, *97*, 1515–1566.
- ⁴⁵ De Silva, A. P.; Gunaratne, H. Q. N.; Gunnlaugsson, T. Fluorescent PET (Photoinducer Electron Transfer) reagents for thiols. *Tetrahedron Lett.* **1998**, *39*, 5077–5080.
- ⁴⁶ Rauh, D.; Simard, J. R.; Getlik, M. Fluorescently or spin-labeled kinases for rapid screening and identification of novel kinase inhibitor scaffolds, and drug discovery uses. PCT Int. Appl. WO2010009886, **2010**.
- ⁴⁷ Oballa, R. M.; Truchon, J. F.; Bayly, C. I.; Chauret, N.; Day, S.; Crane, S.; Berthelette, C. A generally applicable method for assessing the electrophilicity and reactivity of diverse nitrile-containing compounds. *Bioorg. Med. Chem. Lett.* **2007**, *17*, 998–1002.
- ⁴⁸ Arend, M.; Westermann, B.; Risch, N. Modern variants of the Mannich reaction. *Angew. Chem. Int. Ed.* **1998**, *37*, 1044–1070.
- ⁴⁹ Bridges, A. J.; Zhou, H.; Cody, D. R.; Rewcastle, G. W. McMichael, A.; Showalter, H. D. H.; Fry, D. W.; Kraker, A. J.; Denny, W. A. Tyrosine kinase inhibitors. 8. An unusually steep structure–activity relationship for analogues of 4-(3-bromoanilino)-6,7-dimethoxyquinazoline (PD 153035), a potent inhibitor of the epidermal growth factor receptor. *J. Med. Chem.* **1996**, *39*, 267–276.
- ⁵⁰ Simplicio, A. L.; Clancy, J. M.; Gilmer, J. F. Beta-aminoketones as prodrugs with pH-controlled activation. *Int. J. Pharm.* **2007**, *336*, 208–214.
- ⁵¹ Rewcastle, G. W.; Denny, W. A.; Bridges, A. J.; Zhou, H.; Cody, D. R.; McMichael, A.; Fry, D. W. Tyrosine kinase inhibitors: synthesis and structure-activity relationships for 4-[(phenylmethyl)amino]- and 4-[(phenylamino)quinazolines as potent adenosine 5'-triphosphate binding site inhibitors of the tyrosine kinase domain of the epidermal growth factor receptor. *J. Med. Chem.* **1995**, *38*, 3482–3487.
- ⁵² Roth, G. A.; Tai, J. J. A new synthesis of aryl substituted quinazolin-4(1*H*)-ones. *J. Heterocycl. Chem.* **1996**, *33*, 2051–2053.
- ⁵³ Domarkas, J.; Dudouit, F.; Williams, C.; Qiyu, Q.; Banerjee, R.; Brahimi, F.; Jean-Claude, B. J. The combi-targeting concept: Synthesis of stable nitrosoureas designed to inhibit the epidermal growth factor receptor (EGFR). *J. Med. Chem.* **2006**, *49*, 3544–3552.

-
- ⁵⁴ Tang, P. C.; Li, X.; Wang, B.; Wang, J.; Chen, L. 6-Amino quinazoline or 3-cyano quinoline derivatives, preparation methods and pharmaceutical uses thereof. PCT Int. Appl. WO2011/029265, **2011**.
- ⁵⁵ Wissner, A.; Fraser, H. L.; Ingalls, C. L.; Dushin, R. G.; Floyd, M. B.; Cheung, K.; Nittoli, T.; Ravi, M. R.; Tan, X.; Loganzo, F. Dual irreversible kinase inhibitors: Quinazoline-based inhibitors incorporating two independent reactive centers with each targeting different cysteine residues in the kinase domains of EGFR and VEGFR-2. *Bioorg. Med. Chem.* **2007**, *15*, 3635–3648.
- ⁵⁶ Tsou, H. R.; Overbeek-Klumpers, E. G.; Hallett, W. A.; Reich, M. F.; Floyd, M. B.; Johnson, B. D.; Michalak, R. S.; Nilakantan, R.; Discifani, C.; Golas, J.; Rabindran, S. K.; Shen, R.; Shi, X.; Wang, Y.-F.; Upešlaciš, J.; Wissner, A. Optimization of 6,7-disubstituted-4-(arylamino)quinoline-3-carbonitriles as orally active, irreversible inhibitors of human epidermal growth factor receptor-2 kinase activity. *J. Med. Chem.* **2005**, *48*, 1107–1131.
- ⁵⁷ Wissner, A.; Overbeek, E.; Reich, M. F.; Floyd, M. B.; Johnson, B. D.; Mamuya, N.; Rosfjord, E. C.; Discifani, C.; Davis, R.; Shi, X.; Rabindran, S. K.; Gruber, B. C.; Ye, F.; Hallett, W. A.; Nilakantan, R.; Shen, R.; Wang, Y.-F.; Greenberger, L. M.; Tsou, H.-R. Synthesis and structure-activity relationships of 6,7-disubstituted 4-anilinoquinoline-3-carbonitriles. The design of an orally active, irreversible inhibitor of the tyrosine kinase activity of the epidermal growth factor receptor (EGFR) and the human epidermal growth factor receptor-2 (HER-2). *J. Med. Chem.* **2003**, *46*, 49–63.
- ⁵⁸ Chew, W.; Cheal, G. K.; Lunetta, J. F. Methods of synthesizing substituted 3-cyanoquinolines and intermediates thereof. PCT Int. Appl. WO2006/127207, **2006**.
- ⁵⁹ Barlaam, B. C.; Ducray, R.; Kettle, J. G. Pyrazolopyrimidine compounds as antitumor agents. PCT Int. Appl. WO2006/064196, **2006**.
- ⁶⁰ Gilday, J. P.; David, M. Process for the preparation of 4-(3'-chloro-4'-fluoroanilino)-7-methoxy-6-(3-morpholinopropoxy)quinazoline. PCT Int. Appl. WO2004/024703, **2004**.
- ⁶¹ Rewcastle, G. W.; Denny, W. A.; Bridges, A. J.; Zhou, H.; Cody, D. R.; McMichael, A.; Fry, D. W. Tyrosine kinase inhibitors: synthesis and structure-activity relationships for 4-[(phenylmethyl)amino]- and 4-[(phenylamino)quinazolines as potent adenosine 5'-triphosphate binding site inhibitors of the tyrosine kinase domain of the epidermal growth factor receptor. *J. Med. Chem.* **1995**, *38*, 3482–3487.

EPH RECEPTORS AND EPHRINS

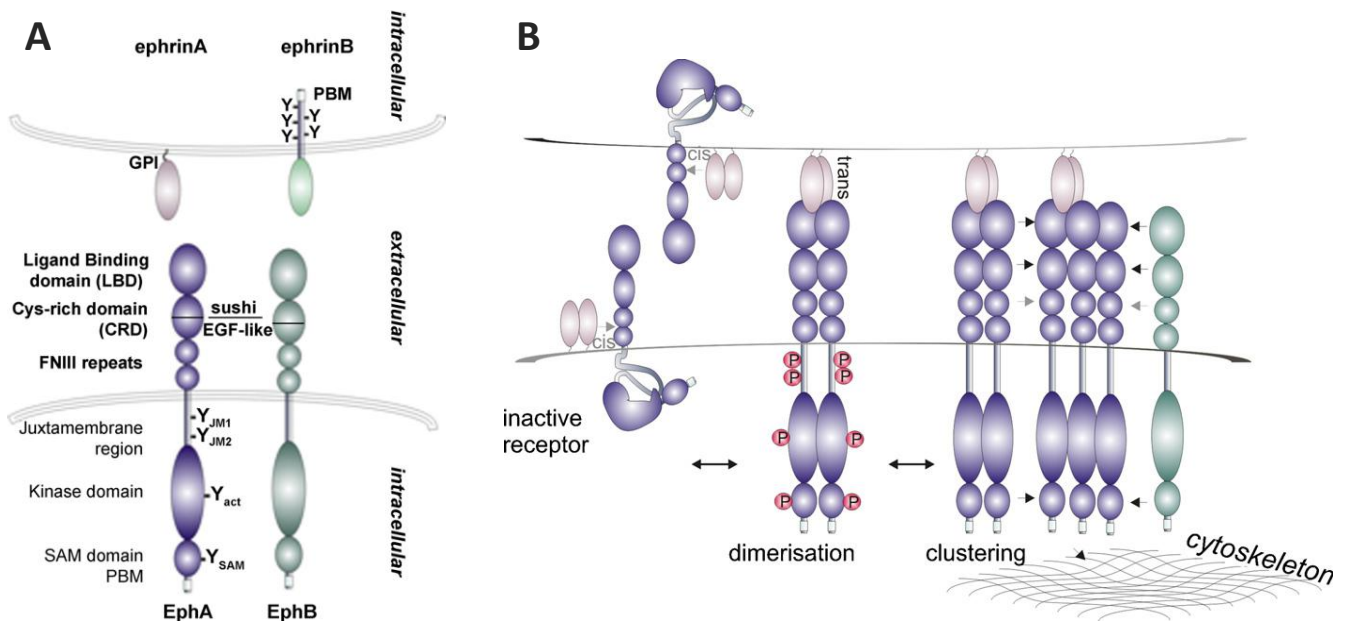
Introduction

The erythropoietin-producing hepatocellular carcinoma (Eph) receptors are the largest family of receptor tyrosine kinases. To date, sixteen members have been identified and classified as EphA (EphA1-10) or EphB (EphB1-6) receptors, on the basis of sequence homologies and binding affinity for their ligands, the ephrins (Eph receptor-interacting proteins). The ephrin ligands are divided into two subclasses, the A subclass (ephrin A1-6), whose members are tethered to the cell membrane by a glycosylphosphatidylinositol (GPI) anchor, and the B subclass (ephrin B1-3), the members of which are transmembrane proteins endowed with a short cytoplasmic region. The receptor-ligand interactions are promiscuous within each class, and some Eph receptors can also bind ephrins of the other class.¹

Eph A and B receptors have a modular structure, consisting of an extracellular globular N-terminal ephrin-binding domain, that contains several ligand-binding interfaces, followed by a cysteine-rich region and two fibronectin type-III repeats, which might be involved in receptor–receptor dimerization interactions. The extracellular motif is connected via a single transmembrane spanning domain to the cytoplasmic region. Intracellularly, the juxtamembrane domain contains two tyrosines that undergo autophosphorylation and is followed by a conserved tyrosine kinase domain. The C-terminal end of Eph receptors serves as a docking site for interacting proteins that may mediate downstream signal transduction processes and includes a sterile α motif (SAM) and a PDZ-binding motif (Figure 1A).^{2,3}

Figure 1. A. Eph and ephrins domain structures (The CRD incorporates tightly packed sushi and EGF-like modules). **B.** Model for Eph receptor clustering and activation. Ephrin binding to one receptor initiates dimerization into an Eph/ephrin hetero-tetramer. Further clustering is facilitated by receptor–receptor interactions between multiple domains of adjacent Ephs, including co-clustering of A and B type

Ephs. Interactions with cytoplasmic proteins and the cytoskeleton allow to transmit biological responses. [Image from Ref 4].



Since both Eph receptors and ephrins are membran-bound proteins, their interaction requires cell-cell contact. The process of receptor activation by ephrins is unique compared with other RTK families and needs a multimeric aggregation of receptors: the interaction of the ligand with its receptor causes the co-clustering of both signaling partners on opposing cells (Figure 1B).^{4,5} The ensuing signals propagate bidirectionally into both the Eph receptor-expressing cells (“forward” signal) and the ephrin-expressing cells (“reverse” signal).¹ Eph receptor forward signaling depends on the tyrosine kinase domain, which mediates autophosphorylation as well as phosphorylation of other proteins, and on the associations of the receptor with various effector proteins.⁶ Ephrin-B “reverse” signaling also depends in part on tyrosine phosphorylation of the ephrin cytoplasmic region (mediated by Src family kinases and some receptor tyrosine kinases) and on associated proteins. Ephrin-A ligands may also be capable of serving as bi-directional signaling molecules, presumably coupling with other transmembrane proteins.⁷

Eph receptors and ephrins along form an important cell-cell communication system, that regulates both cell adhesion and repulsion, by modifying cell morphology, and drives processes as cell migration, proliferation and differenzation. As a consequence, the Eph–ephrin signaling system is responsible for modulation of

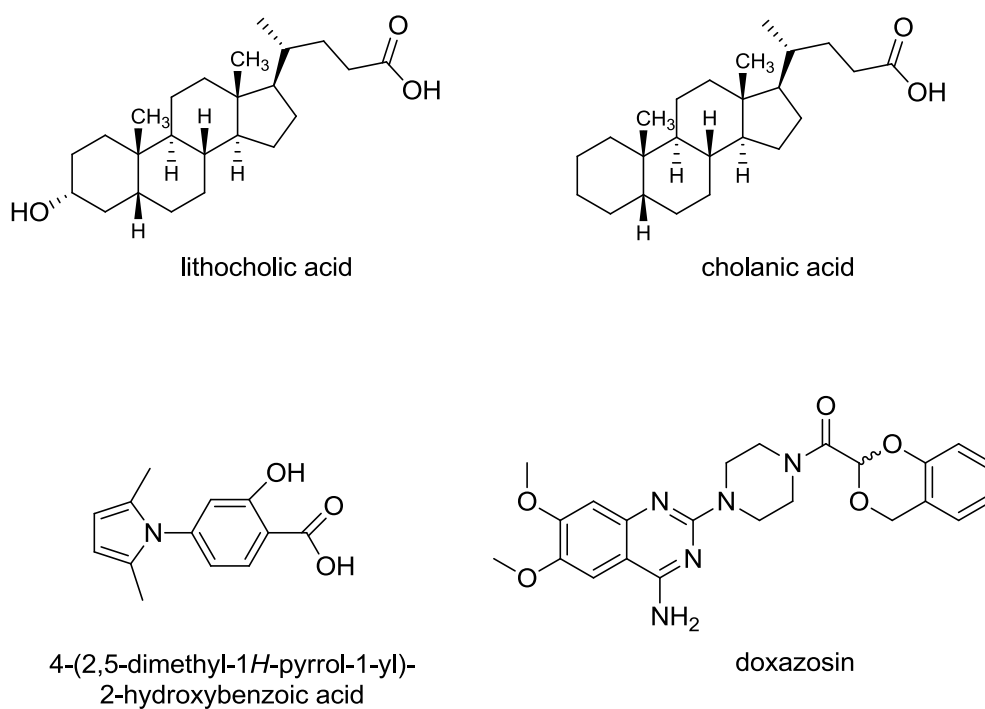
several biological activities involving cellular contact, both during embryonic development and in adult tissues. In fact, these proteins modulate cell movements in morphogenetic processes such as gastrulation, segmentation, angiogenesis, axonal pathfinding, and neural crest cell migration.⁸ Moreover, in the adult, they are involved in the maintenance of cellular architecture in various epithelia,⁹ play key roles in neural plasticity,¹⁰ regeneration of the adult nervous system and remodeling of blood vessels.^{11,12}

The expression of Eph receptors and ephrins is frequently altered in tumors. Many ephrins and Eph receptors have been shown to be up-regulated in several human carcinomas¹³ such as breast,¹⁴ lung,¹⁵ kidney,¹⁶ esophagus,¹⁷ colon, liver, prostate, melanoma, and are often associated with tumor progression and metastasis. Moreover, besides being expressed in cancer cells, Eph receptors and ephrins are also present in tumor vasculature, where they promote tumor angiogenesis and support metastatic dissemination, by enabling aberrant communication between vascular and cancer cells.¹² In particular, the pair of EphB4/ephrinB2¹⁸ and EphA2/ephrinA1¹⁹ seem to be mainly involved in tumor angiogenesis. Despite of these findings, the roles played by Eph receptors in tumor progression remains unclear, due to the evidence that Eph receptors and ephrin ligands can both promote or suppress tumorigenicity in different contexts.²⁰ In this light, the possibility to have available pharmacological tools targeting Eph receptors could allow to elucidate the physiopathological role of the Eph-ephrin system; furthermore, from a therapeutic perspective, the inhibition of the Eph/ephrin-signaling could be a means of preventing tumor angiogenesis. Indeed, inhibition of EphA2 and EphB4 have been shown to effectively block angiogenic processes in vivo, in many cases.²¹

Two main strategies can be used to inhibit Eph receptor dependent signals:^{3,20,22} *i*) blockage of Eph receptor forward signaling by a direct action on the ATP-binding pocket in the receptor kinase domain and *ii*) blockage of both Eph receptor forward and ephrin reverse signals by disruption of the Eph receptor–ephrin interaction. While the first approach is based on the use of small molecules mimicking the structure of ATP, the second one, at the moment, is essentially based on the use of recombinant proteins, including antibodies, soluble forms of Eph receptors and ephrins, and peptides.²³ Only recently a few classes of small molecules able to interfere with the binding of ephrins to Eph receptors have been identified (Figure 2). These include: *i*)

bile acid derivatives, such as lithocholic acid (LCA)^{24,25} and cholic acid,²⁶ two competitive Eph receptor antagonists having a moderate preference for the EphA receptor sub-family; *ii*) salicylic-acid derivatives^{27,28} [exemplified by 4-(2,5-dimethyl-1H-pyrrol-1-yl)-2-hydroxybenzoic acid], which inhibit EphA2 and EphA4 receptor subtypes; *iii*) doxazosin,²⁹ the marketed α 1-adrenoreceptor antagonist that has been recently shown to bind and activate EphA2 and EphA4 receptor subtypes; and *iv*) some polyphenols and polyphenol metabolites.^{30,31,32}

Figure 2. Known modulators of the Eph receptor family.

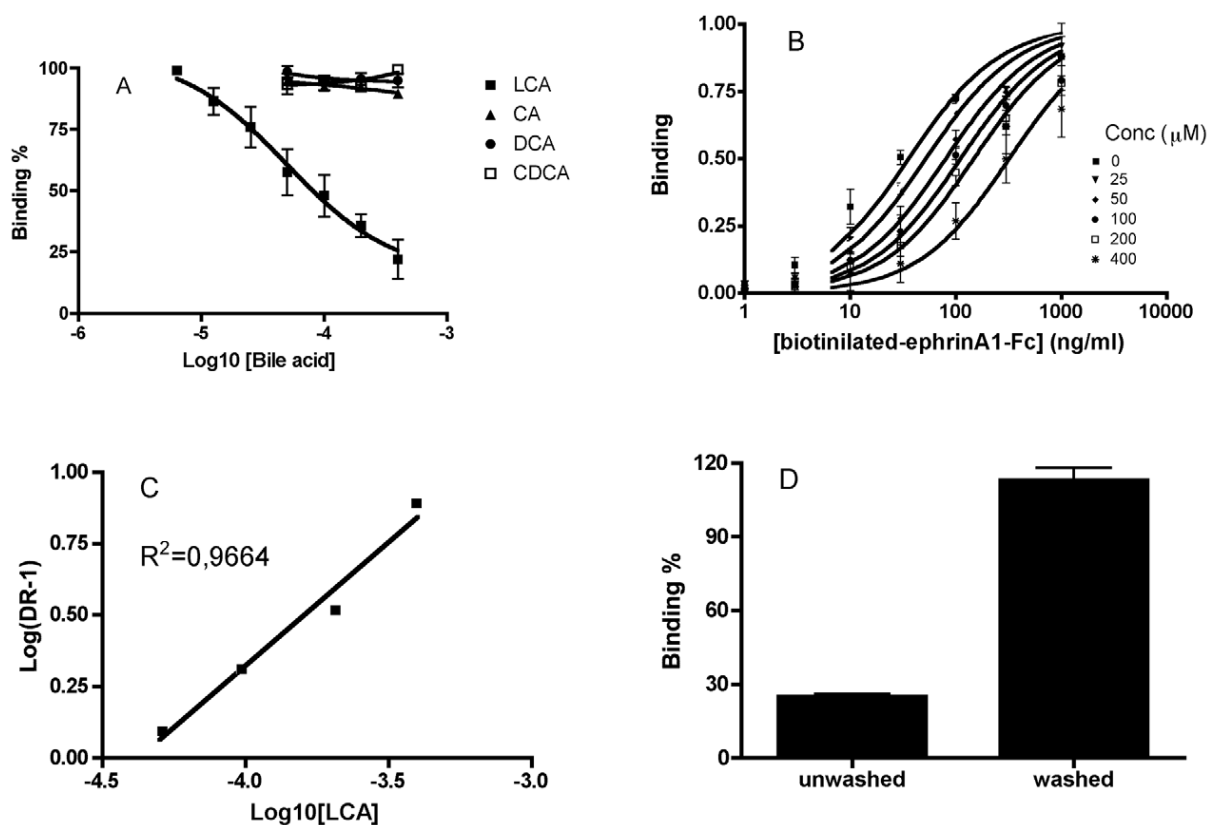


Lithocholic acid is a competitive and reversible Eph receptor ligand

Among the above-mentioned classes of Eph-ephrin system modulators, the present work focus the attention on LCA, which possess a (5 β)-cholan-24-oic acid scaffold able to competitively displace ephrinA1 from the ligand binding domain of EphA2.

LCA was identified as an Eph receptor ligand performing an ELISA binding assay and screening an “in house” chemical library of naturally occurring compounds. Only LCA, among the compounds of the chemical collection, resulted to significantly reduce EphA2-ephrinA1 binding. The experiment was repeated testing LCA along with bile acid analogues: cholic (CA), deoxycholic (DCA) and chenodeoxycholic (CDCA), and only LCA demonstrated to dose-dependently displace binding of ephrinA1 ligand from immobilized EphA2 receptor, with an IC₅₀ of 57 μ M (Figure 3A). To evaluate the nature of the antagonism, saturation curves of EphA2-ephrinA1 binding in presence of different and progressively growing concentrations of LCA (Figure 3B) were plotted. A Schild plot revealed a competitive binding and allowed to calculate the inhibition constant (K_i= 49 μ M) (Figure 3C). Finally, the displacement experiment was repeated with and without the washing of the immobilized EphA2 receptor before adding ephrinA1 ligand and the displacement was detected only where the washing was not performed, suggesting the reversibility of the LCA binding to EphA2-ephrinA1 system (Figure 3D). LCA was also tested towards all the EphA and EphB receptors and it showed to be a promiscuous ligand of all the Eph family members. So, all these data proved the competitive and reversible nature of LCA as Eph-ephrin binding inhibitor.²⁵

Figure 3. Lithocholic acid competitively inhibited EphA2-ephrinA1 binding. **A.** Lithocholic acid dose-dependently displaced binding of ephrin-A1-Fc ectodomain from immobilized EphA2-Fc ectodomain. **B.** Binding of ephrin-A1-Fc ectodomain to immobilized EphA2-Fc ectodomain in the presence of different concentrations of lithocholic acid. **C.** The dissociation constants (K_d) from the previous plot were used to calculate Log (Dose-ratio - 1) and to graph the Schild plot. pK_i of lithocholic acid was estimated by the intersection of the interpolated line with the X-axis. The slope of the interpolated line can be related to the nature of the binding. A slope between 0.8 and 1.2 is related to a competitive binding whereas higher numbers are related to nonspecific interactions. **D.** EphA2-ephrinA1 binding in the presence of 200 μ M LCA with or without washing three times with PBS. [Image from Ref 25].



96 well ELISA high binding plates were incubated O/N with EphA2-Fc and the following day washed and blocked with PBS +0.5% BSA for 1 hour at 37uC. Compounds were added in the wells at proper concentrations 1 hour before the addition of biotinylated ephrinA1-Fc. After 4 hours wells were washed and incubated with a streptavidin-HRP solution for 20 minutes at room temperature. Wells were washed again and incubated with tetra-methylbenzidine. The reaction was stopped with 3N HCl and the absorbance was measured at 450 nm.

The recent resolution of the crystal structure of the ligand-binding domain of the EphA2 receptor in complex with the ephrin-A1 ligand³³ allowed to investigate the putative binding mode of lithocholic acid to EphA2 by molecular docking.

As reported in literature,³³ the ligand-receptor interaction pivots on the G-H loop of ephrin-A1, which inserts itself into a hydrophobic channel on the surface of EphA2. The EphA2/ephrin-A1 interface contains also a second, adjacent, mostly polar docking site, that involves a network of hydrogen bonds and salt bridges; among them, the salt bridge between EphA2 Arg 103 and ephrinA1 Glu 119 seems to be fundamental to strengthen the Eph-ephrin interaction. The EphA2/ephrinA1 binding mode could be described as a “lock, key and latch”-type binding (Figure 4).

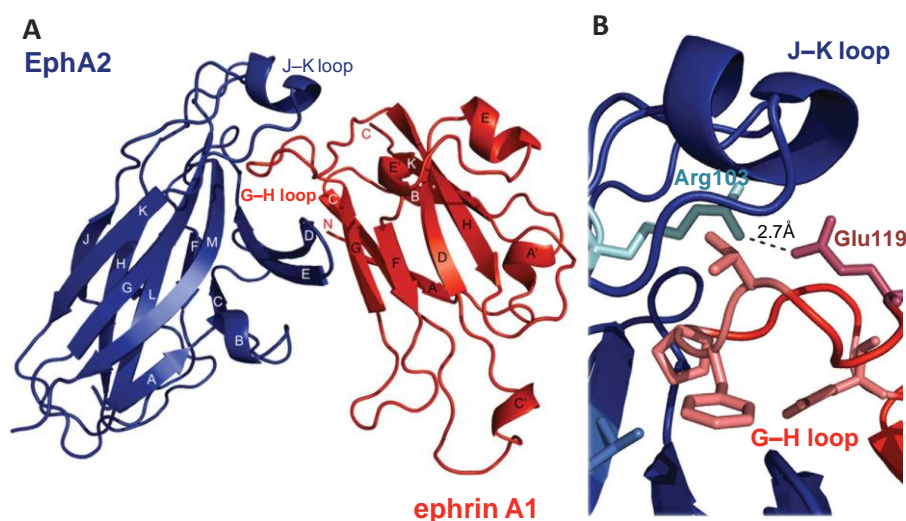


Figure 4. Structure of the EphA2/ephrin-A1 complex. **A.** Structure of the complex of EphA2 (blue) and ephrin-A1 (red). **B.** Stereoview of the ephrin-A1 G–H loop (red) buried in the EphA2 channel (blue). [Image from Ref 33].

Figure 5 shows the solution giving best interaction energy, obtained by docking lithocholic acid within the high affinity ephrin-binding pocket of the EphA2 receptor. The compound occupies the same space as the ephrin-A1 G–H loop, inserting its cyclopenta[*a*]perhydrophenanthrene scaffold into the hydrophobic Eph receptor cavity. The pentanoic acid fragment, emerging from position 17 of the lithocholic acid core, forms a salt bridge with Arg103, mimicking the interaction of Glu119 from ephrin-A1. Finally, 3-hydroxyl group of lithocholic acid weakly interacts with Arg159 of EphA2, which is usually engaged in a hydrogen bond with Asp86 of ephrin-A1.²⁶

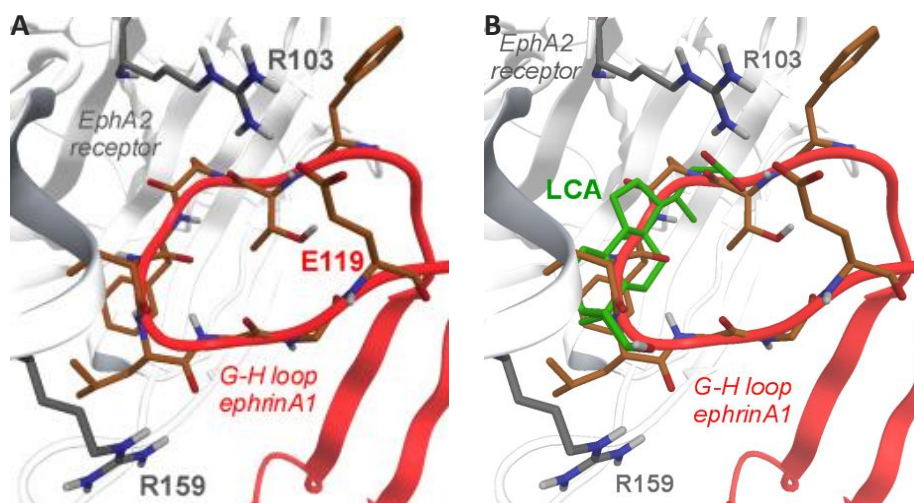


Figure 5. **A.** EphA2 ligand binding domain (white ribbons with gray side chain carbon atoms) in complex with ephrinA1 (red ribbons with orange side chain carbon

atoms). The crucial salt bridge between Arg103 (EphA2) and Glu 119 (ephrinA1) is shown. **B.** Docking of lithocholic acid (LCA, green carbon atoms) in the high-affinity ephrin binding pocket of the EphA2 receptor. The G–H loop of ephrinA1 is also displayed (red ribbons). [Image from Ref 26].

In order to confirm this putative binding mode and verify whether the observed inhibition of the EphA2-ephrinA1 binding mediated by LCA is effectively due to a direct interaction of this compound with the EphA2 receptor and not to a possible binding with the ephrinA1 protein, a surface plasmon resonance (SPR)³⁴ analysis was performed. The dissolved compound was injected over immobilized EphA2–Fc on an optical biosensor surface, and binding was determined based on the change in mass at the sensor surface.³⁵ The change in mass depends linearly on the number of molecules bound. After injection, running buffer was flowed over the surface and dissociation of LCA from the surface was observed. This allowed to measure association and dissociation rate constants (k_{on} , k_{off}) and to obtain the dissociation equilibrium constant (K_D). The SPR sensorgram reported in Figure 6 show that LCA bind the immobilized EphA2 receptor in a concentration-dependent manner. The binding resulted saturable and fully reversible, as the protein-compound complex readily dissociated, restoring the baseline signal. These data are consistent with a 1:1 binding interaction model. Moreover, the SPR analysis proved the specificity of LCA for the EphA2 receptor relative to other members of the Eph–ephrin signaling system, such as ephrin A1 and ephrinB1.

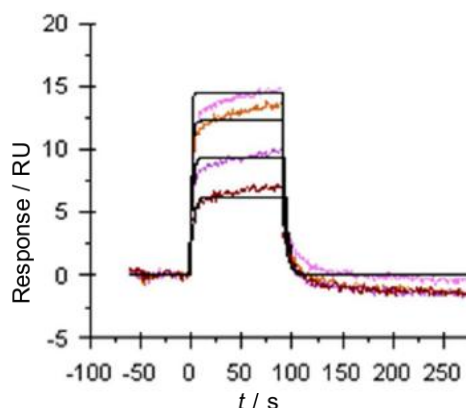
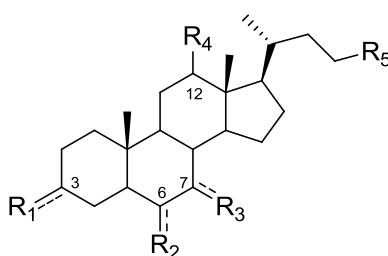


Figure 6. SPR sensorgram for the interaction of LCA with immobilized EphA2-Fc on sensor chip. Tested concentrations are: 3 (red line), 6 (violet line), 12.5 (orange line), and 25 μM (pink line).

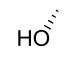
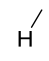
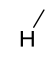
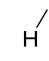
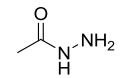
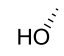
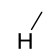
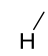
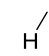
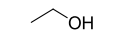
Structure-activity relationships of a first selected set of LCA derivatives

Starting from the theoretical model described above, a focused set of LCA derivatives, commercially available or the novo synthesized, was selected and examined for the ability to disrupt EphA2-ephrinA1 interaction.

Table 1. Structure–activity relationship data for lithocholic acid derivatives.



Compounds	R1	R2	R3	R4	R5	Ki (μM)
1 (LCA)	HO	H	H	H	COOH	49±3.0
2' (CA)	HO	H	HO	HO	COOH	>200
3' (DCA)	HO	H	H	HO	COOH	>200
4' (CDCA)	HO	H	HO	H	COOH	>200
5'	HO	H	O	H	COOH	114±13
6'	HO	O	H	H	COOH	138±20
7'	O	H	H	H	COOH	157±47
8'	O	O	H	H	COOH	114±14
9'	H ₃ C	H	H	H	COOH	88±11
10' (isoLCA)	HO	H	H	H	COOH	25±4
11'	HO ₃ S	H	H	H	COOH	>200
12'	H	H	H	H	COOH	5.1±1.4
13'	HO	H	H	H	COOCH ₃	>200
14'	HO	H	H	H	CONHOH	>200

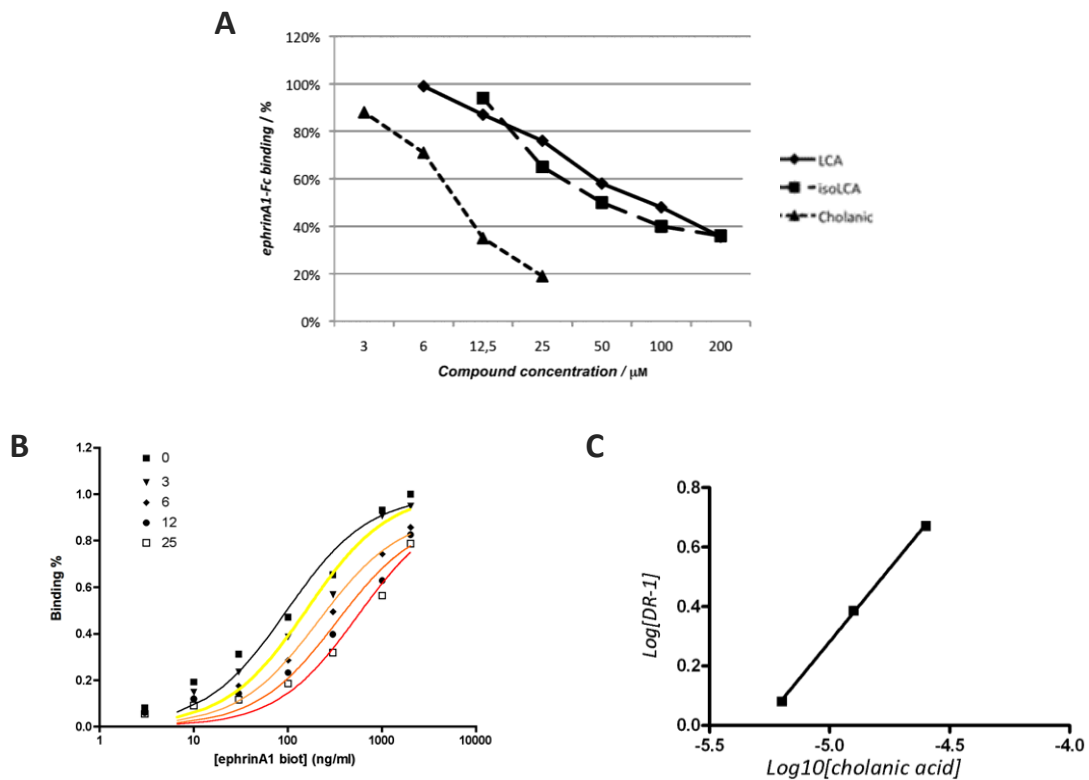
15'						>200
16'						186±27

Compounds **2'-6'** were selected to explore the interaction between the lipophilic scaffold of lithocholic acid and the EphA2 binding site. Compounds **7'-12'** and **13'-16'** were chosen to examine the role played by the two polar ends of lithocholic acid.

The potencies for inhibition of EphA2-ephrin-A1 interaction, as indicated by the K_i values (binding affinity data), revealed that the lithocholic acid derivatives are particularly sensitive to the modulation of the cyclopenta[a]perhydro phenanthrene scaffold. In fact, the introduction of polar groups at 6, 7, and 12 positions was detrimental for activity (compound **2'-6'**). At the same way, the modulation of the carboxylic acid group in position 23 led to less potent or inactive compounds (compound **13'-16'**). Conversely, the 3- α -hydroxyl group didn't seem to be crucial for EphA2 receptor recognition. In fact, removal of this α -hydroxyl group at position 3 led to compound **12'**, *Cholanic acid*, which resulted the most potent compound of the series, with a K_i value of 5 μM (~10-fold more potent than LCA).²⁶

Displacement studies (Figure 7A) showed that cholanic acid displace binding of biotinylated ephrinA1-Fc ectodomain from immobilized EphA2-Fc-ectodomain in a dose-dependent manner. In addition, saturation curves of EphA2-ephrinA1 binding in presence of increasing concentrations of cholanic acid were plotted (Figure 7B). The corresponding Schild plot (Figure 7C) provided well-interpolated regression line that confirmed, as in the case of LCA, a competitive binding.²⁶

Figure 7. Cholanic acid competitively inhibited EphA2-ephrinA1 binding. **A.** Lithocholic, isolithocholic and cholanic acid dose-dependently displaced ephrin-A1-Fc from the immobilized EphA2-Fc ectodomain. **B.** Binding of ephrin-A1-Fc ectodomain to immobilized EphA2-Fc ectodomain in the presence of different concentrations of cholanic acid. **C.** The dissociation constants (K_d) from the displacement experiment was used to calculate $\text{Log}(\text{Dose-ratio} - 1)$ and to graph the Schild plot. pK_i value of cholanic acid was estimated by the intersection of the interpolated line with the X-axis. The slope of the interpolated line can be related to the nature of the binding. A slope between 0.8 and 1.2 is related to a competitive binding, whereas higher numbers are related to non-specific interactions. [Image from Ref 26].



To evaluate the functional effects of cholanic acid, phosphorylation studies were performed using PC3 human prostate adenocarcinoma cells, which endogenously express the EphA2 receptor. These studies proved that cholanic acid dose-dependently inhibited EphA2 phosphorylation induced by ephrinA1-Fc ectodomain. According to binding data, cholanic acid was more potent than lithocholic acid to inhibit EphA2 kinase activation, showing IC_{50} of 12 μM compared to 48 μM of LCA.²⁶

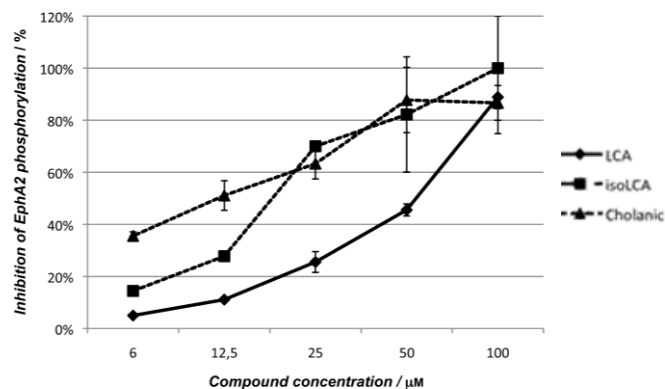


Figure 8. Lithocholic, isolithocholic and cholanic acid inhibit EphA2 phosphorylation in a dose dependent manner. EphA2 phosphorylation was induced by treatment of PC3 cells with $0.25 \mu\text{g/mL}^{-1}$ ephrin-A1-Fc. Cells were

pretreated for 20 minutes with 1% DMSO or the indicated concentration of compounds and then stimulated for 20 minutes with ephrin-A1-Fc. Data are the means \pm SEM of at least three independent experiments.

However, this first exploration of lithocholic acid structure-activity relationships allowed to identify the stereoelectronic requirements for EphA2 binding. In particular, it was found that the simultaneous presence of a large hydrophobic region (represented by the cyclopenta[a]perhydrophenanthrene scaffold) and an anionic hydrogen bond acceptor group (represented by a carboxylate functionality) are pivotal for effective disruption of EphA2–ephrinA1 binding, consistently with the predicted binding mode for the EphA2–lithocholic acid complex.²⁶

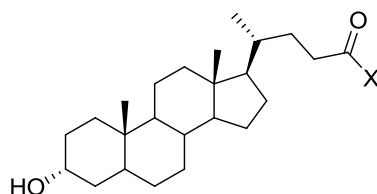
Amino acid derivatives of lithocholic acid as novel antagonists of the EphA2 receptor

The present PhD work makes part of a research project aimed at the identification of novel small molecules able to interfere with the Eph-ephrin interaction, in order to obtain new pharmacological tools and/or new potential anti-oncogenic and anti-angiogenic agents.

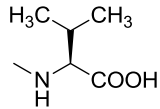
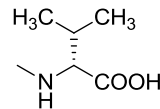
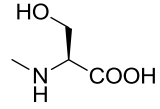
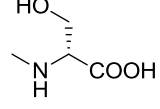
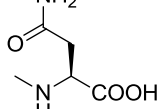
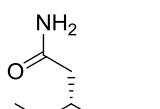
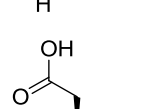
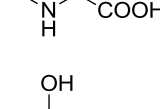
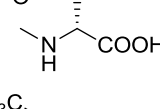
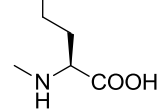
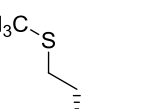
The findings about LCA support the notion that the (5 β)-cholan-24-oic acid scaffold can be used as a template structure to design an improved generation of EphA2 inhibitors.

In the present chapter, the synthesis and structure-activity relationship (SAR) profile of an extended series of α -amino acid conjugates of LCA, designed starting from the theoretical binding mode of the EphA2-LCA complex, is described. The synthesized compounds were examined for their ability to disrupt EphA2-ephrin-A1 complex, using an ELISA binding protocol.²⁵ The measured pIC₅₀ (-log IC₅₀) for the compounds tested are reported in Table 2.

Table 2. pIC₅₀, π and MR variables for amino acid derivatives of lithocholic acid.



Compound	X	pIC ₅₀ \pm SEM [a]	π [b]	MR[b]
1		4.24 \pm 0.07	-	-
2		4.31 \pm 0.09	0	1.03
3		< 3.50	0	1.03
4		4.70 \pm 0.20	0.46	5.51
5		4.51 \pm 0.09	0.46	5.51

6		4.62 ± 0.05	1.43	14.69
7		4.76 ± 0.11	1.43	14.69
8		4.48 ± 0.03	-0.57	7.14
9		4.22 ± 0.09	-0.57	7.14
10		<3.50	-1.0	13.85
11		<3.50	-1.0	13.85
12		<3.50	-0.29	12.54
13		<3.50	-0.29	12.54
14		4.56 ± 0.10	1.12	22.21
15		4.56 ± 0.10	1.12	22.21
16		5.18 ± 0.12	2.00	30.91

17		5.12 ± 0.07	2.00	30.91
18		4.30 ± 0.16	1.69	32.24
19		4.00 ± 0.11	1.69	32.24
20		5.69 ± 0.12	2.36	41.33
21		4.69 ± 0.03	2.36	41.33

[a] Values are means \pm standard error of the mean (SEM) from at least three independent experiments

[b] Descriptors have been calculated with the QSAR module of MOE software.³⁶

These compounds were also examined for the ability to prevent EphA2 phosphorylation in a prostate cancer cell (PC3) line.

Results and discussion

Molecular design and characterization of LCA conjugates

The visual inspection of the EphA2-LCA complex suggested that the simple conjugation of LCA with natural α -amino acids, exemplified by the glycine derivative **2**, would lead to compounds still able to form a salt bridge with Arg103 (Figure 9b) and thus potentially active as EphA2 binders.

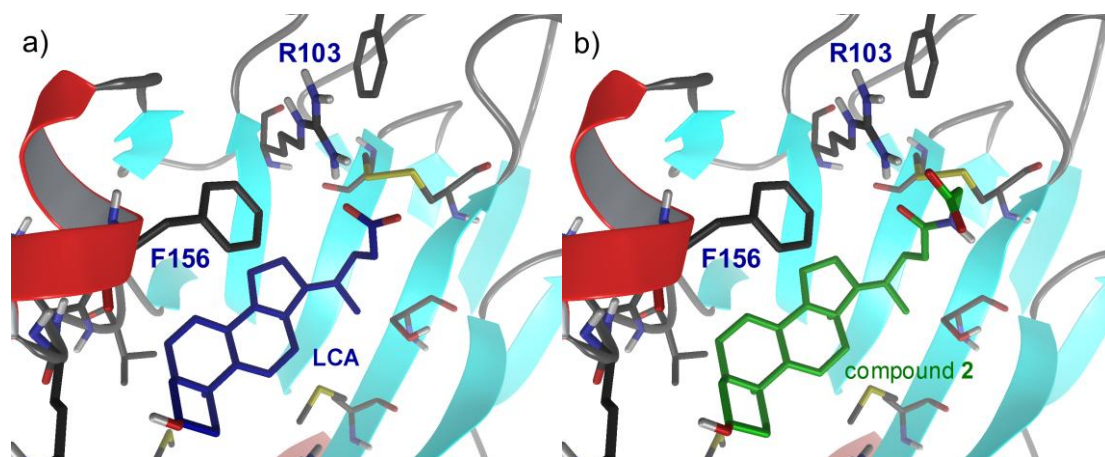
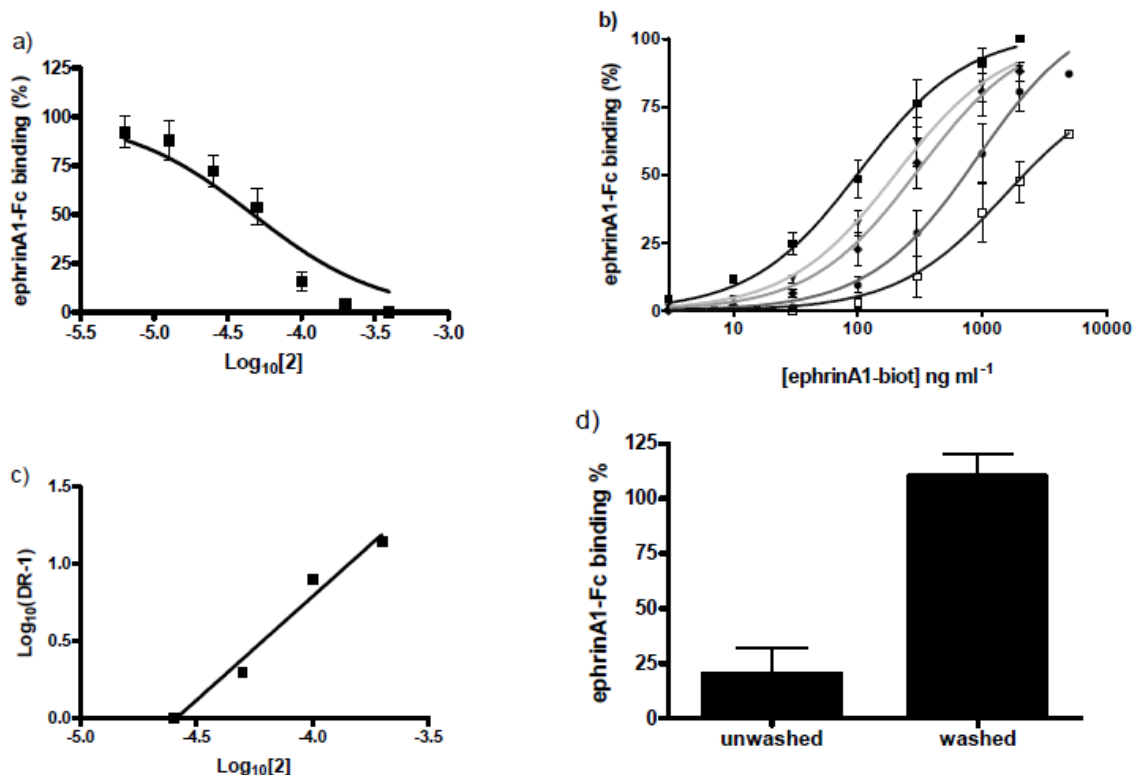


Figure 9. Docking of lithocholic acid (panel **a**), blue carbon atoms) and its glycol-conjugate compound **2** (panel **b**), green carbon atom) within the ligand-binding domain of EphA2.

To verify this hypothesis, the EphA2 binding properties of compound **2** were investigated by using a previously developed ELISA assay. A dose-dependent disruption of the EphA2-ephrinA1 complex was observed when compound **2** was co-incubated with these two proteins (Figure 10A). The pIC_{50} of compound **2** was measured to be 4.31, similarly to what previously found for LCA. To evaluate the nature of the antagonism of compound **2**, saturation curves of EphA2-ephrinA1 binding in the presence of growing concentrations of compound **2** were plotted (Figure 10B). From each of these curves, the K_D or the apparent K_D was calculated and the corresponding Schild plot was built (Figure 10C). The slope of the regression line ($r^2 = 0.98$) of Schild plot indicated the presence of a competitive binding of compound **2** at the EphA2 receptor. The displacement experiment was repeated by incubating 100 μM of compound **2** for 1 hour and washing some wells before adding 50 ng/ml ephrinA1-Fc. The displacement was detected only where the washing was not performed, suggesting that compound **2** acted as reversible binder of the EphA2 receptor. (Figure 10D).

Figure 10. Compound **2** competitively inhibited EphA2-ephrinA1 binding. **a**) Compound **2** displaced ephrin-A1-Fc from the immobilized EphA2-Fc ectodomain in a dose dependent manner. **b**) Binding of ephrin-A1-Fc ectodomain to immobilized EphA2-Fc ectodomain in the presence of increasing concentrations of compound **2**. **c**) The dissociation constants (K_d) from the displacement experiment was used to calculate $\text{Log}(\text{Dose-ratio} - 1)$ and to graph the Schild plot. pK_i value of compound **2** was

estimated by the intersection of the interpolated line with the X-axis. **d)** EphA2-ephrinA1 binding in the presence of 100 μM compound **2** with or without washing three times with PBS.



Structure-activity relationship (SAR) analysis of LCA derivatives

The investigation started testing compounds **1-3** in the ELISA assay. Compounds **1** and **2** were both active at preventing the binding of ephrin-A1 to EphA2, with pIC_{50} of 4.20 and 4.31, respectively. Conversely, compound **3**, the methyl ester derivative of **2**, resulted inactive confirming the importance of a free carboxyl group for maintaining biological activity. Subsequently, it was synthesized and tested eight α -amino acid conjugates (**4-11**), the side chain of which (L- and D-Ala, L- and D-Ser, L- and D-Val, L- and D-Asn) represent the four combinations of positive and negative levels for lipophilicity and steric hindrance, described here by π and MR (molar refractivity) variables, respectively (Figure 11).

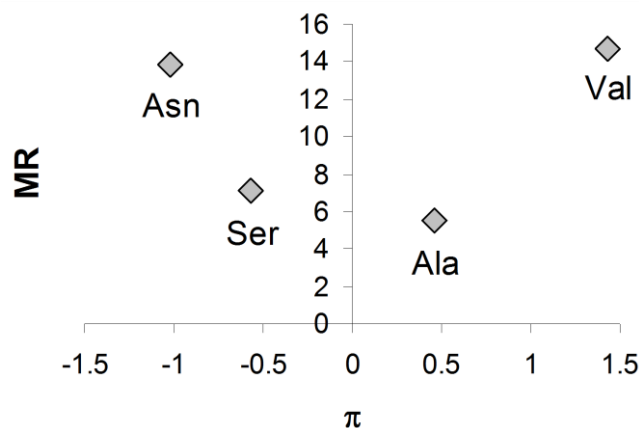


Figure 10. π and MR variables for amino acid selection.

The pIC_{50} values for this first set of compounds indicate that hydrophobic groups (**4-7**) have a favourable impact on pharmacological activity, regardless of the absolute configuration of the chiral centre of the amino acidic moiety. On the other hand, the introduction of hydrophilic groups was tolerated in case of side chains of limited size (**8,9**) but very detrimental for activity in the case of bulkier side chains (**10,11**). Ten additional α -amino acids were coupled with LCA, to further cover the space of lipophilic and steric properties. While conjugation of LCA with L- and D-Asp yielded inactive derivatives (such as compounds **12** and **13**), the introduction of amino acids endowed with a lipophilic side chain always led to active compounds. Compounds **14** and **15**, bearing a methionine side chain, showed a limited increment in the pharmacological activity compared to compound **1**. On the other hand, the introduction of aromatic substituents had a remarkable impact on the pIC_{50} . The two phenylalanine compounds **16** and **17** resulted at least ten times more potent than LCA. Conversely, the replacement of the phenylalanine with the tyrosine side chain led to poorly active compounds (**18** and **19**) possibly due to their reduced lipophilicity. The importance of having a lipophilic group at the α position was further confirmed by the tryptophan conjugates **20** and **21**, which were significantly more active than LCA. In particular, the L-Trp conjugate **20** showed a pIC_{50} of 5.69 resulting the most potent compound of the series.

The availability of the X-ray crystal structure of EphA2 in complex with the ephrin-A1 ligand³³ allowed to investigate the binding mode of compounds **2**, **4-9** and **14-21** by molecular docking and molecular dynamic (MD) simulations. The docking method applied provided binding poses for all these ligands in the EphA2 binding site that are

consistent with the one of compound **2** (Figure 9b). These simulations also highlighted the presence of an accessory hydrophobic site in the ligand-binding channel of the EphA2 receptor where the α -side chain of the investigated compounds can be accommodated. Such a binding mode can thus explain the lack of activity for the relatively more polar derivatives **10-12**, as well as the significant increment in the pIC_{50} values observed for the aromatic derivatives **16,17** and **20,21** bearing a phenylalanine or a tryptophan moiety, respectively. Visual inspection of the EphA2-compound **20** complex underlined the importance of hydrophobic interactions with the EphA2 receptor (Figure 12).

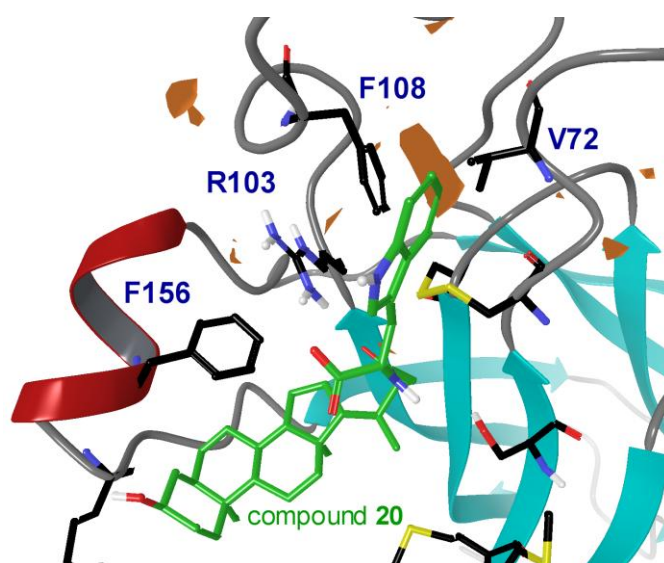


Figure 12. Docking of compound **20** within the ligand binding channel of EphA2.

In particular, the indole ring of compound **20** interacts with Phe108, mimicking the binding of ephrin ligands. Indeed, Phe108 of EphA2 normally interacts with a phenylalanine residue belonging to the conserved ϕ -x-x- ϕ binding motif of ephrin-A1.^{37,38} Overall the binding mode proposed for compound **20** closely resembles that one of the physiological ligand at the EphA2 receptor, suggesting that this small molecule might effectively mimic the G-H loop region of ephrinA1 (Figure 13).

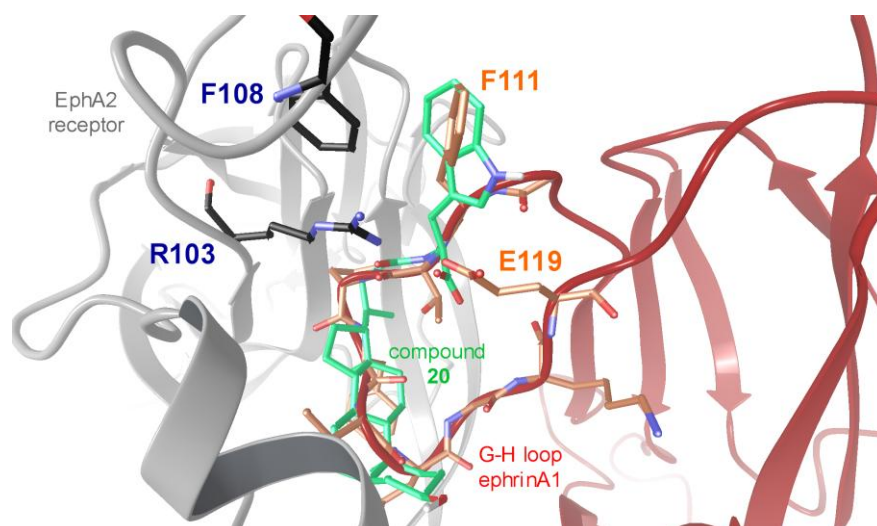


Figure 13. Docking of compound 20 (green carbons) within the ligand binding channel of EphA2 (white cartoons). The structure of ephrinA1 ligand is also displayed (red cartoons), as it appears in the X-ray structure of the EphA2-ephrinA1 complex.³³

Effects on EphA2 phosphorylation in intact cells

LCA derivatives obtained by coupling the carboxylic acid of compound **1** with L-amino acids (**4,6,8,14,16,20**) showed slightly higher pIC_{50} values than the ones resulting from conjugation with the corresponding D-amino acids (**5,7,9,15,17,21**) in the ELISA binding assay. Thus, the attention was focused on the more active subclass of LCA conjugates for further studies. To evaluate the functional effects of compounds **4**, **6**, **8**, **14,16** and **20**, phosphorylation studies were performed using PC3 human prostate adenocarcinoma cells, which endogenously express the EphA2 receptor. The glycine derivative **2**, was also included as a reference compound. All the tested compounds acted as antagonists because they inhibited EphA2 phosphorylation induced by ephrin-A1-Fc in a dose dependent manner (Figure 14).

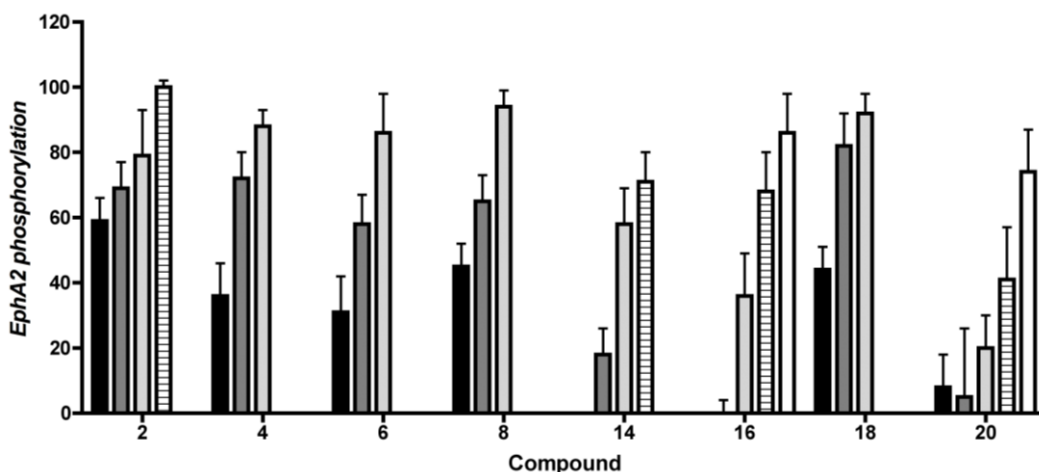


Figure 14. Relative EphA2 phosphorylation in presence of different compound concentrations: 100, 50, 25, 12, 6 μM . EphA2 phosphorylation was induced by treatment of PC3 cells with $0.25 \mu\text{g}/\text{mL}^{-1}$ ephrin-A1-Fc. Cells were pretreated for 20 minutes with 1% DMSO or the indicated concentration of compounds and then stimulated for 20 minutes with ephrin-A1-Fc. Data are the means \pm SEM of at least three independent experiments. EphA2 phosphorylation from cells treated with ephrin-A1-Fc was arbitrarily assigned a value of 100 and from cells treated with Fc a value of 0. Dasatinib, used at 1 μM as reference drug, completely abolished EphA2 phosphorylation (not shown).

The pIC_{50} values measured in the phosphorylation assay roughly parallel the pIC_{50} ones obtained in the EphA2-binding assays. Thus, compounds showing higher affinity for the EphA2 binding site are also more effective in preventing EphA2 activation. Additionally, under these conditions the L-Phe and L-Trp conjugates **18** and **20** (which have pIC_{50} of 4.72 and 4.92, respectively) emerged as the most potent compounds of the series. In particular, compound **20** resulted 5-10 times more potent than compounds **1** (LCA; $\text{pIC}_{50} = 4.32$) and **2** ($\text{pIC}_{50} = 3.86$) in blocking EphA2 activation in the PC3 cell line.

Conclusions

Increasing evidence supports the notion that the Eph–ephrin system, including the EphA2 receptor, plays a critical role in tumor vascularization during carcinogenesis. In particular, the EphA2 receptor is currently being explored as novel target for the development of anti-tumorigenic and anti-angiogenic therapies.²⁴

Few classes of small molecules able to bind the EphA2 receptor have been recently discovered and employed for biological investigations. However, their usefulness as biological tools seems somehow limited by important pharmacological and/or chemical issues. For instance, the marketed doxazosin (Cardura™) binds the EphA2 receptor with micromolar affinity but also has a well known inhibitory activity on the α 1-adrenergic receptor.²⁹ The EphA2/EphA4 salicylic acid antagonists have been recently indicated to suffer from a chemical stability concern. These compounds undergo a modification process that leads to the formation of an unidentified molecular entity able to interact with Eph receptors.^{27,39} In this context, it seemed critical to search for new compounds able to bind the EphA2 receptor, with improved chemical and pharmacological profiles.

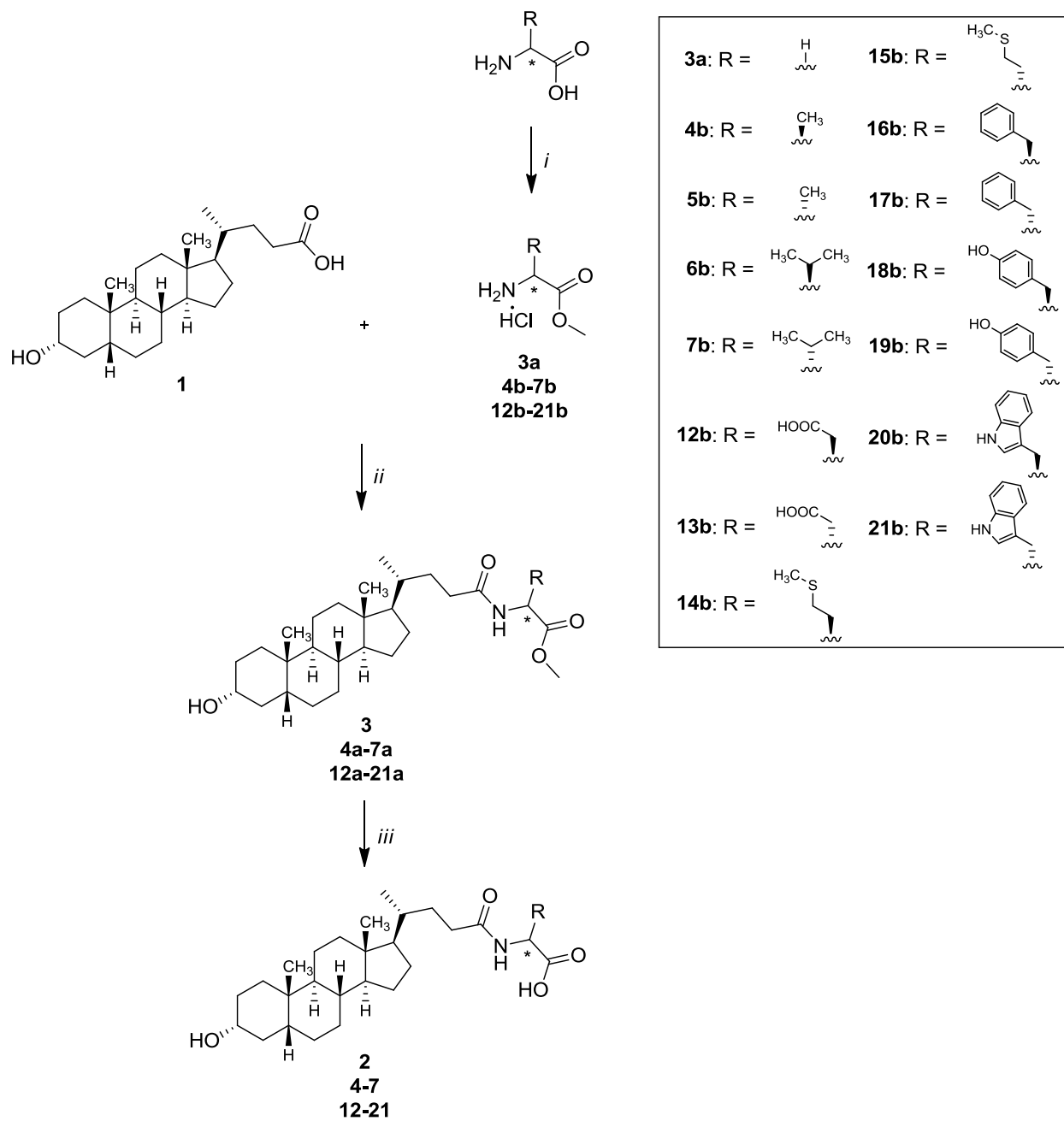
In the present study, it was reported the experimental design and synthesis of a series of α -amino acid-LCA conjugates. As a result of a focused SAR investigation, compound **20** (the L-Trp conjugated of LCA) was identified as the most potent compound of the series. Compound **20** inhibits the EphA2 receptor at low micromolar concentrations ($pIC_{50} = 5.69$) preventing EphA2 activation in intact cells. Indeed, compound **20** blocked EphA2 phosphorylation in the PC3 cell line, with an antagonist potency ($pIC_{50} = 4.92$) similar to that one observed in the binding assay.

Thus compound **20** is emerging as one of the most promising pharmacological tool for elucidating the role of the Eph receptors in physiopathological conditions.

Chemistry

General synthesis of compounds **2**, **4-7**, **12-21**.

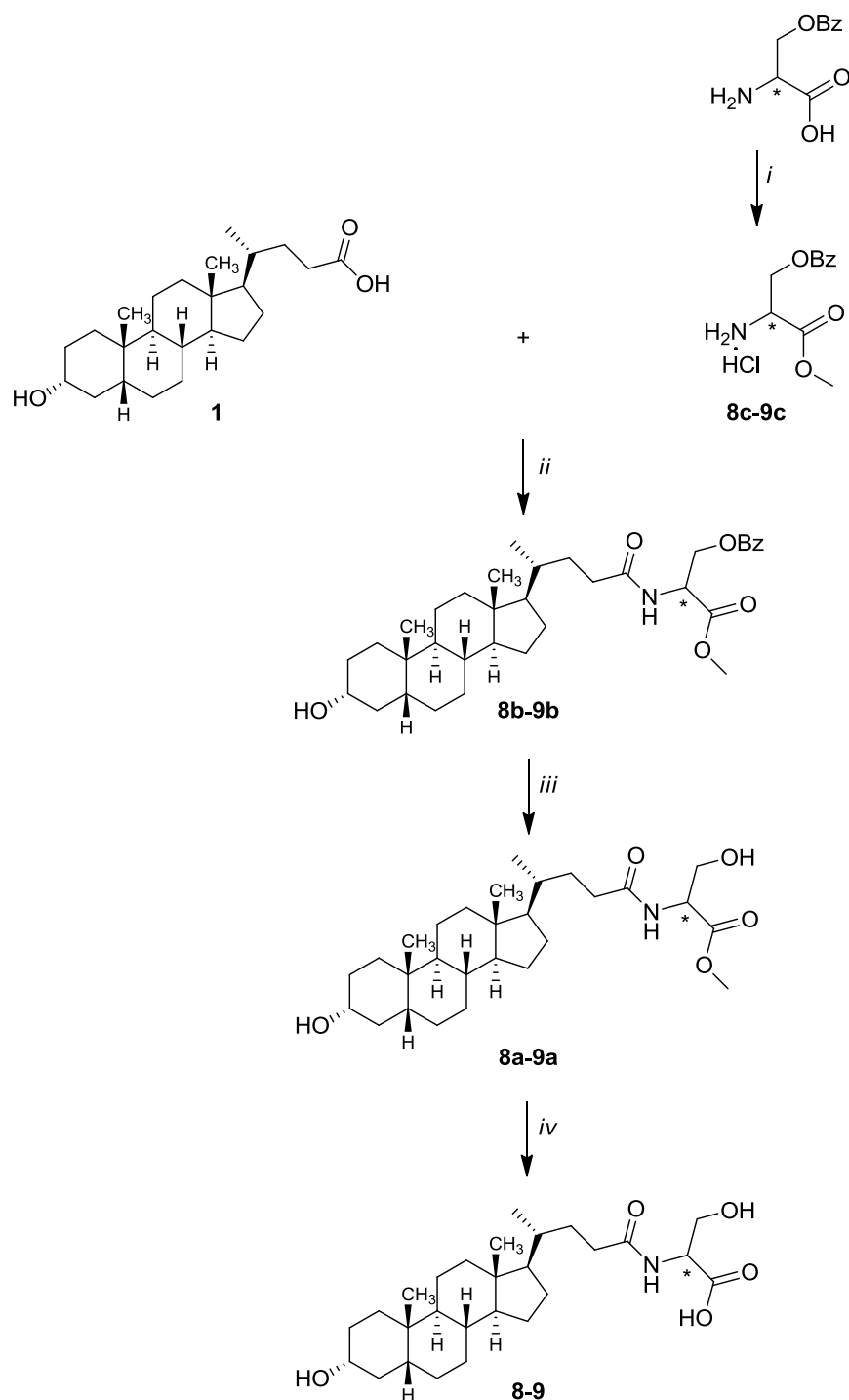
Compounds **2**, **4-7** and **12-21** were synthesized according to the procedure described in Scheme 1. Methyl ester hydrochloride of α -amino acids were purchased from commercial suppliers (**3a**, **4b-7b**, **12b**, **14b**, **16b-18b**, **20b**) or synthesized according to step *i* of Scheme 1, to obtain the corresponding methyl ester hydrochloride derivatives (**13b**, **15b**, **19b** and **21b**). The α -amino acids protected as methyl esters were coupled with LCA (compound **1**) using N-(3-dimethylaminopropyl)-N'-ethylcarbodiimide hydrochloride (EDCI), to give the methyl ester intermediates, **3**, **4a-7a**, **12a-21a**. These intermediates were then hydrolyzed with sodium hydroxide, to achieve the corresponding carboxyl acids. The crude products were crystallized from ethanol-water to give the title compounds **2**, **4-7**, and **12-21**.

Scheme 1^a

^a (i) Acetyl chloride, MeOH, from 0°C to reflux, overnight; (ii) NMM, EDCI, CH₂Cl₂ dry, r.t., overnight ; (iii) NaOH_(aq) 15%, EtOH, r.t, 1 h.

General synthesis of compounds 8-9.

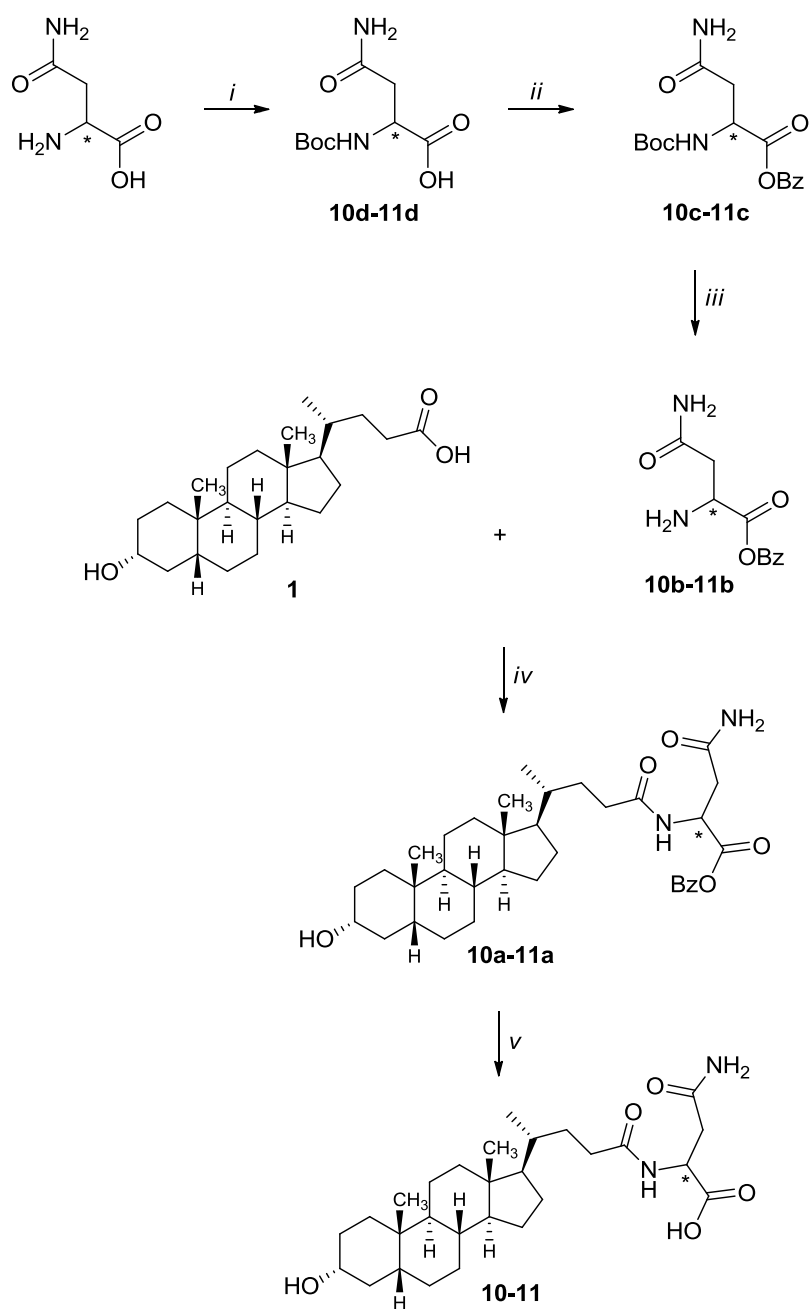
Compounds **8** and **9** were synthesized according to the procedure reported in scheme 2. Methyl ester hydrochloride **8c** and **9c** were prepared starting from L- or D-O-benzyl-serine. Then compound **8c** and **9c** were coupled to **1** (as described above), giving the corresponding methyl ester conjugates **8b** and **9b**. These intermediates were treated with Pd/C 10% under H₂ atmosphere, to remove the benzyl protector group. The obtained intermediates **8a** and **9a** were then hydrolyzed, giving the final products **8** and **9**.

Scheme 2^a

^a (i) Acetyl chloride, MeOH, from 0°C to reflux, overnight; (ii) NMM, EDCI, CH₂Cl₂ dry, r.t. overnight; (iii) Pd/C 10%, MeOH, H₂, 30 psi, 3h; (iv) NaOH_(aq) 15%, EtOH, r.t., 1h.

General synthesis of compounds 10-11.

Compounds **10** and **11** were synthesized according to the procedure reported in scheme 3. The amino group of L- or D-Asparagine was protected with the anhydride Boc_2O . This reaction gave compounds **10d** and **11d**, which were transformed in the corresponding benzyl esters **10c** and **11c**. The Boc protection was then removed giving **10b** and **11b** which in turn were coupled to **1** to obtain compounds **10a** and **11a**. The final products **10** and **11** were obtained by removing the benzyl ester protection via hydrogenation.

Scheme 3^a

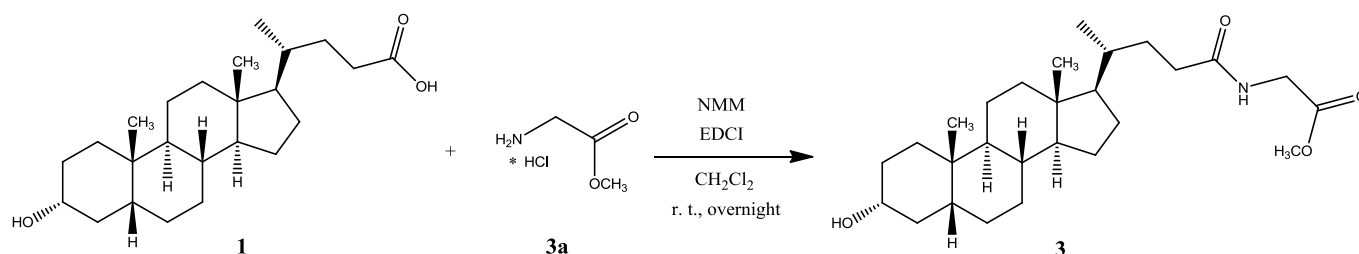
^a (i) Boc_2O , Na_2CO_3 , 1,4-dioxane, water, r.t., overnight; (ii) Cs_2CO_3 , MeOH, BzBr, DMF, r.t., overnight; (iii) TFA, CH_2Cl_2 , r.t., overnight; (iv) NMM, EDCI, CH_2Cl_2 dry, r.t., overnight; (v) Pd/C 10%, MeOH, H_2 , 30 psi, 3h.

Materials and methods

Reagents and solvents were purchased from commercial suppliers (Aldrich and Fluka) and used without further purification. The progress of the reaction was monitored by thin-layer chromatography (TLC) with F₂₅₄ silica-gel precoated sheets (Merck Darmstadt, Germany). UV light, ninhydrin ethanolic solution (0.3% w/v) and potassium permanganate solution (10% w/v) were used for detection. Flash chromatography was performed using Merck silica-gel 60 (Si 60, 40-63 μm , 230-400 mesh ASTM). Catalytic hydrogenation was performed using a Parr 3911 Hydrogenation apparatus. Dichloromethane (DCM) was dried by distillation over calcium hydride. All reactions were carried out using flame-dried glassware under atmosphere of nitrogen. Melting points were determined on a Gallenkamp melting point apparatus and were not corrected. The ¹H-NMR and ¹³C-NMR spectra were recorded on a Bruker Avance 400 spectrometer (400MHz); chemical shifts (δ scale) are reported in parts per million (ppm). ¹H-NMR spectra are reported in the following order: multiplicity, approximate coupling constants (*J* value) in Hertz (Hz) and number of protons; signals were characterized as s (singlet), d (doublet), t (triplet), p (quintuplett), m (multiplet), b (broad). Mass spectra were recorded on an Applied Biosystem API-150 EX system spectrometer with ESI interface. The final compounds were analyzed on a ThermoQuest (Italia) FlashEA 1112 Elemental Analyzer for C, H and N. The percentages found were within $\pm 0.4\%$ of the theoretical values.

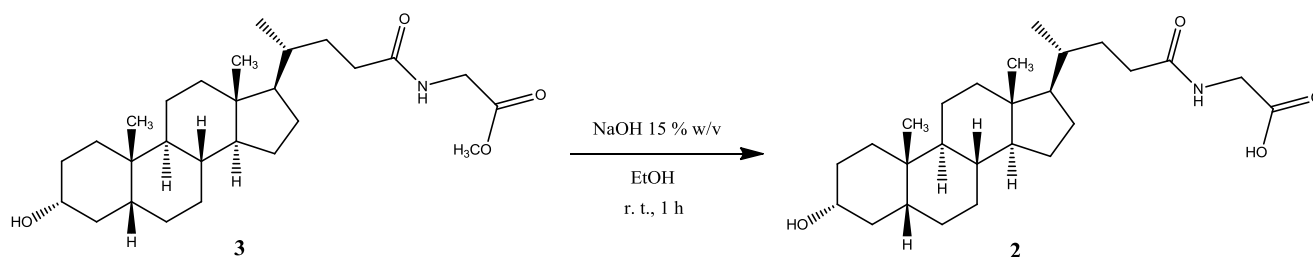
Lithocholic acid (compound **1**) was purchased from Sigma and characterized by elemental analysis. Compounds **2-21**, were synthesized following the procedures described below in the experimental section.

Experimental section

***N*-[(3 α ,5 β)-3-hydroxy-24-oxocholan-24-yl]- Glycine methyl ester (**3**)**

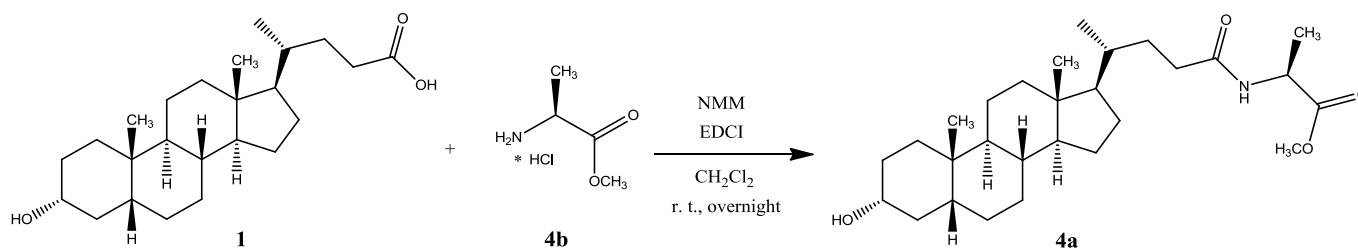
Compound **3** was synthesized following a modification of a described procedure⁴⁰ in which a stirred solution of lithocholic acid **1** (0.8 mmol) L-glycine methyl ester hydrochloride (0.88 mmol) and N-methyl morpholine (NMM) (1.43 mmol) in dry CH₂Cl₂ (15 ml) under nitrogen was added N-(3-dimethylaminopropyl)-N'-ethylcarbodiimide hydrochloride (EDCI) (0.821 mmol). The reaction mixture was stirred at room temperature overnight and then was diluted with 30 ml of CH₂Cl₂, washed with HCl 2N, brine and dried over anhydrous Na₂SO₄. Evaporation of solvent under reduced pressure yielded a white solid that was purified by flash chromatography [SiO₂, CH₂Cl₂:EtOH 98:2]. The crude product was re-crystallized from ethanol-water to give **3**. Yield: 50%. Mp: 157-160°C. ¹H-NMR (400 MHz, DMSO-d₆) δ = 0.60 (s, 3H, CH₃), 0.86-0.87 (m, 6H), 0.91-1.20 (m, 11H), 1.33-1.35 (m, 7H), 1.47-1.68 (m, 5H), 1.74-1.77 (m, 2H), 1.90-1.93 (m, 1H), 1.98-2.05 (m, 1H), 2.10-2.17 (m, 1H), 3.31-3.35 (m, 1H), 3.60 (s, 3H, OCH₃), 3.78 (d, *J* = 6.0, 2H, CH₂), 4.42 (d, *J* = 4.4, 1H, OH), 8.20 (t, *J* = 6.0, 1H, NH). ¹³C-NMR (100 MHz, DMSO-d₆) δ = 12.06, 18.37, 20.83, 23.38, 24.21, 26.42, 27.20, 28.24, 30.55, 31.58, 33.25, 34.58, 35.35, 35.47, 35.85, 36.46, 40.18, 40.43, 41.21, 42.10, 42.75, 52.38, 53.37, 56.00, 56.49, 71.85, 170.64, 173.72. MS (ESI) calc for C₂₇H₄₅NO₄: 447.33; found: 446.3 [M-1].

***N*-[(3 α ,5 β)-3-hydroxy-24-oxocholan-24-yl]- Glycine (**2**)**



Compound **2** was synthesized following a modification of a described procedure⁴¹ in which a solution of compound **3** (0.32 mmol) in ethanol (15 ml) was added a solution of sodium hydroxide 15% w/v (10 ml) and the mixture was stirred at room temperature for 1 hour. Ethanol was removed under reduced pressure and the solution was acidified with concentrated hydrochloric acid until a precipitate was formed. The resulting suspension was filtered under vacuum and the white residue washed with water. The crude product was crystallized from ethanol-water to give the title compound **2** (95%) as a white solid. Mp: 178-181°C. ¹H-NMR (400 MHz, DMSO-d₆) δ = 0.59 (s, 3H, CH₃), 0.86-0.92 (m, 7H), 0.97-1.23 (m, 10H), 1.28-1.34 (m, 7H), 1.47-1.50 (m, 2H), 1.58-1.68 (m, 3H), 1.73-1.79 (m, 2H), 1.90-1.92 (m, 1H), 1.97-2.04 (m, 1H), 2.09-2.16 (m, 1H), 3.32-3.35 (m, 1H), 3.69 (d, J = 6.0, 2H, CH₂), 4.42 (bs, 1H, OH), 8.07 (t, J = 6.0, 1H, NH). ¹³C-NMR (100 MHz, DMSO-d₆) δ = 12.34, 18.75, 20.88, 23.74, 24.32, 26.63, 27.36, 28.18, 30.84, 31.89, 32.50, 34.67, 35.33, 35.62, 35.85, 36.76, 41.00, 41.99, 42.73, 56.09, 56.55, 70.32, 171.91, 173.37. MS (ESI) calc for C₂₆H₄₃NO₄: 433.32; found: 432.5 [M-1].

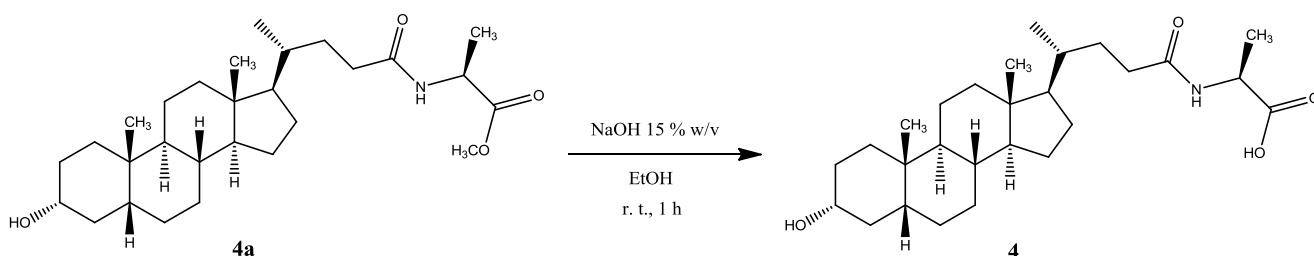
***N*-[(3 α ,5 β)-3-hydroxy-24-oxocholan-24-yl]- L-Alanine methyl ester (**4a**).**



Compound **4a** was synthesized following the procedure described for **3** using L-alanine methyl ester hydrochloride and purified by flash chromatography [SiO₂, CH₂Cl₂:C₂H₅OH 98:2]. The crude product was re-crystallized from ethanol-water to give **4a**. Yield: 66%. Mp: 148-150°C. ¹H-NMR (400 MHz, CDCl₃) δ = 0.64 (s, 3H,

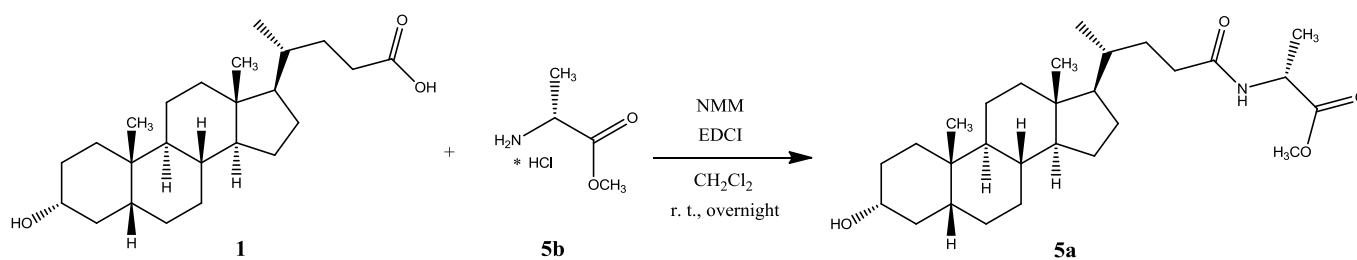
CH₃), 0.91-0.93 (m, 6H), 0.96-1.31 (m, 10H), 1.34-1.41 (m, 9H), 1.50-1.64 (m, 4H), 1.71-1.86 (m, 5H), 1.94-1.97 (m, 1H), 2.06-2.14 (m, 1H), 2.23-2.30 (m, 1H), 3.59-3.65 (m, 1H), 3.75 (s, 3H, OCH₃), 4.60 (p, *J* = 7.2, 1H, CHCH₃), 6.00 (d, *J* = 7.2, 1H, NH). ¹³C-NMR (100 MHz, CDCl₃) δ = 12.03, 18.37, 18.54, 20.80, 23.38, 24.20, 26.41, 27.20, 28.24, 30.50, 31.57, 33.36, 34.56, 35.36, 35.44, 35.83, 36.41, 40.17, 40.40, 42.08, 42.40, 42.72, 47.84, 52.43, 56.00, 56.48, 71.74, 173.12, 173.78. MS (ESI) calc for C₂₈H₄₇NO₄: 461.35; found: 460.5 [M-1]. Anal. calc for C₂₈H₄₇NO₄: C, 72.84; H, 10.26; N, 3.03; found: C, 72.78; H, 10.48; N, 2.90.

***N*-[(3 α ,5 β)-3-hydroxy-24-oxocholan-24-yl]- L-Alanine (4).**



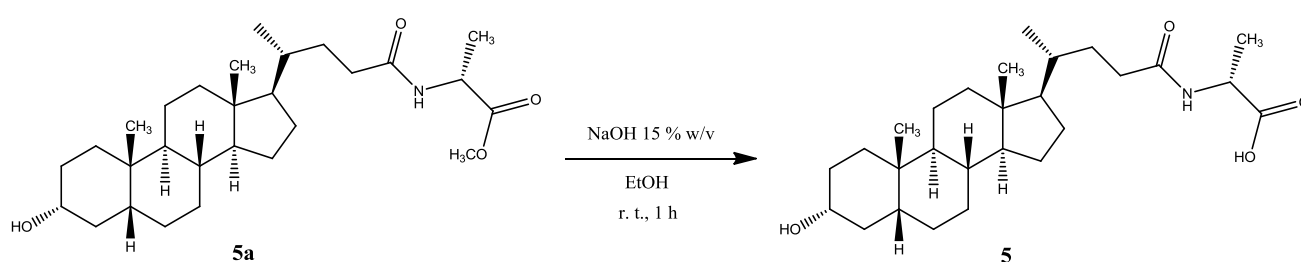
Compound **4** was synthesized following the procedure described for **2** using compound **4a**. The crude product was re-crystallized from (EtOH/H₂O). Yield: 86%. Mp: 218-221°C. ¹H-NMR (400 MHz, DMSO-d₆) δ = 0.59 (s, 3H, CH₃), 0.87-0.91 (m, 7H), 1.00-1.08 (m, 4H), 1.11-1.21 (m, 9H), 1.28-1.34 (m, 7H), 1.47-1.55 (m, 2H), 1.58-1.68 (m, 3H), 1.73-1.79 (m, 2H), 1.90-2.01 (m, 2H), 2.07-2.12 (m, 1H), 3.34-3.36 (m, 1H), 4.10 (p, *J* = 7.2, 1H, CHCH₃), 7.96 (d, *J* = 7.2, 1H, NH). ¹³C-NMR (100 MHz, DMSO-d₆) δ = 12.33, 17.97, 18.79, 20.87, 23.74, 24.32, 26.63, 27.36, 28.20, 30.83, 31.91, 32.55, 34.66, 35.37, 35.61, 35.84, 36.75, 41.99, 42.75, 48.13, 56.08, 56.56, 70.32, 172.64, 174.91. MS (ESI) calc for C₂₇H₄₅NO₄: 447.33; found: 446.4 [M-1]. Anal. calc for C₂₇H₄₅NO₄: C, 72.44; H, 10.13; N, 3.13; found: C, 71.96; H, 10.08; N, 3.09.

***N*-[(3 α ,5 β)-3-hydroxy-24-oxocholan-24-yl]- D-Alanine methyl ester (5a).**



Compound **5a** was synthesized following the procedure described for **3** using D-alanine methyl ester hydrochloride and purified by flash chromatography [SiO_2 , CH_2Cl_2 : $\text{C}_2\text{H}_5\text{OH}$ 98:2]. The crude product was re-crystallized from ethanol-water to give **5a** (EtOH/ H_2O). Yield: 71%. Mp: 221-224°C. $^1\text{H-NMR}$ (400 MHz, DMSO- d_6) δ = 0.56 (s, 3H, OCH_3), 0.82-0.95 (m, 6H), 1.05-1.10 (m, 4H), 1.12-1.23 (m, 9H), 1.28-1.34 (m, 7H), 1.47-1.55 (m, 2H), 1.58-1.68 (m, 3H), 1.73-1.79 (m, 2H), 1.90-2.09 (m, 2H), 2.07-2.12 (m, 1H), 3.30-3.36 (m, 1H), 3.70 (s, 3H, OCH_3), 4.17 (p, J = 7.2, 1H, CHCH_3), 7.95 (d, J = 7.2, 1H, NH). $^{13}\text{C-NMR}$ (100 MHz, DMSO- d_6) δ = 12.25, 18.12, 18.81, 20.77, 23.55, 24.30, 26.52, 27.46, 28.40, 30.73, 32.41, 32.45, 34.67, 35.38, 35.51, 35.81, 36.76, 42.02, 42.43, 42.70, 48.20, 56.21, 56.76, 70.36, 172.84, 174.31. MS (ESI) calc for $\text{C}_{27}\text{H}_{47}\text{NO}_4$: 461.35; found: 460.4 [$\text{M}-1$]. Anal. calc for $\text{C}_{27}\text{H}_{45}\text{NO}_4$: C, 72.44; H, 10.13; N, 3.13; found: C, 72.21; H, 10.05; N, 3.10.

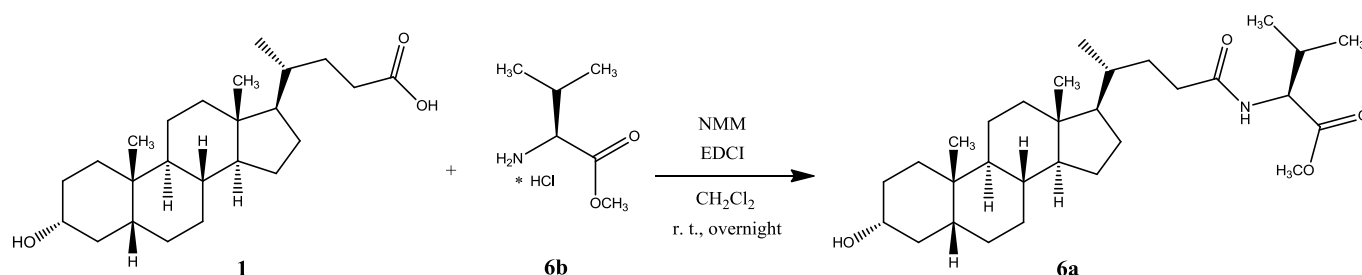
***N*-[(3 α ,5 β)-3-hydroxy-24-oxocholan-24-yl]-D-Alanine (**5**).**



Compound **5** was synthesized following the procedure described for **2** using **5a**. The crude product was re-crystallized from (EtOH/ H_2O) to give **5**. Yield: 97%. Mp: 224-227°C. $^1\text{H-NMR}$ (400 MHz, DMSO- d_6) δ = 0.59 (s, 3H, CH_3), 0.85-0.91 (m, 7H), 1.01-1.06 (m, 4H), 1.09-1.22 (m, 9H), 1.32-1.34 (m, 7H), 1.47-1.50 (m, 2H), 1.58-1.68 (m, 3H), 1.73-1.80 (m, 2H), 1.90-1.92 (m, 1H), 1.95-2.03 (m, 1H), 2.07-2.14 (m, 1H), 3.32-3.38 (m, 1H), 4.15 (p, J = 7.3, 1H, CHCH_3), 4.43 (bs, 1H, OH), 8.05 (d, J = 7.3,

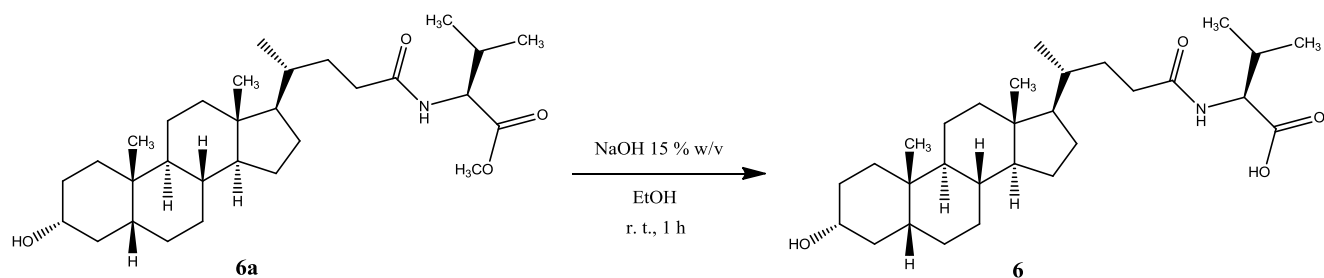
1H, NH). ^{13}C -NMR (100 MHz, DMSO- d_6) δ = 12.33, 17.66, 18.74, 20.87, 23.74, 24.32, 26.63, 27.36, 28.18, 30.84, 31.84, 32.43, 34.67, 35.36, 35.61, 35.84, 36.75, 41.99, 42.75, 47.72, 56.07, 56.54, 70.32, 172.79, 174.77. MS (ESI) calc for $\text{C}_{27}\text{H}_{45}\text{NO}_4$: 447.33; found: 446.4 $[\text{M}-1]^-$. Anal. calc for $\text{C}_{27}\text{H}_{45}\text{NO}_4$: C, 72.44; H, 10.13; N, 3.13; found: C, 72.61; H, 10.29; N, 3.06.

***N*-[(3 α ,5 β)-3-hydroxy-24-oxocholan-24-yl]-L-Valine methyl ester (6a).**



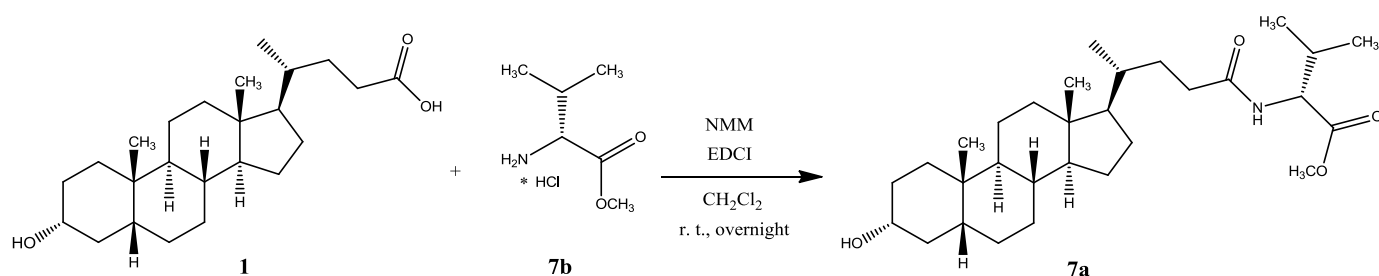
Compound **6a** was synthesized following the procedure described for **3** using L-valine methyl ester hydrochloride and purified by flash chromatography [SiO_2 , CH_2Cl_2 : $\text{C}_2\text{H}_5\text{OH}$ 98:2]. The crude product was re-crystallized from ethanol-water to give **6a** (EtOH/ H_2O). Yield: 77%. Mp: 183-186°C. ^1H -NMR (400 MHz, CDCl_3) δ = 0.64 (s, 3H, CH_3), 0.89-0.94 (m, 12H), 0.96-1.16 (m, 5H), 1.24-1.40 (m, 11H), 1.52-1.64 (m, 4H), 1.71-1.86 (m, 5H), 1.94-1.97 (m, 1H), 2.09-2.17 (m, 2H), 2.26-2.34 (m, 1H), 3.62 (m, 1H), 3.74 (s, 3H, OCH_3), 4.58 (dd, J = 8.8, 4.8, 1H, $\text{CHCH}(\text{CH}_3)_2$), 5.90 (d, J = 8.8, 1H, NH). ^{13}C -NMR (100 MHz, CDCl_3) δ = 12.04, 17.86, 18.36, 18.93, 20.81, 23.37, 24.20, 26.42, 27.20, 28.24, 30.52, 31.35, 31.72, 33.55, 34.57, 35.35, 35.45, 35.84, 36.44, 40.18, 40.42, 42.09, 42.74, 52.11, 56.02, 56.48, 56.79, 71.80, 172.80, 173.47. MS (ESI) calc for $\text{C}_{30}\text{H}_{51}\text{NO}_4$: 489.38; found: 488.5 $[\text{M}-1]^-$. Anal. calc for $\text{C}_{30}\text{H}_{51}\text{NO}_4$: C, 73.57; H, 10.50; N, 2.86; found: C, 73.55; H, 10.47; N, 2.85.

***N*-[(3 α ,5 β)-3-hydroxy-24-oxocholan-24-yl]-L-Valine (6).**



Compound **6** was synthesized following the procedure described for **2** using **6a**. The crude product was re-crystallized from (EtOH/H₂O) to give **6**. Yield: 92%. Mp: 229-232°C. ¹H-NMR (400 MHz, DMSO-d₆) δ = 0.59 (s, 3H, CH₃), 0.84-0.91 (m, 13H), 1.00-1.07 (m, 4H), 1.11-1.17 (m, 6H), 1.32 (m, 7H), 1.50 (m, 2H), 1.58-1.68 (m, 3H), 1.77 (m, 2H), 1.90-1.92 (m, 1H), 1.98-2.07 (m, 2H), 2.16-2.20 (m, 1H), 3.35 (m, 1H), 4.10 (dd, J = 8.40, 6.00, 1H, CHCH(CH₃)₂), 4.43 (bs, 1H, OH), 7.88 (d, J = 8.40, 1H, NH). ¹³C-NMR (100 MHz, DMSO-d₆) δ = 12.33, 18.54, 18.80, 19.63, 20.88, 23.74, 24.31, 26.64, 27.36, 28.17, 30.23, 30.85, 32.10, 32.44, 34.67, 35.41, 35.62, 35.85, 36.76, 41.99, 42.72, 56.04, 56.56, 57.48, 70.33, 173.38, 173.68. MS (ESI) calc for C₂₉H₄₉NO₄: 475.37; found: 474.5 [M-1]. Anal. calc for C₂₉H₄₉NO₄: C, 73.22; H, 10.38; N, 2.94; found: C, 73.26; H, 10.69; N, 2.96.

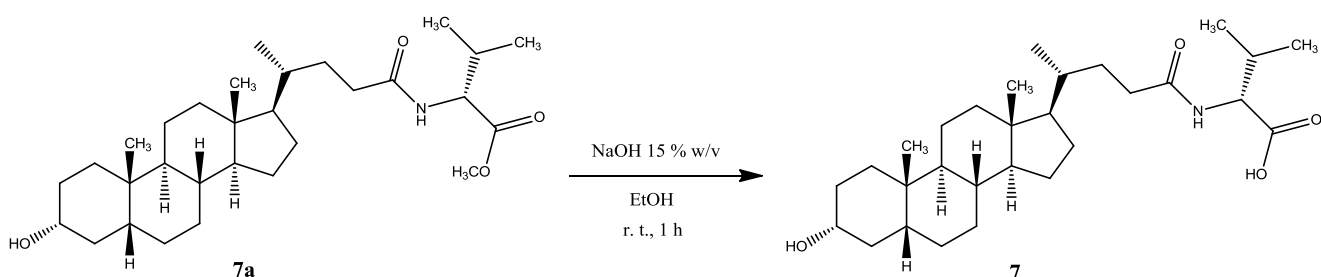
N-[(3 α ,5 β)-3-hydroxy-24-oxocholan-24-yl]- D-Valine methyl ester (**7a**).



Compound **7a** was synthesized following the procedure described for **3** using D-valine methyl ester hydrochloride and purified by flash chromatography [SiO₂, CH₂Cl₂:C₂H₅OH 98:2]. The crude product was re-crystallized from ethanol-water to give **7a** (EtOH/H₂O). Yield: 77%. Mp: 173-176°C. ¹H-NMR (400 MHz, CDCl₃) δ = 0.63 (s, 3H, CH₃), 0.88-0.93 (m, 12H), 0.95-1.15 (m, 5H), 1.23-1.38 (m, 11H), 1.48-1.64 (m, 4H), 1.72-1.86 (m, 5H), 1.93-1.96 (m, 1H), 2.09-2.16 (m, 2H), 2.25-2.33 (m, 1H), 3.58-3.64 (m, 1H), 3.73 (s, 3H, OCH₃), 4.57 (dd, J = 8.8, 5.2, 1H, CHCH(CH₃)₂),

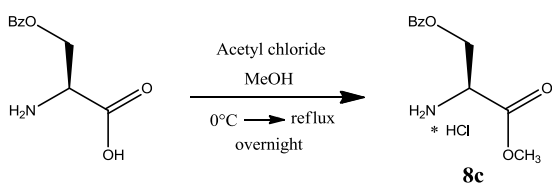
5.92 (d, $J = 8.8$, 1H, NH). $^{13}\text{C-NMR}$ (100 MHz, CDCl_3) $\delta = 12.04$, 17.85, 18.33, 18.93, 20.81, 23.37, 24.20, 26.41, 27.20, 28.21, 30.52, 31.33, 31.66, 33.58, 34.57, 35.39, 35.84, 36.44, 40.18, 40.41, 42.09, 42.74, 52.10, 56.03, 56.48, 56.81, 71.79, 172.79, 173.42. MS (ESI) calc for $\text{C}_{30}\text{H}_{51}\text{NO}_4$: 489.38; found: 490.6 $[\text{M}+\text{H}]^+$, 512.5 $[\text{M}+\text{Na}]^+$. Anal. calc for $\text{C}_{30}\text{H}_{51}\text{NO}_4$: C, 73.57; H, 10.50; N, 2.86; found: C, 73.59; H, 10.66; N, 2.86.

N-[(3 α ,5 β)-3-hydroxy-24-oxocholan-24-yl]- *D*-Valine (**7**).



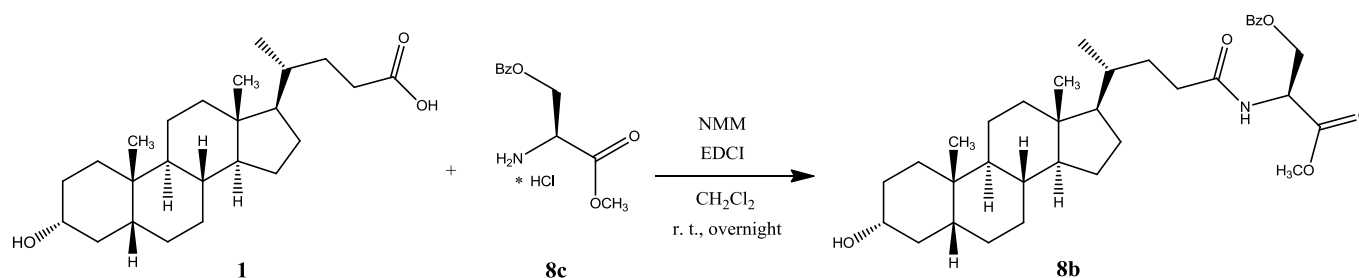
Compound **7** was synthesized following the procedure described for compound **2** starting from **7a**. The crude product was re-crystallized from (EtOH/ H_2O) to give **7**. Yield: 92%. Mp: 215-218°C. $^1\text{H-NMR}$ (400 MHz, DMSO-d_6) $\delta = 0.61$ (s, 3H, CH_3), 0.87-0.94 (m, 13H), 1.02-1.27 (m, 10H), 1.29-1.38 (m, 7H), 1.50-1.61 (m, 3H), 1.64-1.71 (m, 2H), 1.76-1.83 (m, 2H), 1.91-1.94 (m, 1H), 2.00-2.07 (m, 2H), 2.12-2.17 (m, 1H), 3.37-3.39 (m, 1H), 4.15 (dd, $J = 8.4$, 6.00, 1H, $\text{CHCH}(\text{CH}_3)_2$), 7.62 (d, $J = 8.0$, 1H, NH). $^{13}\text{C-NMR}$ (100 MHz, DMSO-d_6) $\delta = 12.35$, 18.54, 18.78, 19.53, 20.94, 23.68, 24.29, 26.64, 27.43, 28.06, 30.31, 30.95, 32.03, 32.74, 34.75, 35.26, 35.74, 35.99, 36.92, 42.18, 42.85, 56.34, 56.67, 57.61, 70.43, 173.23, 173.39. MS (ESI) calc for $\text{C}_{29}\text{H}_{49}\text{NO}_4$: 475.37; found: 474.5 $[\text{M}-1]^-$. Anal. calc for $\text{C}_{29}\text{H}_{49}\text{NO}_4 \cdot 0.1\text{H}_2\text{O}$: C, 72.94; H, 10.38; N, 2.93; found: C, 72.66; H, 10.47; N, 2.91.

O-Benzyl-*L*-Serine methyl ester hydrochloride (**8c**).



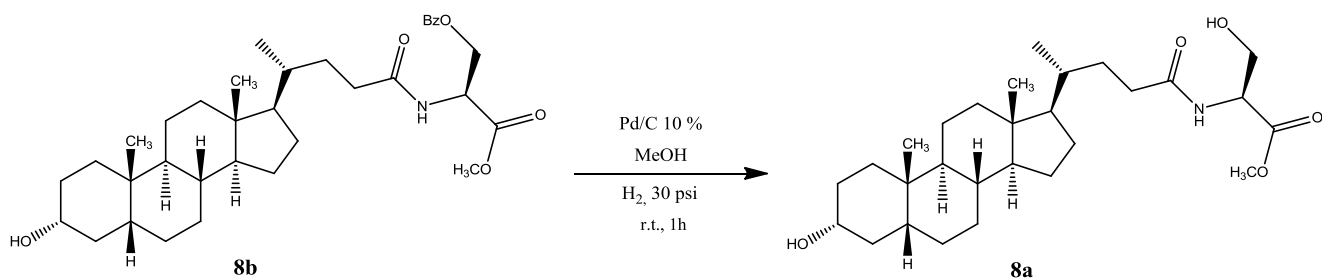
Compound **8c** was synthesized following a described procedure⁴² starting from O-Benzyl-L-Serine.

***N*-[(3 α ,5 β)-3-hydroxy-24-oxocholan-24-yl]-O-Benzyl-L-Serine methyl ester (**8b**).**



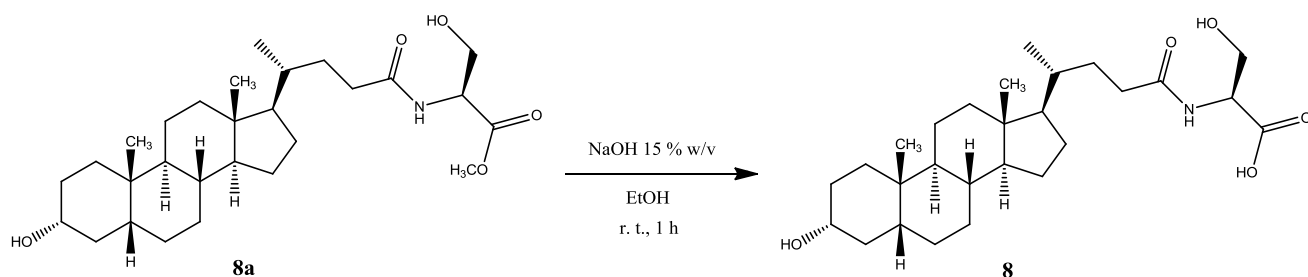
Compound **8b** was synthesized following the procedure described for **3** starting from O-benzyl-L-Serine methyl ester hydrochloride **8c** and purified by flash chromatography [SiO₂, CH₂Cl₂:C₂H₅OH 98:2]. The crude product was re-crystallized from ethanol-water to give **8b** (EtOH/H₂O). Yield: 79%. Mp: 145-148°C. ¹H-NMR (400 MHz, CDCl₃) δ = 0.63 (s, 3H, CH₃), 0.91-0.93 (m, 6H), 0.95-1.16 (m, 5H), 1.23-1.40 (m, 11H), 1.48-1.63 (m, 4H), 1.71-1.84 (m, 5H), 1.94-1.97 (m, 1H), 2.09-2.17 (m, 1H), 2.24-2.32 (m, 1H), 3.61-3.57 (m, 1H), 3.68 (dd, J = 9.44, 3.16 Hz, 1H, CHCHH), 3.74 (s, 3H, OCH₃), 3.89 (dd, J = 9.44, 3.08 Hz, 1H CHCHH), 4.48 (d, J = 12.2 Hz, 1H, CHHPh), 4.53 (d, J = 12.2 Hz, 1H, CHHPh), 4.76 (dt, J = 8.2, 3.1 Hz, 1H, CHCH₂), 6.30 (d, J = 7.9 Hz, 1H, NH), 7.25-7.36 (m, 5H, Ar). ¹³C-NMR (100 MHz, CDCl₃) δ = 12.06, 18.38, 20.82, 23.38, 24.22, 26.42, 27.20, 28.24, 30.54, 31.53, 33.37, 34.58, 35.36, 35.45, 35.85, 36.45, 40.19, 40.42, 42.10, 42.75, 52.46, 52.52, 56.02, 56.50, 69.78, 71.83, 73.27, 127.66, 127.91, 128.46, 137.51, 170.92, 173.39. MS (ESI) calc for C₃₅H₅₃NO₅: 567.39; found: 568.6 [M+H]⁺, 590.5 [M+Na]⁺, 606.4 [M+K]⁺. Anal. calc for C₃₅H₅₃NO₅: C, 74.04; H, 9.41; N, 2.47; found: C, 74.13; H, 9.63; N, 2.43.

***N*-[(3 α ,5 β)-3-hydroxy-24-oxocholan-24-yl]-L-Serine methyl ester (**8a**).**



Compound **8b** (0.405 mmol) was dissolved in 25 ml of MeOH in a bottle reaction, Pd/C 10% (0.01032 mmol) was added to the solution and the mixture was shaken under H₂ atmosphere (30 psi) for 3h on a Parr apparatus. The reaction mixture was filtered over a pad of Celite and the solvent was removed under reduced pressure. The residue was then purified by flash chromatography (CH₂Cl₂/HCOOH/EtOH: 89.5/0.5/10), giving the title compound as a white solid **8a**. Yield: 98%. Mp: 165-170°C. ¹H-NMR (400 MHz, CD₃OD) δ = 0.69 (s, 3H, CH₃), 0.94-0.98 (m, 6H), 1.06-1.19 (m, 5H), 1.25-1.49 (m, 13H), 1.61-1.63 (m, 2H), 1.72-1.82 (m, 3H), 1.86-1.90 (m, 2H), 2.01-2.04 (m, 1H), 2.16-2.24 (m, 1H), 2.28-2.36 (m, 1H), 3.49-3.56 (m, 1H), 3.73 (s, 3H, OCH₃), 3.78 (dd, *J* = 11.2, 4.3 Hz, 1H, CHCHH), 3.87 (dd, *J* = 11.2, 5.0 Hz, 1H, CHCHH), 4.52-4.97 (m, H, CHCH₂). ¹³C-NMR (100 MHz, CD₃OD) δ = 11.12, 17.49, 20.56, 22.55, 23.88, 26.26, 26.97, 27.85, 29.79, 31.63, 32.34, 34.28, 35.09, 35.39, 35.78, 35.84, 40.15, 40.49, 42.14, 42.52, 51.36, 54.78, 56.11, 56.54, 61.43, 71.01, 171.01, 175.44. MS (ESI) calc for C₂₈H₄₇NO₅: 477.35; found: 478.5 [M+H]⁺, 500.4 [M+Na]⁺. Anal. calc for C₂₈H₄₇NO₅ • 1H₂O: C, 67.84; H, 9.96; N, 2.82; found: C, 68.12; H, 10.08; N, 2.70.

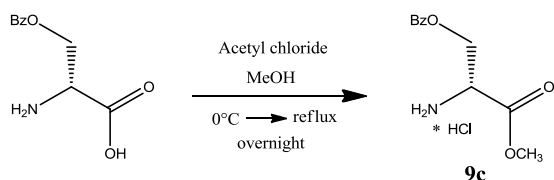
***N*-[(3 α ,5 β)-3-hydroxy-24-oxocholan-24-yl]- L-Serine (**8**).**



Compound **8** was synthesized following the procedure described for compound **2** starting from **8a**. The crude product was re-crystallized from (EtOH/H₂O) to give **8**

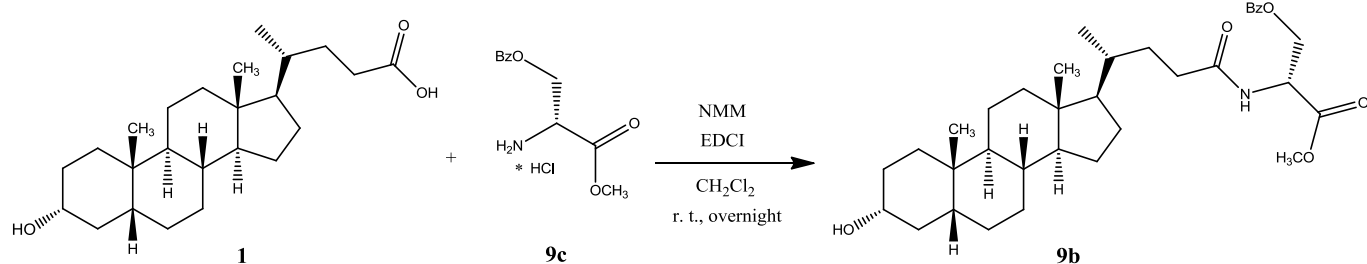
Yield: 87%. Mp: 180-183°C. $^1\text{H-NMR}$ (400 MHz, DMSO- d_6) δ = 0.44 (s, 3H, CH_3), 0.87-0.91 (m, 6H), 1.02-1.06 (m, 7H), 1.11-1.17 (m, 6H), 1.33-1.43 (m, 5H), 1.50 (m, 2H), 1.58-1.68 (m, 3H), 1.77-1.85 (m, 2H), 1.90-1.92 (m, 1H), 2.00-2.06 (m, 1H), 2.14-2.16 (m, 1H), 3.57-3.66 (m, 2H, CHCHH), 4.24-4.29 (m, 1H, CHCH_2), 4.41 (bs, 1H, OH), 7.88 (d, J = 7.60, 1H, NH). $^{13}\text{C-NMR}$ (100 MHz, DMSO- d_6) δ = 12.33, 18.80, 20.87, 23.73, 24.32, 26.63, 27.36, 28.19, 30.83, 31.90, 32.51, 34.66, 35.38, 35.61, 35.85, 36.75, 41.99, 42.72, 55.01, 56.11, 56.56, 61.90, 70.32, 172.63, 173.15. MS (ESI) calc for $\text{C}_{27}\text{H}_{45}\text{NO}_5$: 463.33; found: 462.5 $[\text{M-H}]^-$. Anal. calc for $\text{C}_{27}\text{H}_{45}\text{NO}_5$: C, 69.94; H, 9.78; N, 3.02; found: C, 69.77; H, 10.10; N, 2.89.

O-Benzyl-D-Serine methyl ester hydrochloride(**9c**).



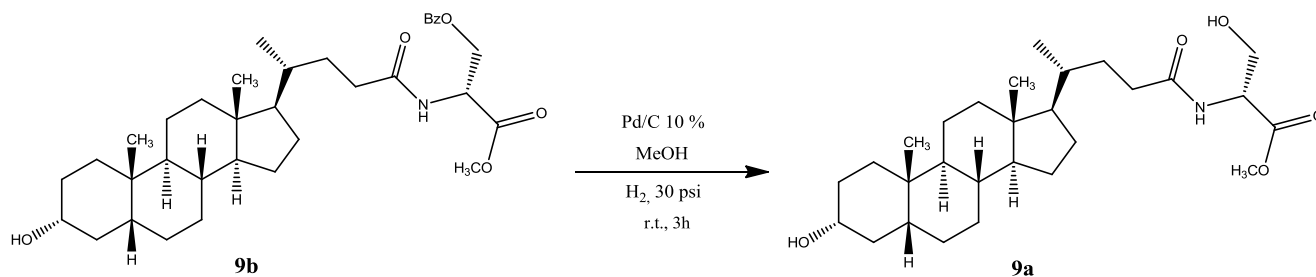
Compound **9c** was synthesized following a modification of a described procedure⁴³ in which acetyl chloride (3.84 mmol) was added dropwise to a methanol (10 ml) at 0°C. The mixture was stirred for 15 min and O-benzyl-D-serine (0.512 mmol) was then added portionwise to the solution. The resulting mixture was heated to reflux overnight. The solvent was evaporated under reduced pressure afforded **9c** as a white solid that was immediately used in the next step without further purification. Yield (99%). $^1\text{H-NMR}$ (400 MHz, D_2O) δ = 3.84 (s, 3H, OCH_3), 3.95 (dd, J = 14.8, 4.4 Hz, 1H, CHCHH), 4.02 (dd, J = 14.8, 5.8 Hz, 1H, CHCHH), 4.39 (dd, J = 6.0, 4.0 Hz, 1H, CHCH_2), 4.59 (d, J = 15.6 Hz, 1H, CHHPh), 4.68 (d, J = 16.0 Hz, 1H, CHHPh), 7.40-7.48 (m, 5H, Ar). (ESI) calc for $\text{C}_{11}\text{H}_{15}\text{NO}_3$: 209.24 found: 205.23 $[\text{M+H}]^+$.

N-[(3 α ,5 β)-3-hydroxy-24-oxocholan-24-yl]- O-Benzyl-D-Serine methyl ester (**9b**).



Compound **9b** was synthesized following the procedure described for **3** starting from O-benzyl-D-Serine methyl ester hydrochloride **9c** and purified by flash chromatography [SiO_2 , CH_2Cl_2 : $\text{C}_2\text{H}_5\text{OH}$ 98:2]. The crude product was re-crystallized from ethanol-water to give **9b** ($\text{EtOH}/\text{H}_2\text{O}$). Yield: 79%. Mp: 187-190°C. $^1\text{H-NMR}$ (400 MHz, CDCl_3) δ = 0.64 (s, 3H, CH_3), 0.92-0.93 (m, 6H), 0.96-1.00 (m, 1H), 1.08-1.16 (m, 5H), 1.24-1.40 (m, 11H), 1.48-1.63 (m, 5H), 1.75-1.84 (m, 4H), 1.94-1.97 (m, 1H), 2.08-2.16 (m, 1H), 2.26-2.32 (m, 1H), 3.59-3.65 (m, 1H), 3.68 (dd, J = 9.2, 3.2 Hz, 1H, CHCHH), 3.74 (s, 3H, OCH_3), 3.89 (dd, J = 9.2, 3.2 Hz, 1H, CHCHH), 4.48 (d, J = 12.4 Hz, 1H, CHHPh), 4.53 (d, J = 12.0 Hz, 1H, CHHPh), 4.76 (dt, J = 8.4, 3.2 Hz, 1H, CHCH_2), 6.28 (d, J = 8.0 Hz, 1H, 1H), 7.26-7.36 (m, 5H, Ar). $^{13}\text{C-NMR}$ (100 MHz, CDCl_3) δ = 12.06, 18.37, 20.83, 23.39, 24.22, 26.43, 27.21, 28.23, 30.54, 31.52, 33.38, 34.58, 35.37, 35.46, 35.86, 36.46, 40.19, 40.42, 42.10, 42.75, 52.47, 52.52, 56.02, 56.48, 69.81, 71.81, 73.28, 127.65, 127.91, 128.45, 137.52, 170.91, 173.39. MS (ESI) calc for $\text{C}_{35}\text{H}_{53}\text{NO}_5$: 567.39; found: 568.6 $[\text{M}+\text{H}]^+$, 590.5 $[\text{M}+\text{Na}]^+$, 606.4 $[\text{M}+\text{K}]^+$. Anal. calc for $\text{C}_{35}\text{H}_{53}\text{NO}_5$: C, 74.04; H, 9.41; N, 2.47; found: C, 74.20; H, 9.63; N, 2.42.

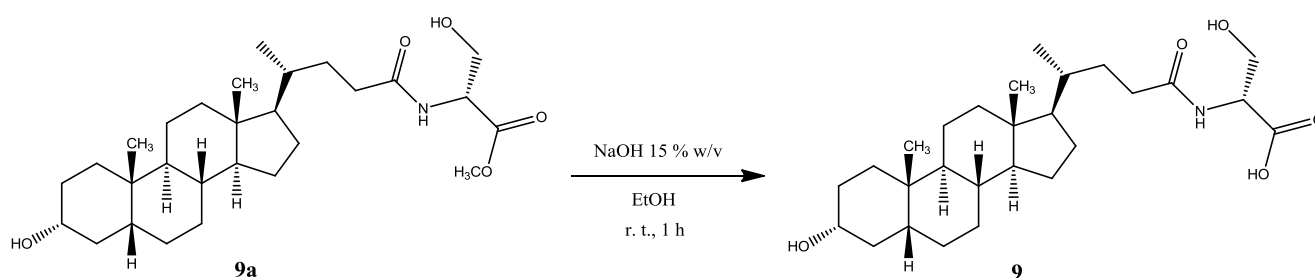
N-[(3 α ,5 β)-3-hydroxy-24-oxocholan-24-yl]- D-Serine methyl ester (**9a**).



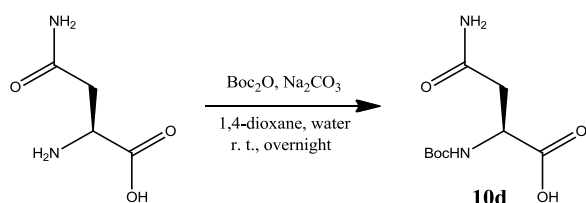
Compound **9a** was synthesized following the procedure described for **8a** starting from compound **9b**. Yield: 98 %. Mp: 173-176°C. $^1\text{H-NMR}$ (400 MHz, CDCl_3) δ = 0.64

(s, 3H, CH₃), 0.92-0.93 (m, 6H), 0.96-1.00 (m, 1H), 1.08-1.16 (m, 5H), 1.24-1.40 (m, 11H), 1.48-1.57 (m, 3H), 1.63-1.84 (m, 6H), 1.94-1.97 (m, 1H), 2.08-2.16 (m, 1H), 2.26-2.32 (m, 1H), 3.59-3.65 (m, 1H), 3.68 (dd, *J* = 9.2, 3.2 Hz, 1H, CHCHH), 3.74 (s, 3H, OCH₃), 3.89 (dd, *J* = 9.2, 3.2 Hz, 1H, CHCHH), 4.48 (d, *J* = 12.4 Hz, 1H, CHHPh), 4.53 (d, *J* = 12.0 Hz, 1H, CHHPh), 4.76 (dt, *J* = 8.4, 3.2 Hz, 1H, CHCH₂), 6.28 (d, *J* = 8.0 Hz, 1H, NH), 7.26-7.36 (m, 5H, Ar). ¹³C-NMR (100 MHz, CDCl₃) δ = 12.10, 18.35, 20.78, 23.40, 24.29, 26.48, 27.31, 28.21, 30.52, 31.48, 33.35, 34.54, 35.30, 35.31, 36.58, 36.37, 40.31, 40.56, 42.20, 42.65, 52.48, 52.53, 56.07, 56.45, 69.71, 71.78, 73.24, 127.23, 127.80, 128.78, 137.45, 170.51, 173.68. MS (ESI) calc for C₂₈H₄₇NO₅: 477.35; found: 500.4 [M+Na]⁺. Anal. calc for C₃₅H₅₃NO₅: C, 74.04; H, 9.41; N, 2.47; found: C, 74.30; H, 9.55; N, 2.58

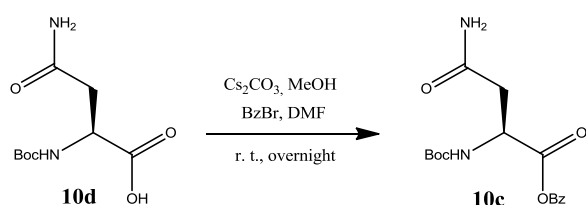
***N*-[(3 α ,5 β)-3-hydroxy-24-oxocholan-24-yl]-D-Serine (9).**



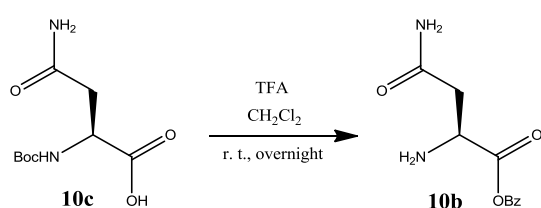
Compound **9** was synthesized following the procedure described for compound **2** starting from compound **9a**. The crude product was re-crystallized from (EtOH/H₂O) to give **9** Yield: 88%. Mp: 165-167°C. ¹H-NMR (400 MHz, DMSO-d₆) δ = 0.59 (s, 3H, CH₃), 0.86-0.91 (m, 7H), 1.01-1.07 (m, 4H), 1.14-1.17 (m, 6H), 1.33-1.46 (m, 7H), 1.50-1.58 (m, 3H), 1.61-1.68 (m, 2H), 1.77-1.84 (m, 2H), 1.90-1.92 (m, 1H), 2.00-2.07 (m, 1H), 2.14-2.16 (m, 1H), 3.56-3.63 (m, 2H, CHCHH), 4.23 (m, 1H, CHCH₂), 4.41 (bs, 1H, OH), 7.89 (d, *J* = 7.6, 1H, NH). ¹³C-NMR (100 MHz, DMSO-d₆) δ = 12.34, 18.77, 20.88, 23.74, 24.32, 26.63, 27.36, 28.19, 30.84, 31.86, 32.49, 34.67, 35.40, 35.61, 35.85, 36.75, 41.99, 42.73, 54.99, 56.09, 56.55, 61.91, 70.33, 172.62, 173.13. MS (ESI) calc for C₂₇H₄₅NO₅: 463.33; found: 461.9 [M-H]⁻. Anal. calc for C₂₇H₄₅NO₅ · 0.1H₂O: C, 69.67; H, 9.79; N, 3.00; found: C, 69.32; H, 10.09; N, 2.89.

N-(tert-Butoxycarbonyl)-L-Asparagine (10d).

Compound **10d** was synthesized according to a described procedure⁴⁴ starting from L-Asparagine.

N-(tert-Butoxycarbonyl)-L-Asparagine Benzyl ester (10c).

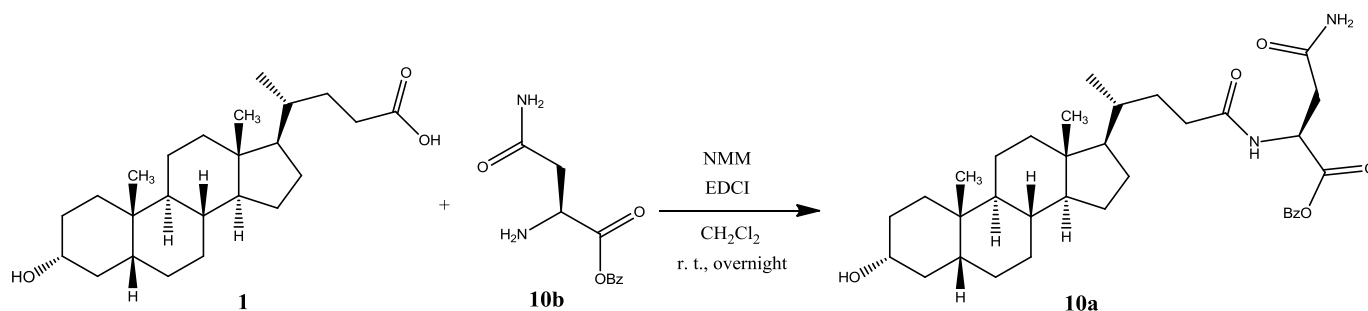
Compound **10c** was synthesized according to a described procedure⁴⁴ starting from **10d**.

L-Asparagine Benzyl ester (10b).

Compound **10b** was synthesized following a modification procedure⁴⁵ in which a solution of **10c** (1.148 mmol) in CH_2Cl_2 (10 ml) was added trifluoroacetic acid (1ml) the resulting solution was stirred at room temperature overnight. Evaporation of solvent under reduced pressure afforded to **10b** as a white solid that was immediately used in the next step without further purification. Yield 98%. $^1\text{H-NMR}$ (400 MHz, CDCl_3) δ = 2.52 (dd, J = 16.0, 8.8 Hz, 1H, CHCHH), 2.70 (dd, J = 16.0, 3.6 Hz, 1H, CHCHH), 3.84 (dd, J = 8.8, 3.6 Hz, 1H, CHCH₂), 5.14 (d, J = 12.4 Hz,

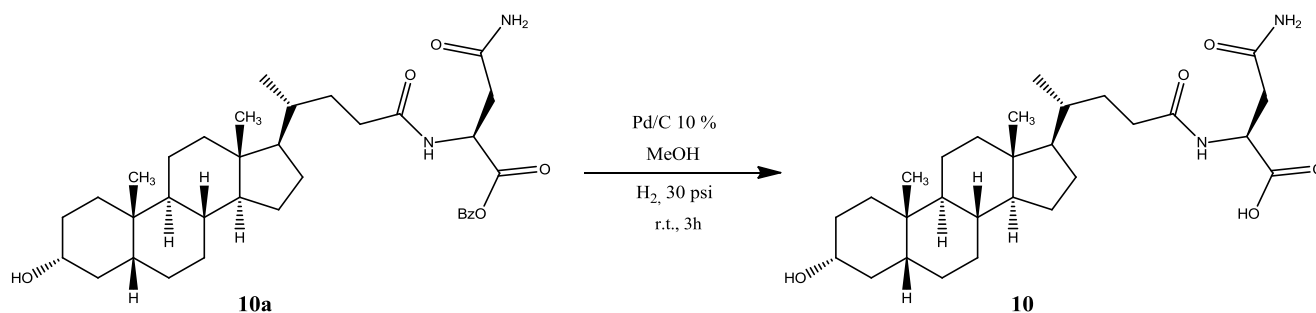
1H, *CHHP*h), 5.18 (d, $J = 12.4$ Hz, 1H, *CHHP*h), 5.53 (bs, 1H, *CONHH*), 6.85 (bs, 1H, *CONHH*), 7.35-7.38 (m, 5H, Ar). ^{13}C -NMR (100 MHz, CDCl_3) $\delta = 39.35, 51.46, 67.23, 128.33, 128.51, 128.65, 135.36, 172.60, 174.17$.

***N*-[(3 α ,5 β)-3-hydroxy-24-oxocholan-24-yl]- L-Asparagine benzyl ester (10a).**



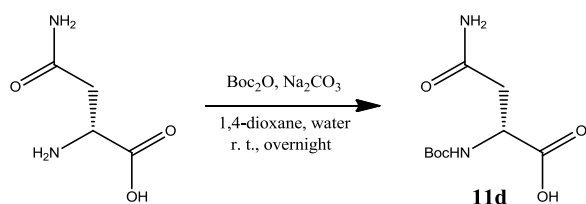
Compound **10a** was synthesized following the procedure described for **3** starting from L-Asparagine benzyl ester **10b** and purified by flash chromatography [SiO_2 , CH_2Cl_2 : $\text{C}_2\text{H}_5\text{OH}$ from 98:2 to 95:5]. The crude product was re-crystallized from ethanol-water to give **10a** (EtOH/ H_2O). Yield: 72%. Mp: 65-68°C. ^1H -NMR (400 MHz, CDCl_3) $\delta = 0.60$ (s, 3H, CH_3), 0.87-0.90 (m, 6H), 0.94-1.13 (m, 7H), 1.29-1.38 (m, 8H), 1.50 (m, 2H), 1.62 (m, 1H), 1.72-1.78 (m, 5H), 1.91-1.94 (m, 1H), 2.06-2.14 (m, 3H), 2.22-2.28 (m, 1H), 2.75 (dd, $J = 16.2, 4.4$ Hz, 1H, *CHCHH*), 2.93 (dd, $J = 16.2, 4.8$ Hz, 1H, *CHCHH*), 3.60 (m, 1H), 4.80 (dt, $J = 8.0, 4.6$ Hz, 1H, *CHCH}_2*), 5.14 (d, $J = 12.4$ Hz, 1H, *CHHP*h), 5.18 (d, $J = 12.4$ Hz, 1H, *CHHP*h), 5.69 (bs, 1H, *CONHH*), 6.18 (bs, 1H, *CONHH*), 6.89 (d, $J = 8.0$ Hz, 1H, NH), 7.26-7.35 (m, 5H, Ar). ^{13}C -NMR (100 MHz, CDCl_3) $\delta = 12.02, 18.36, 20.80, 23.37, 24.19, 26.42, 27.19, 28.19, 30.48, 31.55, 33.32, 34.56, 35.35, 35.44, 35.83, 36.40, 36.91, 40.16, 40.42, 42.09, 42.72, 48.92, 55.98, 56.47, 58.28, 67.46, 71.78, 128.18, 128.37, 128.56, 135.32, 137.32, 171.03, 172.54, 173.93$. MS (ESI) calc for $\text{C}_{35}\text{H}_{52}\text{N}_2\text{O}_5$: 580.39; found: 581.5 [$\text{M}+\text{H}$] $^+$, 603.4 [$\text{M}+\text{Na}$] $^+$, 619.5 [$\text{M}+\text{K}$] $^+$. Anal. calc for $\text{C}_{35}\text{H}_{52}\text{N}_2\text{O}_5$: C, 72.38; H, 9.02; N, 4.82; found: C, 72.42; H, 9.12; N, 4.93.

***N*-[(3 α ,5 β)-3-hydroxy-24-oxocholan-24-yl]- L-Asparagine (10).**



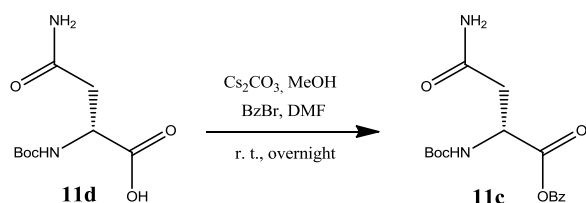
Compound **10a** (0.516 mmol) was dissolved in 20 ml of MeOH in a bottle reaction, Pd/C 10% (0.01032 mmol) was added to the solution and mixture was shaken under H₂ atmosphere (30 psi) for 3h on a Parr apparatus. The reaction mixture was filtered over a pad of Celite and the solvent was removed under reduced pressure. The residue was then purified by flash chromatography (CH₂Cl₂/HCOOH/EtOH 89.5/0.5/10), giving the title compound as a white solid **10**. The crude product was recrystallized from EtOH/H₂O. Yield: 98%. Mp: 164-167°C. ¹H-NMR (400 MHz, DMSO-d₆) δ = 0.59 (s, 3H, CH₃), 0.85-0.87 (m, 7H), 1.01-1.08 (m, 4H), 1.12-1.22 (m, 6H), 1.28-1.35 (m, 7H), 1.47-1.55 (m, 2H), 1.55-1.68 (m, 3H), 1.74-1.77 (m, 2H), 1.90-1.92 (m, 1H), 1.95-2.01 (m, 1H), 2.07-2.14 (m, 1H), 2.41 (dd, J = 15.5, 7.2 Hz, 1H, CHCHH), 2.49-2.54 (m, 1H, CHCHH), 3.35 (m, 1H), 4.45 (dd, J = 7.2, J = 7.0 Hz, 1H, CHCH₂), 6.84 (s, 1H, CONHH), 7.30 (s, 1H, CONHH), 7.93 (d, J = 7.9 Hz, 1H, NH). ¹³C-NMR (100 MHz, DMSO-d₆) δ = 12.34, 18.78, 20.88, 23.73, 24.31, 26.63, 27.36, 28.17, 30.85, 31.88, 32.59, 34.67, 35.33, 35.63, 35.86, 36.77, 37.27, 42.01, 42.74, 49.19, 56.11, 56.56, 70.34, 163.51, 171.73, 172.85, 173.45. MS (ESI) calc for C₂₈H₄₆N₂O₅: 490.34; found: 489.2 [M-H]⁻. Anal. calc for C₂₈H₄₆N₂O₅: C, 68.54; H, 9.45; N, 5.71; found: C, 68.28; H, 9.82; N, 5.54.

N-(tert-Butoxycarbonyl)-D-Asparagine (**11d**).



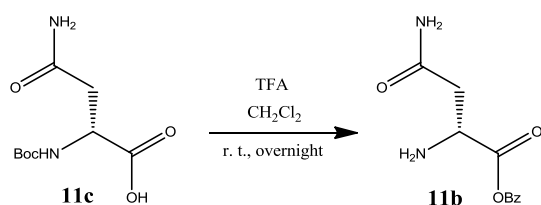
Compound **11d** was synthesized according to a described procedure⁴⁶ starting from D-Asparagine.

N-(tert-Butoxycarbonyl)-D-Asparagine Benzyl ester (**11c**).



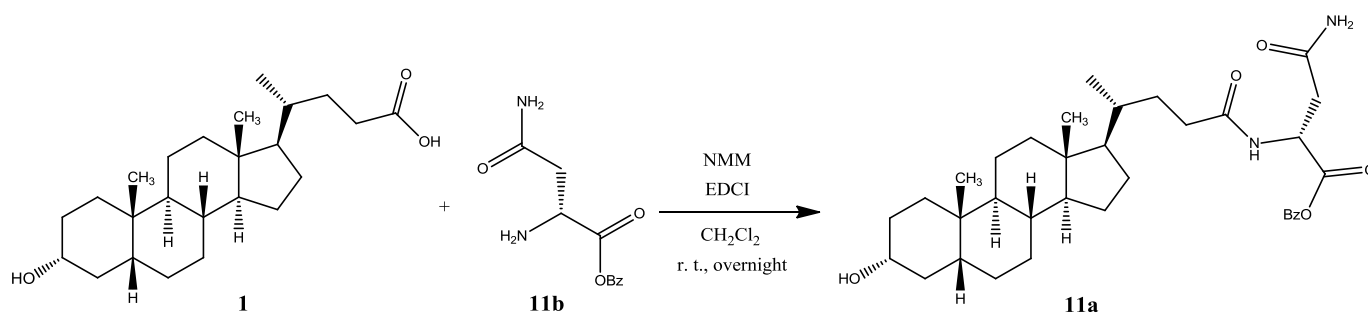
Compound **11c** was synthesized according to a described procedure⁴⁷ starting from **11d**.

D-Asparagine benzyl ester (**11b**).



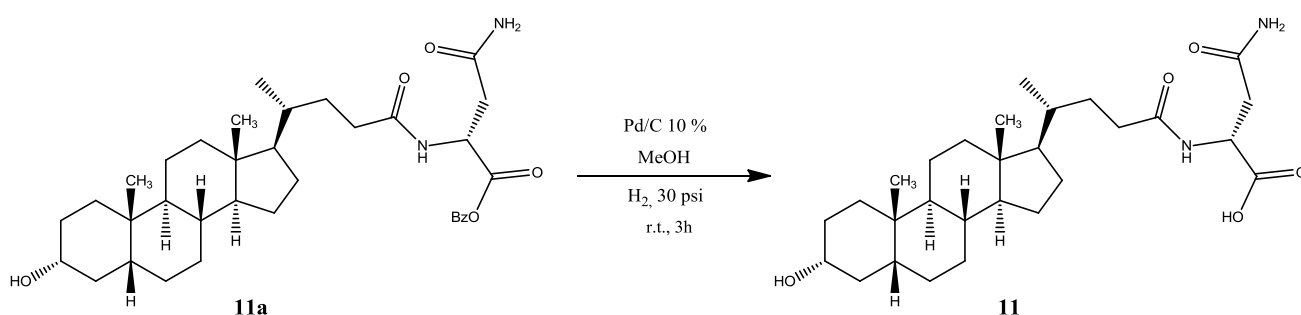
Compound **11b** was synthesized according to a described procedure⁴⁷ starting from **11c**.

N-[(3 α ,5 β)-3-hydroxy-24-oxocholan-24-yl]- D-Asparagine benzyl ester (**11a**).



Compound **11a** was synthesized following the procedure described for **3** starting from D-Asparagine benzyl ester **11b** and purified by flash chromatography [SiO_2 , $\text{CH}_2\text{Cl}_2:\text{C}_2\text{H}_5\text{OH}$ from 98:2 to 95:5]. The crude product was re-crystallized from ethanol-water to give **11a** (EtOH/ H_2O). Yield: 65%. Mp: 169-173°C. $^1\text{H-NMR}$ (400 MHz, DMSO-d_6) δ = 0.58 (s, 3H, CH_3), 0.84-0.91 (m, 7H), 1.00-1.07 (m, 4H), 1.15-1.18 (m, 6H), 1.32-1.35 (m, 7H), 1.50-1.55 (m, 2H), 1.58-1.68 (m, 3H), 1.74-1.77 (m, 2H), 1.89-1.92 (m, 1H), 1.94-2.01 (m, 1H), 2.07-2.16 (m, 1H), 2.46-2.50 (m, 1H, CHCHH), 2.57 (dd, J = 15.6, 6.0 Hz, 1H, CHCHH), 3.32-3.35 (m, 1H), 4.43 (d, J = 4.4 Hz, 1H, OH), 4.56-4.62 (m, 1H, CHCH_2), 5.05-5.07 (m, 2H, CHHPh), 6.91 (s, 1H, CONHH), 7.30-7.36 (m, 6H, 5Ar, CONHH), 8.17 (d, J = 8.00 Hz, 1H, NH). $^{13}\text{C-NMR}$ (100 MHz, DMSO-d_6) δ = 12.35, 18.73, 20.87, 23.74, 24.31, 26.64, 27.36, 28.17, 30.85, 31.87, 32.47, 34.67, 35.40, 35.62, 35.85, 36.77, 37.12, 41.99, 42.72, 49.33, 56.04, 56.54, 66.28, 70.33, 128.02, 128.34, 128.78, 136.51, 171.33, 171.90, 173.08. MS (ESI) calc for $\text{C}_{35}\text{H}_{52}\text{N}_2\text{O}_5$: 580.39; found: 581.3 $[\text{M}+\text{H}]^+$, 603.4 $[\text{M}+\text{Na}]^+$, 619.4 $[\text{M}+\text{K}]^+$. Anal. calc for $\text{C}_{35}\text{H}_{52}\text{N}_2\text{O}_5$: C, 72.38; H, 9.02; N, 4.82; found: C, 72.57; H, 9.22; N, 4.97.

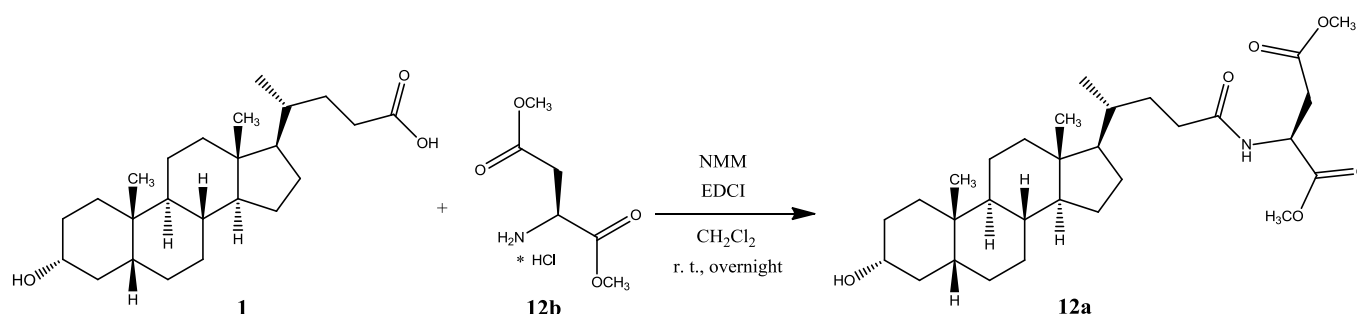
***N*-[(3 α ,5 β)-3-hydroxy-24-oxocholan-24-yl]- D-Asparagine (**11**).**



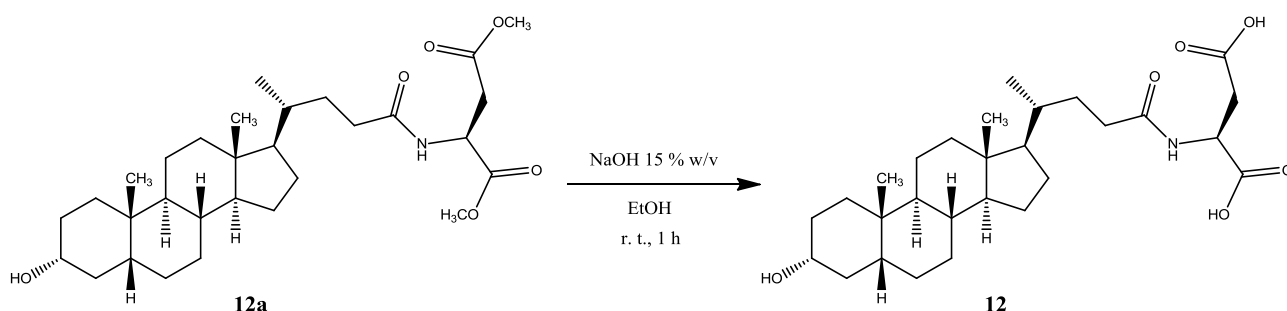
Compound **11** was synthesized following the procedure for **10** starting from **11a** and purified by flash chromatography ($\text{CH}_2\text{Cl}_2/\text{HCOOH}/\text{EtOH}$ 89.5/0.5/10). The crude product was re-crystallized from (EtOH/ H_2O) to give **11**. Yield: 99%. Mp: 167-170°C. $^1\text{H-NMR}$ (400 MHz, DMSO-d_6) δ = 0.59 (s, 3H, CH_3), 0.85-0.91 (m, 7H), 1.01-1.08 (m, 4H), 1.11-1.21 (m, 6H), 1.32-1.34 (m, 7H), 1.50-1.55 (m, 2H), 1.58-1.68 (m, 3H), 1.68-1.77 (m, 2H), 1.90-1.94 (m, 1H), 1.96-2.02 (m, 1H), 2.07-2.13 (m, 1H), 2.40 (dd, J = 15.5, 7.1 Hz, 1H, CHCHH), 2.48-2.54 (m, 1H, CHCHH), 3.31-3.38 (m, 1H), 4.45

(dd, $J = 7.2, J = 7.0$ Hz, 1H, CHCH₂), 6.86 (s, 1H, CONHH), 7.31 (s, 1H, CONHH), 7.96 (d, $J = 7.92$ Hz, 1H, NH). ¹³C-NMR (100 MHz, DMSO-d₆) $\delta = 12.35, 18.74, 20.88, 23.73, 24.32, 26.63, 27.36, 28.18, 30.85, 31.87, 32.56, 34.67, 35.34, 35.62, 35.86, 36.77, 37.28, 42.00, 42.74, 49.17, 56.10, 56.55, 70.33, 163.53, 171.72, 172.82, 173.46$. MS (ESI) calc for C₂₈H₄₆N₂O₅: 490.34; found: 489.2 [M-H]⁻. Anal. calc for C₂₈H₄₆N₂O₅ • 0.1H₂O: C, 68.29; H, 9.45; N, 5.69; found: C, 67.96; H, 9.71; N, 5.63.

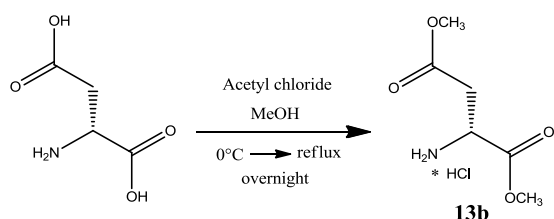
***N*-[(3 α ,5 β)-3-hydroxy-24-oxocholan-24-yl]- L-Aspartic acid dimethyl ester (**12a**).**



Compound **12a** was synthesized following the procedure described for **3** starting from L-Aspartic acid dimethyl ester hydrochloride and purified by flash chromatography [SiO₂, CH₂Cl₂:C₂H₅OH 98:2]. The crude product was re-crystallized from ethanol-water to give **12a** (EtOH/H₂O). Yield: 67%. Mp: 164-167°C. ¹H-NMR (400 MHz, CDCl₃) $\delta = 0.64$ (s, 3H, CH₃), 0.91-0.93 (m, 6H), 0.96-1.16 (m, 7H), 1.24-1.27 (m, 4H), 1.31-1.43 (m, 7H), 1.63-1.67 (m, 2H), 1.71-1.87 (m, 5H), 1.94-1.97 (m, 1H), 2.09-2.17 (m, 1H), 2.24-2.32 (m, 1H), 2.84 (dd, $J = 17.2, 4.4$ Hz, 1H, CHCHH), 3.03 (dd, $J = 17.2, 4.4$ Hz, 1H, CHCHH), 3.59-3.66 (m, 1H), 3.69 (s, 3H, OCH₃), 3.76 (s, 3H, OCH₃), 4.87 (dt, $J = 8.0, 4.4$ Hz, 1H, CHCH₂), 6.44 (d, $J = 8.0$ Hz, 1H, NH). ¹³C-NMR (100 MHz, CDCl₃) $\delta = 12.03, 18.33, 20.81, 23.37, 24.20, 26.41, 27.19, 28.22, 30.53, 31.49, 33.35, 34.57, 35.35, 35.41, 35.84, 36.11, 36.45, 40.18, 40.42, 42.09, 42.74, 48.30, 52.01, 52.78, 56.02, 56.48, 71.80, 171.32, 171.66, 173.32$. MS (ESI) calc for C₃₀H₄₉NO₆: 519.36; found: 520.3 [M+H]⁺, 542.5 [M+Na]⁺, 558.3 [M+K]⁺. Anal. calc for C₃₀H₄₉NO₆: C, 69.33; H, 9.50; N, 2.70; found: C, 69.13; H, 9.69; N, 2.65.

***N*-[(3 α ,5 β)-3-hydroxy-24-oxocholan-24-yl]- L-Aspartic acid (**12**).**

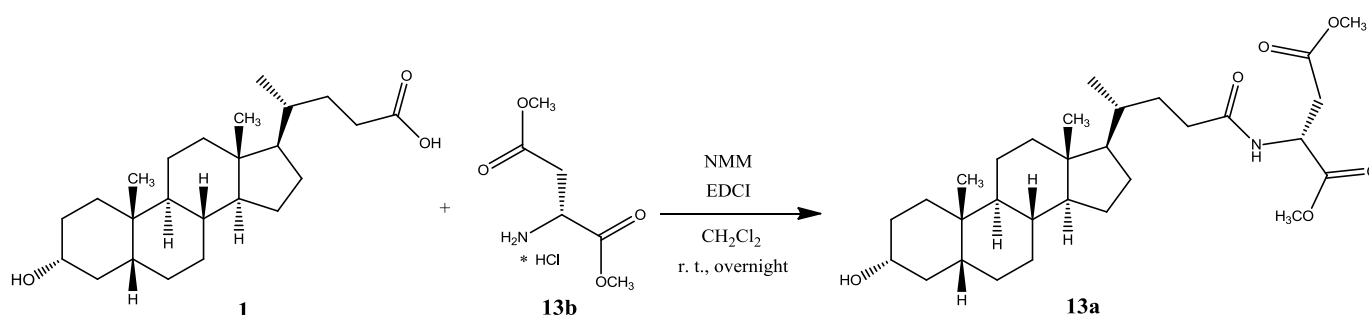
Compound **12** was synthesized following the procedure described for **2** using compound **12a** starting from compound **12a**. The crude product was re-crystallized from (EtOH/H₂O) to give **12**. Yield: 92%. Mp: 207-210°C. ¹H-NMR (400 MHz, DMSO-d₆) δ = 0.59 (s, 3H, CH₃), 0.86-0.91 (m, 7H), 1.01-1.08 (m, 4H), 1.11-1.17 (m, 6H), 1.32 (m, 7H), 1.50 (m, 2H), 1.58-1.68 (m, 3H), 1.77 (m, 2H), 1.90-1.92 (m, 1H), 1.95-2.03 (m, 1H), 2.08-2.11 (m, 1H), 2.52 (dd, J = 16.4, 7.2 Hz, 1H, CHCHH), 2.65 (dd, J = 16.4, 5.6 Hz, 1H, CHCHH), 4.42-4.50 (m, 2H, OH+ CHCH₂), 8.09 (d, J = 8.0 Hz, 1H, NH). ¹³C-NMR (100 MHz, DMSO-d₆) δ = 12.33, 18.76, 20.88, 23.74, 24.32, 26.63, 27.36, 28.18, 30.85, 31.88, 32.53, 34.67, 35.32, 35.62, 35.85, 36.52, 36.76, 41.99, 42.73, 48.98, 56.09, 56.56, 70.33, 172.14, 172.93, 173.03. MS (ESI) calc for C₂₈H₄₅NO₆: 491.32; found: 490.5 [M-H]⁻. Anal. calc for C₂₈H₄₅NO₆: C, 68.40; H, 9.22; N, 2.85; found: C, 68.33; H, 9.40; N, 2.79.

D-Aspartic acid dimethyl ester hydrochloride (13b**).**

Compound **13b** was synthesized following a modification of a described procedure⁴⁸ in which acetyl chloride (15.40 mmol) was added dropwise to a methanol (10 ml) at 0°C. The mixture was stirred for 15 min and D-aspartic acid (4.8 mmol) was then added portionwise to the solution. The resulting mixture was heated to reflux

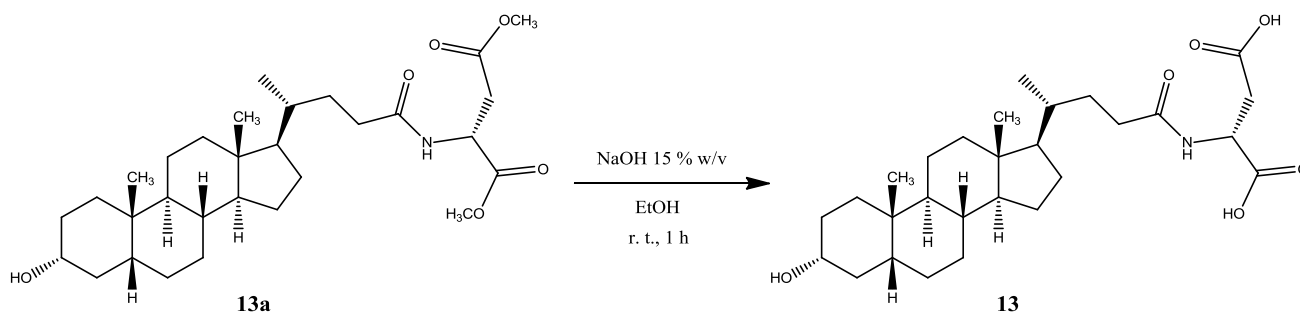
overnight. The solvent was evaporated under reduced pressure afforded the D-Aspartic acid dimethyl ester hydrochloride **13b** as a white solid that was immediately used in the next step without further purification. Yield (73%). $^1\text{H-NMR}$ (400 MHz, D_2O) δ = 3.04 (dd, J = 18.0, 4.8 Hz, 1H, CHCHH), 3.12 (dd, J = 18.0, 6.0 Hz, 1H, CHCHH), 3.66 (s, 3H, OCH_3), 3.75 (s, 3H, OCH_3), 4.40-4.42 (m, 1H, CHCH $_2$). (ESI) calc for $\text{C}_6\text{H}_{12}\text{NO}_4$: 162.16 found: 163.14 $[\text{M}+\text{H}]^+$.

***N*-[(3 α ,5 β)-3-hydroxy-24-oxocholan-24-yl]- D-Aspartic acid dimethyl ester (**13a**).**



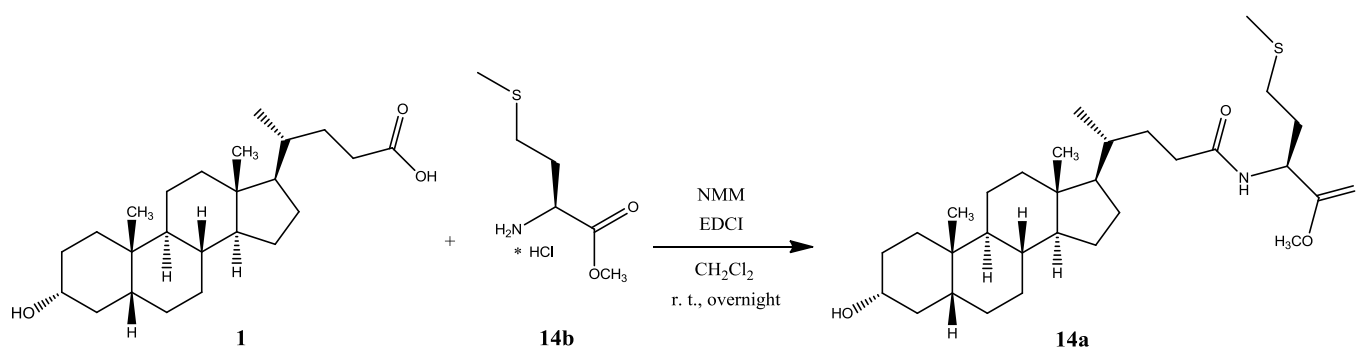
Compound **13a** was synthesized following the procedure described for **3** starting from D-Aspartic acid dimethyl ester hydrochloride **13b** and purified by flash chromatography [SiO_2 , CH_2Cl_2 : $\text{C}_2\text{H}_5\text{OH}$ 98:2]. The crude product was re-crystallized from ethanol-water to give **13a** (EtOH/ H_2O). Yield: 65%. Mp: 179-182°C. $^1\text{H-NMR}$ (400 MHz, CDCl_3) δ = 0.62 (s, 3H, CH_3), 0.89-0.90 (m, 6H), 0.94-1.11 (m, 7H), 1.14-1.38 (m, 11H), 1.63-1.65 (m, 1H), 1.70-1.86 (m, 6H), 1.92-1.95 (m, 1H), 2.06-2.14 (m, 1H), 2.24-2.32 (m, 1H), 2.83 (dd, J = 17.20, 4.40 Hz, 1H, CHCHH), 3.01 (dd, J = 17.20, 4.40 Hz, 1H, CHCHH), 3.57-3.64 (m, 1H), 3.68 (s, 3H, OCH_3), 3.74 (s, 3H, CH_3), 4.84 (dt, J = 8.00, 4.40 Hz, 1H, CHCH $_2$), 6.49 (d, J = 7.60 Hz, 1H, NH). $^{13}\text{C-NMR}$ (100 MHz, CDCl_3) δ = 12.02, 18.32, 20.81, 23.37, 24.20, 26.41, 27.19, 28.21, 30.52, 31.49, 33.34, 34.57, 35.35, 35.42, 35.84, 36.13, 36.44, 40.17, 40.41, 42.09, 42.73, 48.33, 52.01, 52.78, 56.00, 56.47, 71.79, 171.31, 171.64, 173.36. MS (ESI) calc for $\text{C}_{30}\text{H}_{49}\text{NO}_6$: 519.36; found: 518.3 $[\text{M}-\text{H}]^-$. Anal. calc for $\text{C}_{30}\text{H}_{49}\text{NO}_6$: C, 69.33; H, 9.50; N, 2.70; found: C, 69.20; H, 9.67; N, 2.63.

***N*-[(3 α ,5 β)-3-hydroxy-24-oxocholan-24-yl]- D-Aspartic acid (**13**).**



Compound **13** was synthesized following the procedure described for **2** using **13a**. The crude product was re-crystallized from (EtOH/H₂O) to give **13**. Yield: 96%. Mp: 200-204°C. ¹H-NMR (400 MHz, DMSO-d₆) δ = 0.59 (s, 3H, CH₃), 0.86-0.91 (m, 7H), 1.01-1.08 (m, 4H), 1.11-1.17 (m, 6H), 1.32-1.50 (m, 9H), 1.58-1.68 (m, 3H), 1.77 (m, 2H), 1.90-1.92 (m, 1H), 1.96-2.03 (m, 1H), 2.08-2.13 (m, 1H), 2.45-2.49 (m, 1H, CHCHH), 2.60 (dd, J = 16.4, 7.2 Hz, 1H, CHCHH), 4.40 (m, 1H, CHCH₂), 7.98 (d, J = 7.6 Hz, 1H, NH). ¹³C-NMR (100 MHz, DMSO-d₆) δ = 12.33, 18.74, 20.87, 23.74, 24.32, 26.63, 27.36, 28.18, 30.85, 31.88, 32.55, 34.67, 35.32, 35.62, 35.85, 36.76, 37.52, 41.99, 42.73, 48.96, 56.07, 56.55, 70.33, 172.36, 172.72, 173.23. MS (ESI) calc for C₂₈H₄₅NO₆: 491.32; found: 490.6 [M-H]. Anal. calc for C₂₈H₄₅NO₆ • 0.25H₂O: C, 67.78; H, 9.24; N, 2.82; found: C, 67.97; H, 9.36; N, 2.88.

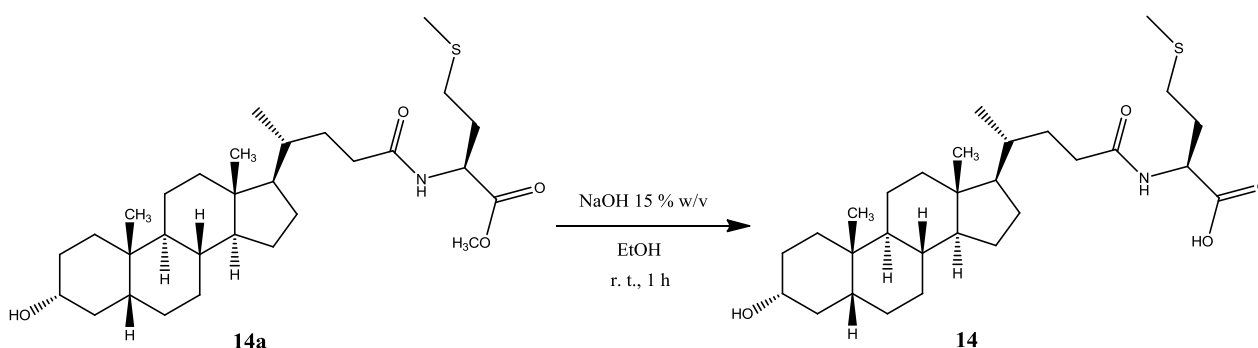
***N*-[(3 α ,5 β)-3-hydroxy-24-oxocholan-24-yl]- L-Methionine methyl ester (**14a**).**



Compound **14a** was synthesized following the procedure described for **3** using L-Methionine methyl ester hydrochloride and purified by flash chromatography [SiO₂, CH₂Cl₂:C₂H₅OH 98:2]. The crude product was re-crystallized from ethanol-water to give **14a** (EtOH/H₂O). Yield: 67%. Mp: 149-152°C.⁴⁹ ¹H-NMR (400 MHz, CDCl₃) δ = 0.64 (s, 3H, CH₃), 0.91-0.93 (m, 6H), 0.96-1.13 (m, 5H), 1.26 (m, 4H), 1.38 (m, 7H),

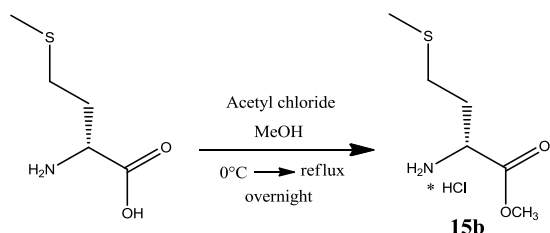
1.64 (m, 5H), 1.77-1.84 (m, 4H), 1.97 (m, 2H), 2.09 (s, 3H, SCH₃), 2.14 (m, 2H), 2.29 (m, 1H), 2.51 (m, 2H, CHCHH). 3.59-3.62 (m, 1H), 3.76 (s, 3H, OCH₃), 4.70-4.75 (m, 1H, CHCH₂), 6.12 (d, *J* = 7.7) Hz, 1H, NH). ¹³C-NMR (100 MHz, CDCl₃) δ = 12.04, 15.50, 18.37, 20.81, 23.37, 24.20, 26.41, 27.19, 28.26, 29.99, 30.53, 31.60, 31.77, 33.43, 34.57, 35.35, 35.44, 35.84, 36.45, 40.18, 40.42, 42.09, 42.74, 51.41, 52.51, 56.00, 56.48, 71.81, 172.67, 173.40. MS (ESI) calc for C₃₀H₅₁NO₄S: 521.35; found: 520.3 [M-H]⁻.

***N*-[(3 α ,5 β)-3-hydroxy-24-oxocholan-24-yl]- L-Methionine (14).**



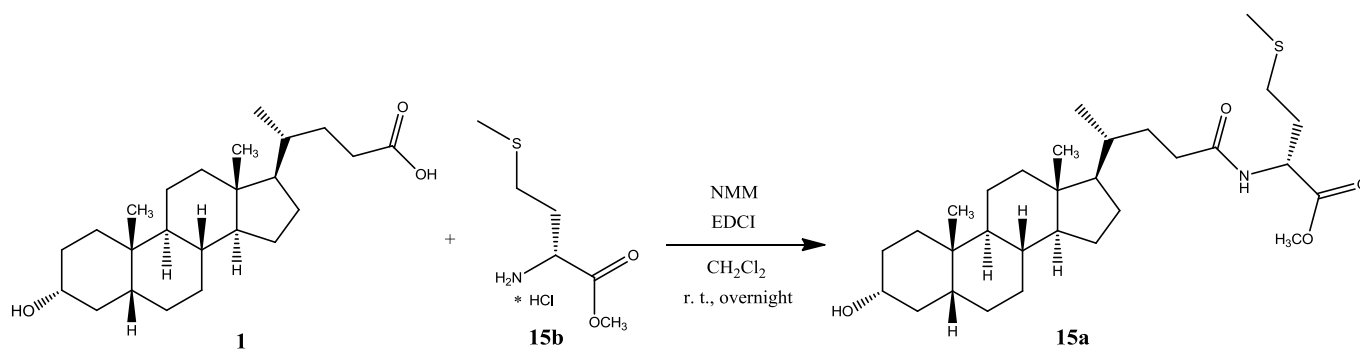
Compound **14** was synthesized following the procedure described for compound **2** using **14a**. The crude product was re-crystallized from (EtOH/H₂O) to give **14**. Yield: 100%. Mp: 178-182°C. ¹H-NMR (400 MHz, DMSO-d₆) δ = 0.59 (s, 3H, CH₃), 0.86-0.91 (m, 6H), 1.01-1.06 (m, 4H), 1.11-1.18 (m, 6H), 1.33-1.34 (m, 7H), 1.47-1.50 (m, 2H), 1.58-1.68 (m, 3H), 1.76-1.83 (m, 3H), 1.90-1.98 (m, 2H), 2.02-1.96 (m, 4H, -SCH₃+CH), 2.07-2.14 (m, 2H, CHCHH +CH), 2.39-2.46 (m, 1H, CHCHH), 4.23-4.29 (m, 1H, CHCH₂), 4.42 (bs, 1H, OH), 8.04 (d, *J* = 7.60 Hz, 1H, NH). ¹³C-NMR (100 MHz, DMSO-d₆) δ = 12.32, 15.02, 18.77, 20.88, 23.74, 24.32, 26.63, 27.36, 28.21, 30.23, 30.84, 31.14, 31.23, 31.92, 32.50, 34.67, 35.31, 35.61, 35.85, 36.76, 41.99, 42.73, 51.24, 56.02, 56.55, 70.32, 173.27, 173.96. MS (ESI) calc for C₂₉H₄₉NO₄S: 507.34; found: 506.5 [M-H]⁻. Anal. calc for C₂₉H₄₉NO₄S: C, 68.60; H, 9.73; N, 2.76; found: C, 68.41; H, 9.99; N, 2.74.

D-Methionine methyl ester hydrochloride (15b).



Compound **15b** was synthesized following a modification of a described procedure⁵⁰ in which acetyl chloride (5.03 mmol) was added dropwise to a methanol (15 ml) at 0°C . The mixture was stirred for 15 min and D-Methionine (1.67 mmol) was then added portionwise to the solution. The resulting mixture was heated to reflux overnight. The solvent was evaporated under reduced pressure afforded the D-Methionine methyl ester hydrochloride **15b** as a white solid that was immediately used in the next step without further purification. Yield 86%. $^1\text{H-NMR}$ (400 MHz, D_2O) $\delta = 2.02$ (s, 3H, SCH_3), 2.56-2.62 (m, 2H, CHCHH), 3.76 (s, 1H, OCH_3), 4.20-4.23 (m, 1H, CHCH_2). MS (ESI) calc for $\text{C}_5\text{H}_{11}\text{NO}_2\text{S}$: 149.21 found: 150.12 $[\text{M}+\text{H}]^+$.

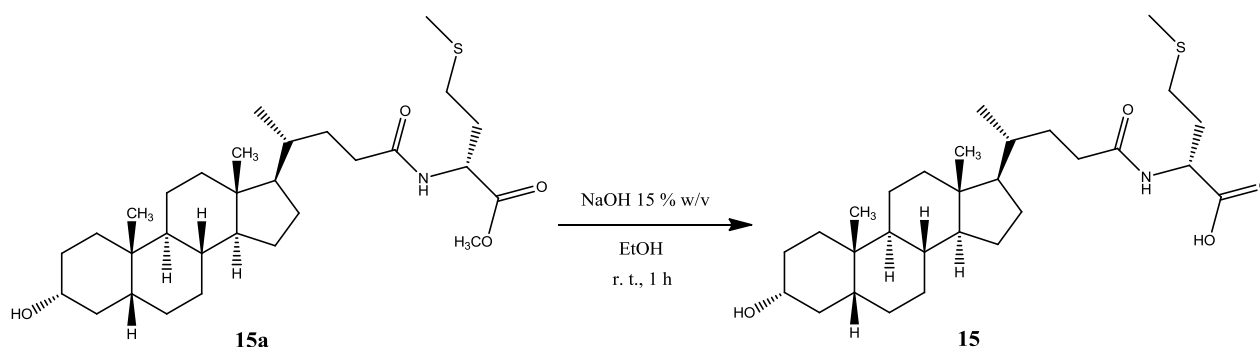
N-[(3 α ,5 β)-3-hydroxy-24-oxocholan-24-yl]- D-Methionine methyl ester (**15a**).



Compound **15a** was synthesized following the procedure described for **3** using D-Methionine methyl ester hydrochloride **15b** and purified using flash chromatography ($\text{CH}_2\text{Cl}_2/\text{EtOH}$: 98/2) and re-crystallized from ($\text{EtOH}/\text{H}_2\text{O}$). Yield: 65%. Mp: 143-146 $^{\circ}\text{C}$. $^1\text{H-NMR}$ (400 MHz, CDCl_3) $\delta = 0.64$ (s, 3H, CH_3), 0.91-1.01 (m, 4H), 1.21-1.45 (m, 10H), 1.49-1.59 (m, 3H), 1.65 (m, 2H), 1.71-1.90 (m, 5H), 1.92-2.02 (m, 2H), 2.09 (s, 3H, SCH_3), 2.11-2.21 (m, 2H), 2.25-2.33 (m, 1H), 2.46-2.54 (m, 2H, CHCHH), 3.57-3.66 (m, 1H), 3.76 (s, 3H, OCH_3), 4.72 (ddd, $J = 7.4, 5.5, 2.2$ Hz, 1H, CHCH_2), 6.13 (d, $J = 7.8$ Hz, 1H, NH). $^{13}\text{C-NMR}$ (100 MHz, CDCl_3) $\delta = 12.05, 15.49,$

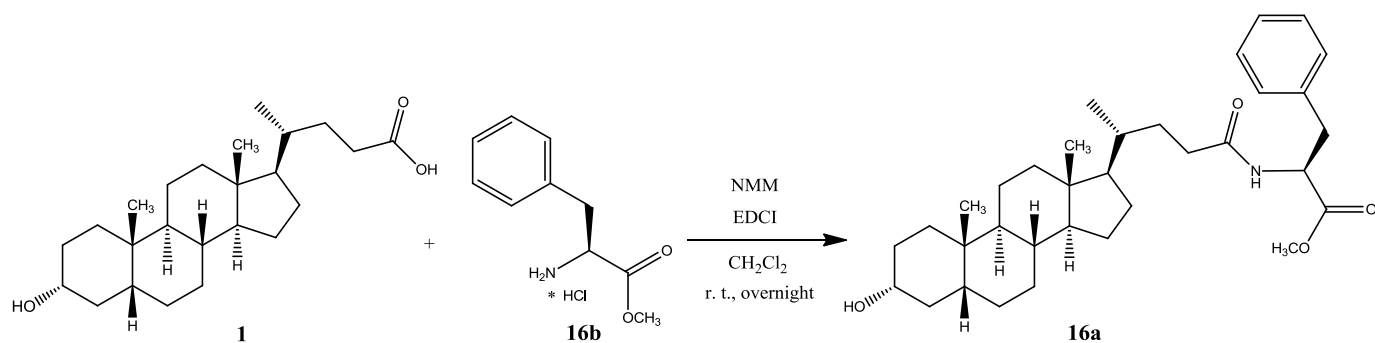
18.36, 20.81, 23.37, 24.20, 26.41, 27.19, 28.23, 29.99, 30.52, 31.57, 31.77, 33.43, 34.56, 35.35, 35.43, 35.83, 36.44, 40.18, 40.41, 42.09, 42.74, 51.40, 52.51, 56.00, 56.48, 71.79, 172.67, 173.40. MS (ESI) calc for $C_{30}H_{51}NO_4S$: 521.35; found: 520.3 $[M-H]^-$. Anal. calc for $C_{30}H_{51}NO_4S$: C, 69.05; H, 9.85; N, 2.68; found: C, 68.56; H, 9.99; N, 2.50.

***N*-[(3 α ,5 β)-3-hydroxy-24-oxocholan-24-yl]- D-Methionine (15).**



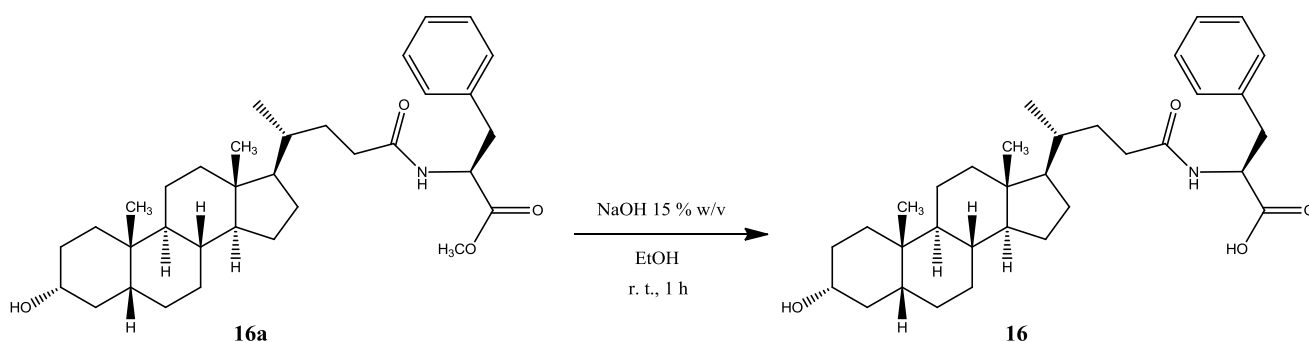
Compound **15** was synthesized following the procedure described for compound **2** starting from **15a**. The crude product was re-crystallized from (EtOH/H₂O) to give **15**. Yield: 96%. Mp: 169-172°C. ¹H-NMR (400 MHz, DMSO-d₆) δ = 0.59 (s, 3H, CH₃), 0.86-0.88 (m, 6H), 0.91-1.22 (m, 11H), 1.32-1.34 (m, 7H), 1.50-1.54 (m, 2H), 1.58-1.68 (m, 3H), 1.77-1.84 (m, 3H), 1.90-1.92 (m, 2H), 2.01 (s, 3H, SCH₃), 2.01-2.11 (m, 3H), 2.42-2.49 (m, 2H, CHCHH), 3.35 (m, 1H), 4.25-4.31 (m, 1H, CHCH₂), 4.42 (bs, 1H, OH), 8.05 (d, J = 7.6 Hz, 1H, NH). ¹³C-NMR (100 MHz, DMSO-d₆) δ = 12.33, 15.02, 18.70, 20.87, 23.74, 24.32, 26.64, 27.36, 28.20, 30.21, 30.84, 31.18, 31.90, 32.55, 34.67, 35.28, 35.61, 35.84, 36.76, 41.99, 42.73, 51.17, 56.11, 56.56, 70.32, 173.17, 173.97. MS (ESI) calc for $C_{29}H_{49}NO_4S$: 507.34; found: 506.4 $[M-H]^-$. Anal. calc for $C_{29}H_{49}NO_4S \cdot 0.2H_2O$: C, 68.11; H, 9.74; N, 2.74; found: C, 67.94; H, 9.72; N, 2.69.

***N*-[(3 α ,5 β)-3-hydroxy-24-oxocholan-24-yl]- L-Phenylalanine methyl ester (16a).**



Compound **16a** was synthesized following procedure described for compound **3** starting from L-phenylalanine methyl ester hydrochloride and purified by flash chromatography [SiO_2 , CH_2Cl_2 : $\text{C}_2\text{H}_5\text{OH}$ 98:2]. The crude product was re-crystallized from (EtOH/ H_2O) to give **16a**. Yield: 80%. Mp: 185-187°C. $^1\text{H-NMR}$ (400 MHz, CDCl_3) δ = 0.63 (s, 3H, CH_3), 0.88-0.97 (m, 7H), 1.00-1.15 (m, 5H), 1.21-1.30 (m, 5H), 1.38-1.40 (m, 7H), 1.63-1.67 (m, 2H), 1.71-1.88 (m, 5H), 1.93-1.96 (m, 1H), 2.03-2.11 (m, 1H), 2.19-2.26 (m, 1H), 3.09 (dd, J = 13.6, 5.6 Hz, 1H, CHCHH), 3.15 (dd, J = 13.6, 5.6 Hz, 1H, CHCHH), 3.62 (m, 1H), 3.73 (s, 3H, OCH_3), 4.89 (dt, J = 8.0, 5.6 Hz, 1H, CHCH_2), 5.87 (d, J = 7.6 Hz, 1H, NH), 7.09 (d, J = 6.4 Hz, 2H, Ar), 7.25-7.31 (m, 3H, Ar). $^{13}\text{C-NMR}$ (100 MHz, CDCl_3) δ = 12.06, 18.35, 20.82, 23.38, 24.21, 26.43, 27.20, 28.20, 30.53, 31.58, 33.37, 34.57, 35.36, 35.40, 35.85, 36.45, 37.89, 40.17, 40.43, 42.10, 42.73, 52.30, 52.92, 55.98, 56.48, 71.80, 127.10, 128.54, 129.27, 135.91, 172.22, 173.14. MS (ESI) calc for $\text{C}_{34}\text{H}_{51}\text{NO}_4$: 537.38; found: 536.4 $[\text{M-H}]^-$. Anal. calc for $\text{C}_{34}\text{H}_{51}\text{NO}_4$: C, 75.94; H, 9.56; N, 2.60; found: C, 75.85; H, 9.85; N, 2.52.

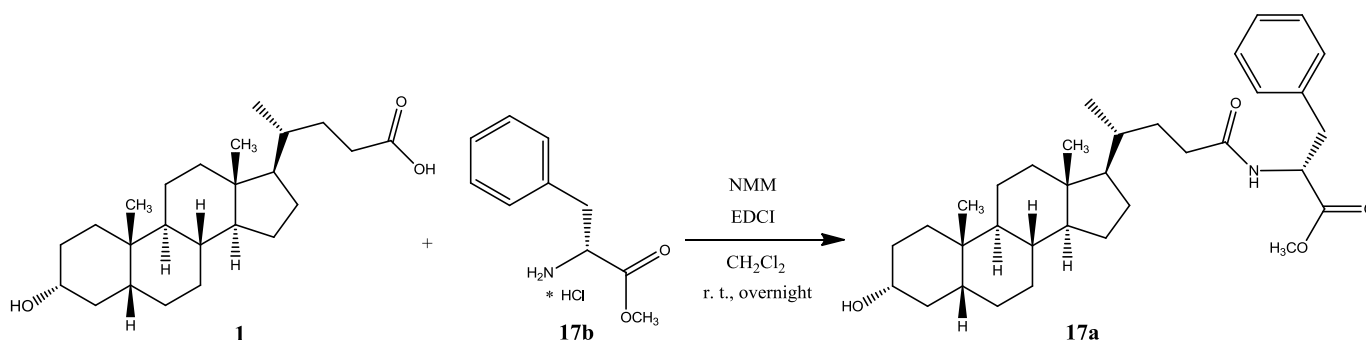
N-[(3 α ,5 β)-3-hydroxy-24-oxocholan-24-yl]- L-Phenylalanine (**16**).



Compound **16** was synthesized following the procedure described for compound **2** starting from compound **16a**. The crude product was re-crystallized from (EtOH/ H_2O)

to give **16**. Yield: 95%. Mp: 225-228°C. $^1\text{H-NMR}$ (400 MHz, DMSO- d_6) δ = 0.57 (s, 3H, CH_3), 0.81-0.92 (m, 7H), 1.00-1.17 (m, 10H), 1.32-1.41 (m, 7H), 1.50-1.77 (m, 7H), 1.88-1.98 (m, 2H), 2.01-2.07 (m, 1H), 2.82 (dd, J = 13.6, 10.0 Hz, 1H, CHCHH), 3.02 (dd, J = 13.6, 4.4 Hz, 1H, CHCHH), 4.37-4.43 (m, 1H, CHCH_2), 7.22 (m, 5H, Ar), 8.06 (d, J = 8.0 Hz, 1H, NH). $^{13}\text{C-NMR}$ (100 MHz, DMSO- d_6) δ = 12.33, 18.73, 20.87, 23.74, 24.31, 26.63, 27.36, 28.12, 30.85, 31.88, 32.49, 34.67, 35.29, 35.62, 35.84, 36.76, 37.20, 41.99, 42.70, 53.81, 56.01, 56.54, 70.32, 126.77, 128.54, 129.52, 138.27, 173.05, 173.68. MS (ESI) calc for $\text{C}_{33}\text{H}_{49}\text{NO}_4$: 523.37; found: 522.4 $[\text{M-H}]^-$. Anal. calc for $\text{C}_{33}\text{H}_{49}\text{NO}_4$: C, 75.68; H, 9.43; N, 2.67; found: C, 75.68; H, 9.64; N, 2.72.

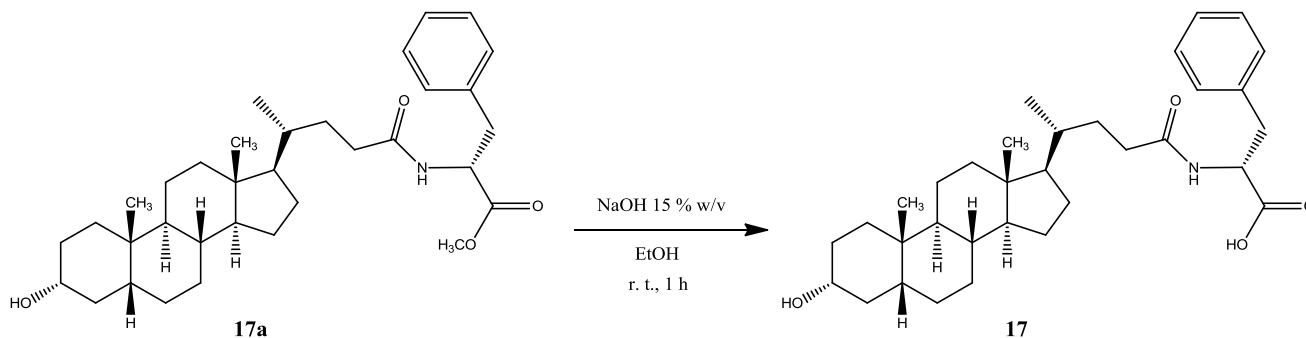
***N*-[(3 α ,5 β)-3-hydroxy-24-oxocholan-24-yl]- D-Phenylalanine methyl ester (**17a**).**



Compound **17a** was synthesized following the procedure described for compound **3** starting from D-phenylalanine methyl ester hydrochloride and purified by flash chromatography [SiO_2 , CH_2Cl_2 : $\text{C}_2\text{H}_5\text{OH}$ 98:2]. The crude product was re-crystallized from ethanol-water to give **17a** (EtOH/ H_2O . Yield: 40%. Mp: 228-231°C. $^1\text{H-NMR}$ (400 MHz, CDCl_3) δ = 0.65 (s, 3H, CH_3), 0.88-0.95 (m, 7H), 1.05-1.17 (m, 5H), 1.22-1.35 (m, 5H), 1.37-1.41 (m, 7H), 1.60-1.66 (m, 2H), 1.69-1.85 (m, 5H), 1.92-1.98 (m, 1H), 2.07-2.15 (m, 1H), 2.20-2.28 (m, 1H), 3.23(dd, J = 13.6, 5.6 Hz, 1H, CHCHH), 3.28 (dd, J = 13.6, 5.6 Hz, 1H, CHCHH), 3.61 (m, 1H), 3.73 (s, 3H, OCH_3), 4.78 (dt, J = 8.0, 5.6 Hz, 1H, CHCH_2), 5.82 (d, J = 7.6 Hz, 1H, NH), 7.10 (d, J = 6.4 Hz, 2H, Ar), 7.20-7.29 (m, 3H, Ar). $^{13}\text{C-NMR}$ (100 MHz, CDCl_3) δ = 12.10, 18.25, 20.80, 23.34, 24.27, 26.53, 27.10, 28.30, 30.58, 31.57, 33.33, 34.54, 35.37, 35.48, 35.85, 36.47, 37.93, 40.21, 40.48, 42.20, 42.83, 52.28, 52.88, 52.97, 55.88, 56.51, 71.84, 127.15, 128.55, 129.25, 135.96, 172.31, 173.17. MS (ESI) calc for $\text{C}_{34}\text{H}_{51}\text{NO}_4$: 537.38; found:

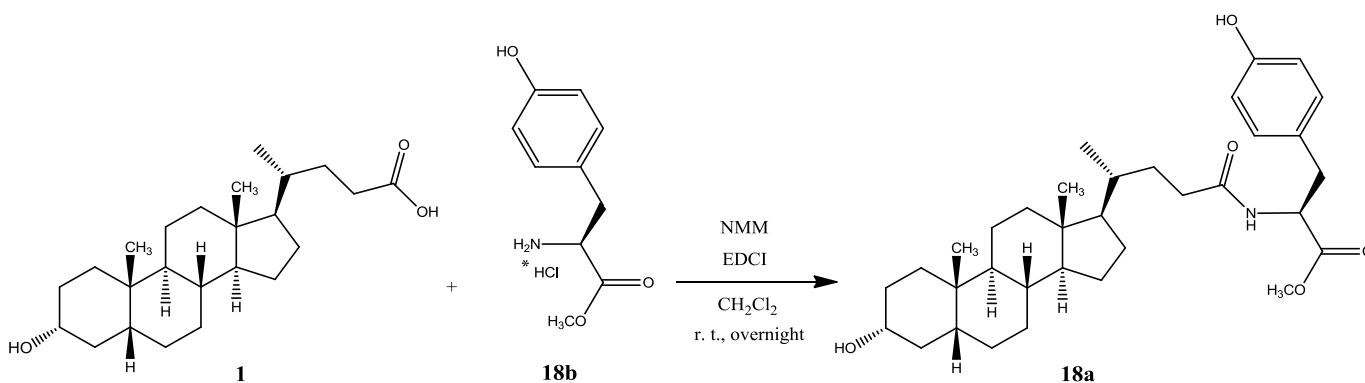
536.4 [M-H]⁻. Anal. calc for C₃₄H₅₁NO₄ • 3H₂O: C, 69.00; H, 9.71; N, 2.34; found: C, 69.20; H, 9.67; N, 2.63.

***N*-[(3 α ,5 β)-3-hydroxy-24-oxocholan-24-yl]- D-Phenylalanine (17).**



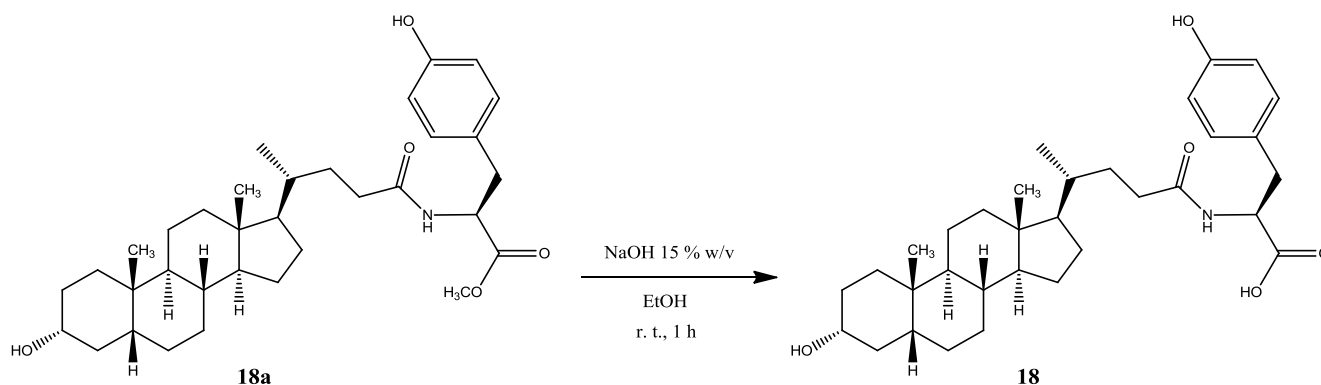
Compound **17** was synthesized following the procedure described for **2** using **17a**. The crude product was re-crystallized from (EtOH/H₂O) to give **17**. Yield: 93%. Mp: 155-158°C. ¹H-NMR (400 MHz, DMSO-d₆) δ = 0.56 (s, 3H, CH₃), 0.79-0.92 (m, 7H), 0.99-1.22 (m, 10H), 1.27-1.34 (m, 7H), 1.47-1.77 (m, 7H), 1.88-1.99 (m, 2H), 2.03-2.12 (m, 1H), 2.82 (dd, *J* = 13.6, 10.0 Hz, 1H, CHCHH), 3.03 (dd, *J* = 13.6, 4.4 Hz, 1H, CHCHH), 4.32-4.37 (m, 2H, CHCH₂+ OH), 7.17-7.26 (m, 5H, Ar), 8.06 (d, *J* = 8.0 Hz, 1H, NH). ¹³C-NMR (100 MHz, DMSO-d₆) δ = 12.34, 18.64, 20.87, 23.74, 24.30, 26.62, 27.36, 28.13, 30.85, 31.83, 32.54, 34.67, 35.24, 35.62, 35.85, 36.77, 37.22, 42.00, 42.71, 53.72, 56.17, 56.54, 70.33, 126.77, 128.53, 129.51, 138.24, 172.93, 173.66. MS (ESI) calc for C₃₃H₄₉NO₄: 523.37; found: 522.1 [M-H]⁻. Anal. calc for C₃₃H₄₉NO₄ • 0.5H₂O: C, 74.40; H, 9.46; N, 2.63; found: C, 74.43; H, 9.55; N, 2.59.

***N*-[(3 α ,5 β)-3-hydroxy-24-oxocholan-24-yl]- L-Tyrosine methyl ester (18a).**



Compound **18a** was synthesized following the procedure described for compound **3** starting from L-tyrosine methyl ester hydrochloride. and purified by flash chromatography [SiO_2 , CH_2Cl_2 : $\text{C}_2\text{H}_5\text{OH}$ from 98:2 to 95:5]. The crude product was re-crystallized from ethanol-water to give **18a** (EtOH/ H_2O . Yield: 87%. Mp: 203-206°C. $^1\text{H-NMR}$ (400 MHz, CD_3OD) δ = 0.66 (s, 3H, CH_3), 0.91-1.01 (m, 7H), 1.08-1.45 (m, 17H), 1.61-1.67 (m, 3H), 1.72-1.90 (m, 4H), 1.98-2.11 (m, 2H), 2.17-2.23 (m, 1H), 2.16-2.83 (dd, J = 14.0, 9.2 Hz, 1H, CHCHH), 3.04 (dd, J = 14.0, 5.6 Hz, 1H, CHCHH), 3.51-3.53 (m, 1H), 3.68 (s, 3H, OCH_3), 4.58 (dd, J = 9.2, 5.6 Hz, 1H, CHCH_2), 6.69 (d, J = 8.4 Hz, 2H, Ar), 7.01 (d, J = 8.8 Hz, 2H, Ar). $^{13}\text{C-NMR}$ (100 MHz, CD_3OD) δ = 11.12, 17.43, 20.55, 22.55, 23.87, 26.26, 26.97, 27.83, 29.79, 31.78, 32.35, 34.28, 35.09, 35.35, 35.77, 35.83, 36.22, 40.13, 40.48, 42.14, 42.49, 51.20, 54.01, 56.07, 56.50, 71.02, 114.81, 127.42, 129.76, 156.00, 172.41, 175.29. MS (ESI) calc for $\text{C}_{34}\text{H}_{51}\text{NO}_5$: 553.38; found: 552.3 $[\text{M-H}]^-$. Anal. calc for $\text{C}_{34}\text{H}_{51}\text{NO}_5$: C, 73.74; H, 9.28; N, 2.53; found: C, 73.08; H, 9.10; N, 2.46.

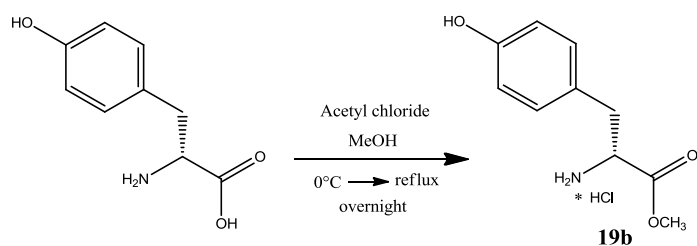
***N*-[(3 α ,5 β)-3-hydroxy-24-oxocholan-24-yl]- L-Tyrosine (**18**).**



Compound **18** was synthesized following the procedure described for **2** using **18a**. The crude product was re-crystallized from (EtOH/ H_2O) to give **18**. Yield: 93%. Mp: 219-223°C. $^1\text{H-NMR}$ (400 MHz, DMSO-d_6) δ = 0.58 (s, 3H, CH_3), 0.82-0.94 (m, 7H), 1.01-1.32 (m, 17H), 1.47-1.77 (m, 7H), 1.89-1.98 (m, 2H), 2.02-2.08 (m, 1H), 2.70 (dd, J = 13.6, 9.6 Hz, 1H, CHCHH), 2.89 (dd, J = 13.6, 4.0 Hz, 1H, CHCHH), 4.28-4.32 (m, 1H, CHCH_2), 4.43 (bs, 1H, CH_2OH), 6.61 (d, J = 8.0 Hz, 2H, Ar), 6.98 (d, J = 8.0 Hz, 2H, Ar), 8.0 (d, J = 8.0 Hz, 1H, NH), 9.20 (s, 1H, ArOH). $^{13}\text{C-NMR}$ (100 MHz, DMSO-d_6) δ = 12.33, 18.75, 20.88, 23.74, 24.32, 26.64, 27.36, 28.13, 30.84, 31.92,

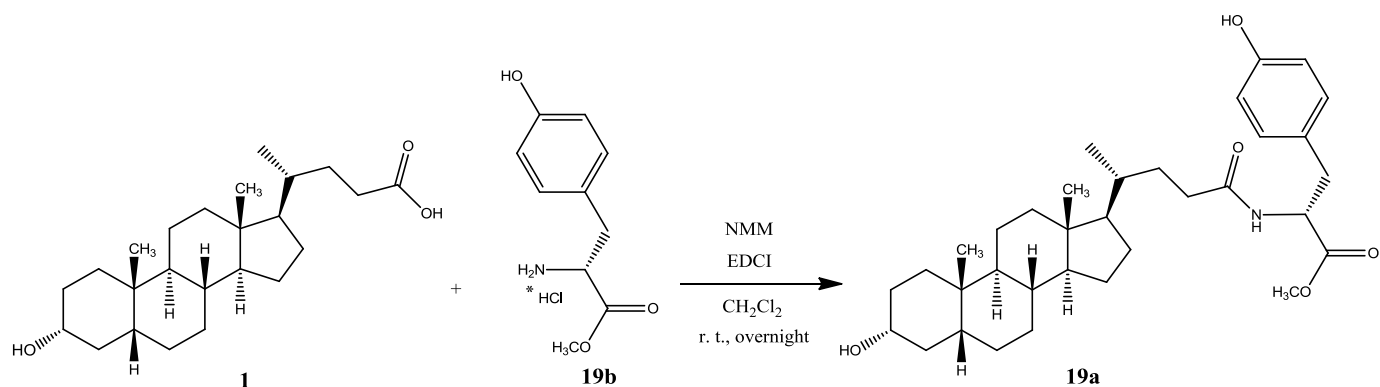
32.51, 34.67, 35.31, 35.62, 35.85, 36.45, 36.76, 41.99, 42.71, 54.17, 56.04, 56.55, 70.33, 115.35, 128.19, 130.41, 156.35, 173.05, 173.78. MS (ESI) calc for $C_{33}H_{49}NO_5$: 539.36; found: 538.4 $[M-H]^-$. Anal. calc for $C_{33}H_{49}NO_5 \cdot 1.25H_2O$: C, 70.49; H, 9.23; N, 2.49; found: C, 70.34; H, 9.10; N, 2.48.

D-Tyrosine methyl ester hydrochloride (**19b**).



Compound **19b** was synthesized following the procedure described in literature⁵¹ using D-Tyrosine.

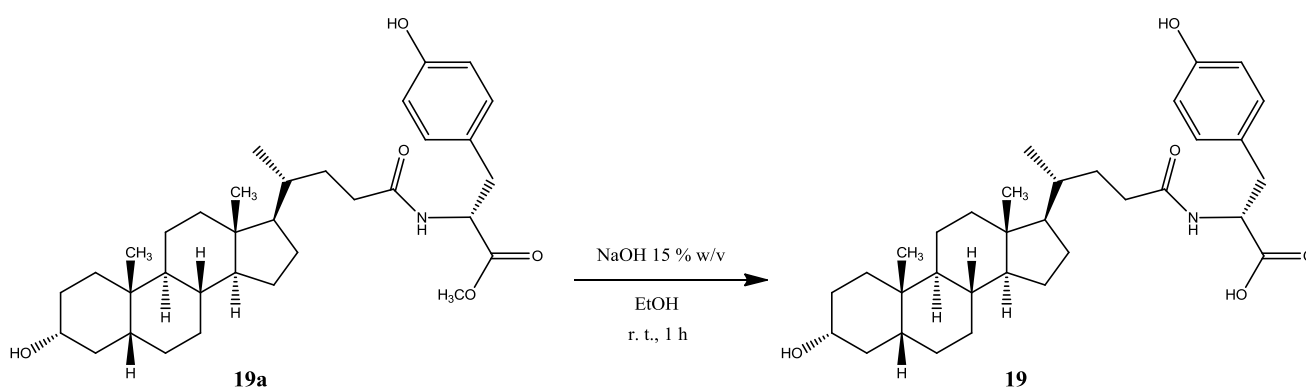
N-[(3 α ,5 β)-3-hydroxy-24-oxocholan-24-yl]- D-Tyrosine methyl ester (**19a**).



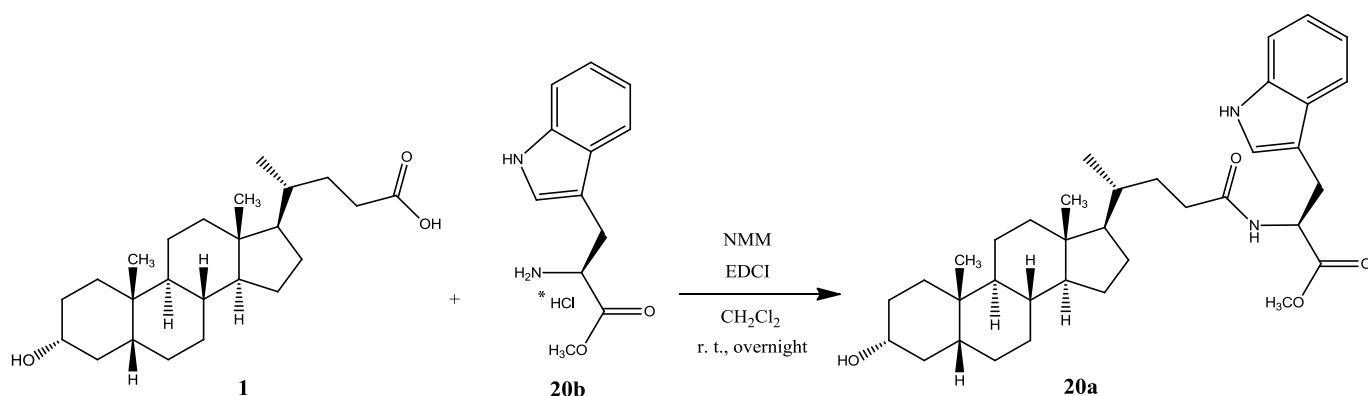
Compound **19b** was synthesized following the procedure described for compound **3** starting from D-tyrosine methyl ester hydrochloride **19b** and purified by flash chromatography [SiO_2 , CH_2Cl_2 : C_2H_5OH from 98:2]. The crude product was re-crystallized from ethanol-water to give **19a** (EtOH/ H_2O . Yield: 68%. Mp: 228-232°C. 1H -NMR (400 MHz, DMSO- d_6) δ = 0.57 (s, 3H, CH_3), 0.81-0.91 (m, 7H), 1.00-1.32 (m, 17H), 1.50-1.77 (m, 7H), 1.89-2.07 (m, 3H), 2.73 (dd, J = 13.6, 9.6 Hz, 1H, $CHCHH$), 2.83 (dd, J = 13.6, 5.2 Hz, 1H, $CHCHH$), 3.41-3.44 (m, 1H), 3.56 (s, 3H, OCH_3), 4.31-4.36 (m, 1H, $CHCH_2$), 4.43 (d, J = 4.0 Hz, 1H, CH_2OH), 6.62 (d, J = 8.4

Hz, 2H, Ar), 6.96 (d, $J = 8.0$ Hz, 2H, Ar), 8.16 (d, $J = 7.6$ Hz, 1H, NH), 9.19 (s, 1H, ArOH). ^{13}C -NMR (100 MHz, DMSO- d_6) $\delta = 12.31, 18.65, 19.02, 20.87, 23.74, 24.31, 26.63, 27.35, 28.15, 30.85, 31.79, 32.44, 34.67, 35.28, 35.61, 35.84, 36.45, 36.76, 41.99, 42.71, 52.16, 54.23, 56.12, 56.49, 56.54, 70.33, 115.41, 127.72, 130.38, 156.42, 172.83, 173.06$. MS (ESI) calc for $\text{C}_{34}\text{H}_{51}\text{NO}_5$: 553.38; found: 552.3 [M-H] $^-$. Anal. calc for $\text{C}_{34}\text{H}_{51}\text{NO}_5 \cdot 0.25\text{H}_2\text{O}$: C, 73.15; H, 9.29; N, 2.51; found: C, 73.12; H, 9.58; N, 2.44.

***N*-[(3 α ,5 β)-3-hydroxy-24-oxocholan-24-yl]-D-Tyrosine (19).**

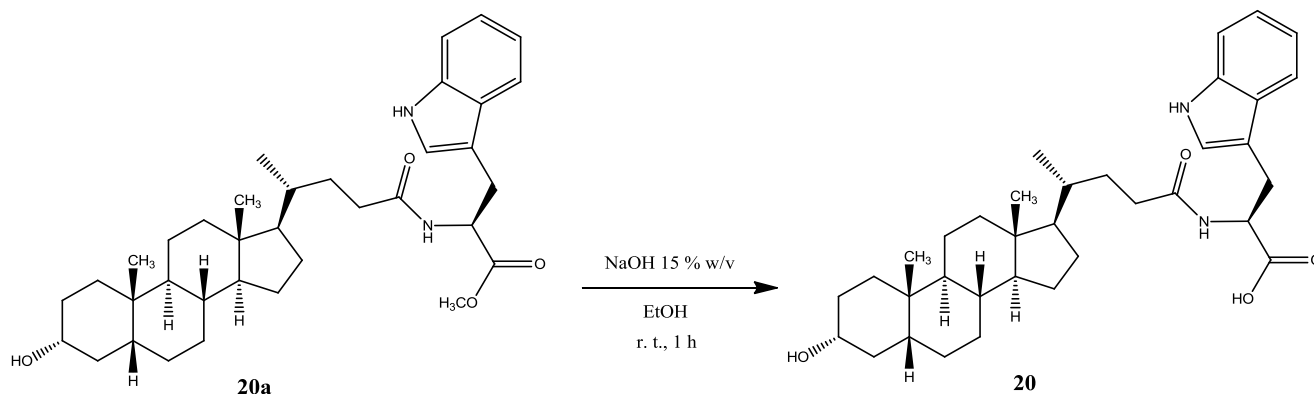


Compound **19** was synthesized following the procedure described for **2** using compound **19a**. The crude product was re-crystallized from (EtOH/ H_2O) to give **19**. Yield: 75%. Mp: 211-214 $^\circ\text{C}$. ^1H -NMR (400 MHz, DMSO- d_6) $\delta = 0.56$ (s, 3H, CH_3), 0.82 (d, $J = 6.40$ Hz, 3H), 0.86 (s, 3H, CH_3) 0.89-0.91 (m, 6H), 1.00-1.09 (m, 5H), 1.12-1.17 (m, 5H), 1.27-1.34 (m, 7H), 1.50-1.54 (m, 2H), 1.58-1.68 (m, 3H), 1.74-1.77 (m, 2H), 1.88-1.91 (m, 1H), 1.96-2.02 (m, 1H), 2.04-2.06 (m, 1H), 2.70 (dd, $J = 13.6, 9.6$ Hz, 1H, CHCHH), 2.89 (dd, $J = 13.6, 4.4$ Hz, 1H, CHCHH), 3.34-3.39 (m, 1H), 4.26-4.32 (m, 1H, CHCH $_2$), 6.61 (d, $J = 8.5$ Hz, 2H, Ar), 6.98 (d, $J = 8.5$ Hz, 2H, Ar), 7.98 (d, $J = 8.1$ Hz, 1H, NH). ^{13}C -NMR (100 MHz, DMSO- d_6) $\delta = 12.31, 18.66, 20.88, 23.75, 24.31, 26.63, 27.36, 28.14, 30.84, 31.87, 32.57, 34.67, 35.28, 35.62, 35.84, 36.48, 36.76, 41.99, 42.71, 54.12, 56.18, 56.55, 70.33, 115.32, 128.20, 130.41, 156.31, 172.91, 173.82$. MS (ESI) calc for $\text{C}_{33}\text{H}_{49}\text{NO}_5$: 539.36; found: 538.4 [M-H] $^-$. Anal. calc for $\text{C}_{33}\text{H}_{49}\text{NO}_5$: C, 73.43; H, 9.15; N, 2.59; found: C, 73.22; H, 8.81; N, 2.54.

***N*-[(3 α ,5 β)-3-hydroxy-24-oxocholan-24-yl]- L-Tryptophan methyl ester (20a).**

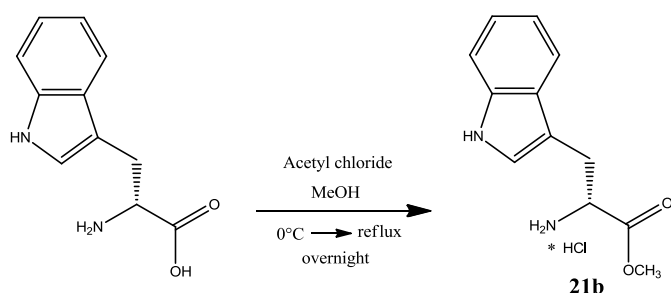
Compound **20a** was synthesized following the procedure described for compound **3** starting from L-tryptophan methyl ester hydrochloride. and purified by flash chromatography [SiO₂, CH₂Cl₂:C₂H₅OH from 99:1]. The crude product was recrystallized from ethanol-water to give **20a** (EtOH/H₂O. Yield: 67%. Mp: 156-159°C. ¹H-NMR (400 MHz, DMSO-d₆) δ = 0.58 (s, 3H, CH₃), 0.83-0.86 (m, 6H), 1.01-1.17 (m, 11H), 1.32 (bs, 7H), 1.50-1.77 (m, 7H), 1.89-1.91 (m, 1H), 2.00 (m, 1H), 2.08 (m, 1H), 3.00 (dd, J = 14.4, 8.4 Hz, 1H, CHCHH), 3.11 (dd, J = 14.0, 5.2 Hz, 1H, CHCHH), 3.32-3.36 (m, 1H), 3.55 (s, 3H, OCH₃), 4.43 (d, J = 4.4 Hz, 1H, CH₂OH), 4.47 (m, 1H, CHCH₂), 6.96 (t, J = 7.2 Hz, 1H, Ar), 7.05 (t, J = 7.2 Hz, 1H, Ar), 7.11 (s, 1H, Ar), 7.32 (d, J = 8.0 Hz, 1H, Ar), 7.47 (d, J = 7.6 Hz, 1H, Ar), 8.19 (d, J = 7.2 Hz, 1H, NH). ¹³C-NMR (100 MHz, DMSO-d₆) δ = 12.32, 18.74, 20.87, 23.74, 24.32, 26.64, 27.36, 27.53, 28.13, 30.85, 31.81, 32.43, 34.67, 35.32, 35.62, 35.85, 36.77, 41.99, 42.71, 52.18, 53.32, 56.03, 56.54, 70.33, 110.07, 111.87, 118.46, 118.83, 121.39, 124.04, 127.54, 136.56, 173.04, 173.17. MS (ESI) calc for C₃₆H₅₂NO₄: 576.39; found: 575.3 [M-H]⁻. Anal. calc for C₃₆H₅₂N₂O₄ • 0.5H₂O: C, 73.80; H, 9.12; N, 4.78; found: C, 73.73; H, 9.41; N, 4.80.

***N*-[(3 α ,5 β)-3-hydroxy-24-oxocholan-24-yl]- L-Tryptophan (20).**

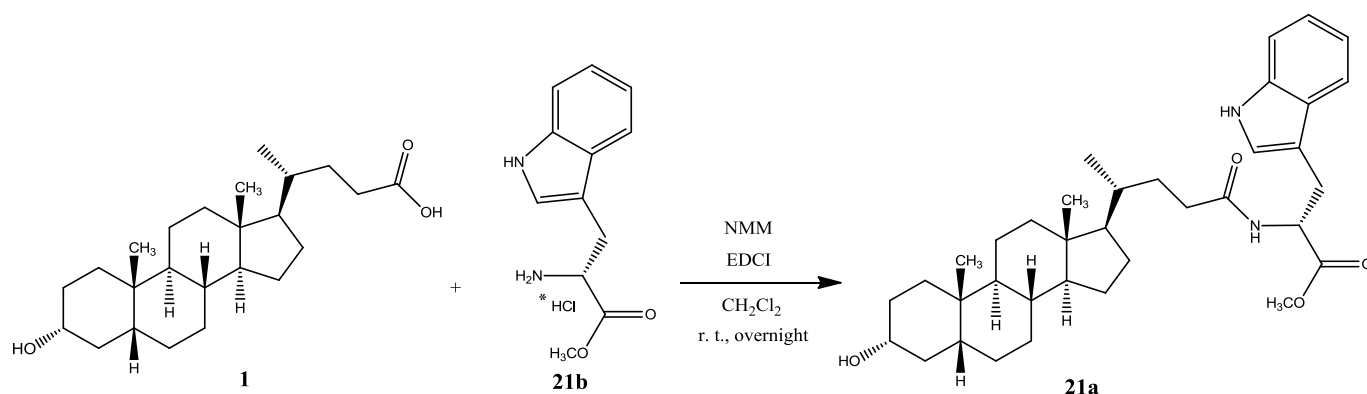


Compound **20** was synthesized following the procedure described for **2** using **20a**. The crude product was re-crystallized from (EtOH/H₂O) to give **20**. Yield: 95%. Mp: 194-197°C.⁵² ¹H-NMR (400 MHz, DMSO-d₆) δ = 0.57 (s, 3H, CH₃), 0.82-0.91 (m, 6H), 1.00-1.17 (m, 10H), 1.32 (m, 7H), 1.50-1.68 (m, 5H), 1.77 (m, 2H), 1.88-1.91 (m, 1H), 1.99 (m, 1H), 2.08 (m, 1H), 2.97 (dd, J = 14.6, 8.7 Hz, 1H, CHCHH), 3.14 (dd, J = 14.6, 4.9 Hz, 1H, CHCHH), 4.43 (m, 2H, CHCH₂ + CH₂OH), 6.95 (t, J = 7.2 Hz, 1H, Ar), 7.04 (t, J = 7.2 Hz, 1H, Ar), 7.11 (m, 1H, Ar), 7.31 (d, J = 8.08 Hz, 1H, Ar), 7.51 (d, J = 7.8 Hz, 1H, Ar), 8.04 (d, J = 7.8 Hz, 1H, NH). ¹³C-NMR (100 MHz, DMSO-d₆) δ = 12.32, 18.77, 20.87, 23.74, 24.32, 26.63, 27.36, 27.57, 28.13, 30.84, 31.84, 32.53, 34.67, 35.34, 35.62, 35.84, 36.76, 41.99, 42.70, 53.37, 56.04, 56.54, 70.33, 110.50, 111.81, 118.62, 118.74, 121.30, 123.94, 127.68, 136.53, 173.05, 174.04. MS (ESI) calc for C₃₅H₅₀N₂O₄: 562.38; found: 561.4 [M-H]⁻.

D-Tryptophan methyl ester hydrochloride (**21b**).

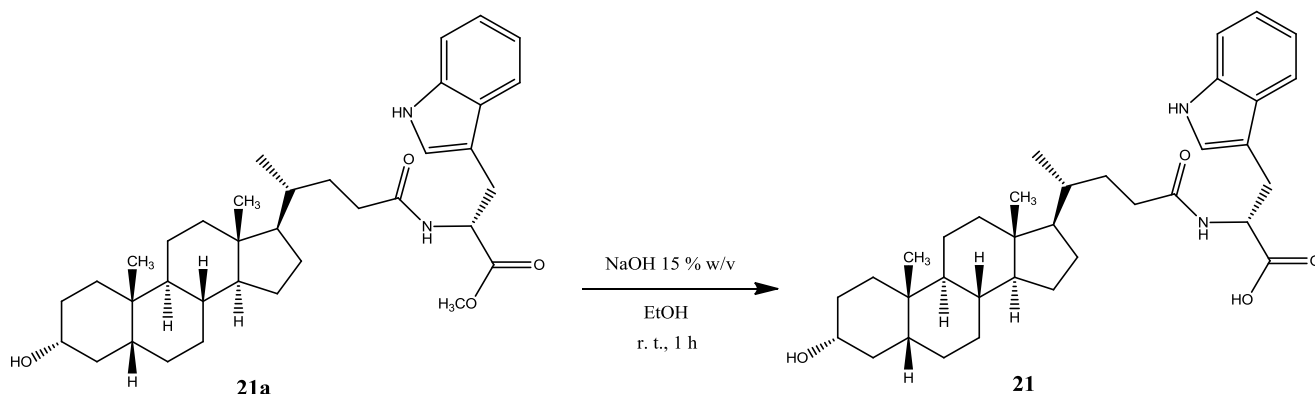


Compound **21b** was synthesized following a described procedure⁵³ using from D-Tryptophan.

***N*-[(3 α ,5 β)-3-hydroxy-24-oxocholan-24-yl]- D-Tryptophan methyl ester (21a).**

Compound **21a** was synthesized following the procedure described for compound **3** starting from D-tryptophan methyl ester hydrochloride **21b** and purified by flash chromatography [SiO₂, CH₂Cl₂:C₂H₅OH from 98:2]. The crude product was recrystallized from ethanol-water to give **21a** (EtOH/H₂O. Yield: 74%. Mp: 221-224°C. ¹H-NMR (400 MHz, DMSO-d₆) δ = 0.55 (s, 3H, CH₃), 0.83 (d, *J* = 6.44 Hz, 3H), 0.86 (s, 3H, CH₃), 1.01-1.14 (m, 11H), 1.32 (m, 7H), 1.50-1.77 (m, 7H), 1.88-1.90 (m, 1H), 2.00 (m, 1H), 2.10 (m, 1H), 3.00 (dd, *J* = 14.56, 8.52 Hz, 1H, CHCHH), 3.12 (dd, *J* = 14.52, 5.68 Hz, 1H, CHCHH), 3.55 (s, 3H, OCH₃), 4.43 (d, *J* = 4.56 Hz, 1H, CH₂OH), 4.48 (m, 1H, CHCH₂), 6.96 (t, *J* = 7.0 Hz, 1H, Ar), 7.0 (t, *J* = 6.9 Hz, 1H, Ar), 7.11 (d, *J* = 2.4, 1H, Ar), 7.31 (d, *J* = 8.0 Hz, 1H, Ar), 7.47 (d, *J* = 7.8 Hz, 1H, Ar), 8.19 (d, *J* = 7.6 Hz, 1H, NH). ¹³C-NMR (100 MHz, DMSO-d₆) δ = 12.28, 18.68, 20.87, 23.74, 24.31, 26.63, 27.36, 27.55, 28.14, 30.85, 31.75, 32.44, 34.67, 35.30, 35.62, 35.84, 36.76, 41.99, 42.70, 52.18, 53.49, 56.07, 56.53, 70.33, 110.04, 111.87, 118.43, 118.82, 121.38, 124.04, 127.53, 136.55, 173.04, 173.11. MS (ESI) calc for C₃₆H₅₂NO₄: 576.39; found: 575.3 [M-H]⁻. Anal. calc for C₃₆H₅₂N₂O₄: C, 74.96; H, 9.09; N, 4.86; found: C, 74.94; H, 9.48; N, 4.87.

***N*-[(3 α ,5 β)-3-hydroxy-24-oxocholan-24-yl]- D-Tryptophan (21).**



Compound **21** was synthesized following the procedure described for **2** using compound **21a**. The crude product was re-crystallized from (EtOH/H₂O) to give **21**. Yield: 98%. Mp: 175-178°C. ¹H-NMR (400 MHz, DMSO-d₆) δ = 0.54 (s, 3H, CH₃), 0.81-0.88 (m, 6H), 0.98-1.06 (m, 5H), 1.09-1.14 (m, 6H), 1.31-1.34 (m, 7H), 1.50-1.68 (m, 5H), 1.77-1.82 (m, 2H), 1.88-1.90 (m, 1H), 1.97-1.99 (m, 1H), 2.07-2.09 (m, 1H), 2.97 (dd, J = 14.56, 8.72 Hz, 1H, CHCHH), 3.13 (dd, J = 14.5, 4.8 Hz, 1H, CHCHH), 4.43-4.50 (m, 2H, CHCH₂ + CH₂OH), 6.95 (t, J = 7.0 Hz, 1H, Ar), 7.04 (t, J = 7.0 Hz, 1H, Ar), 7.10 (d, 1H, J = 2.5, Ar), 7.31 (d, J = 8.0 Hz, 1H, Ar), 7.51 (d, J = 7.8 Hz, 1H, Ar), 8.01 (d, J = 7.8 Hz, 1H, NH). ¹³C-NMR (100 MHz, DMSO-d₆) δ = 12.28, 18.69, 20.87, 23.74, 24.31, 26.63, 27.36, 27.59, 28.12, 30.85, 31.82, 32.55, 34.67, 35.29, 35.62, 35.84, 36.76, 41.99, 42.70, 53.32, 56.12, 56.53, 70.34, 110.47, 111.81, 118.60, 118.76, 121.30, 123.92, 127.66, 136.53, 172.99, 174.06. MS (ESI) calc for C₃₅H₅₀N₂O₄: 562.38; found: 561.5 [M-H]. Anal. calc for C₃₅H₅₀N₂O₄ • 0.5H₂O: C, 73.52; H, 8.99; N, 4.90; found: C, 73.81; H, 9.21; N, 4.63.

References

- ¹ E. B. Pasquale. Eph receptor signalling casts a wide net on cell behaviour. *Nat. Rev. Mol. Cell. Biol.* **2005**, 6, 462-475.
- ² J. Wykosky, W. Debinski. The EphA2 receptor and ephrinA1 ligand in solid tumors: functional and therapeutic targeting. *Mol. Cancer. Res.* **2008**, 6, 1795-1806.
- ³ K. Kullander, R. Klein. Mechanisms and functions of Eph and ephrin signalling. *Nat. Rev. Mol. Cell. Biol.* **2002**, 3, 475-486.
- ⁴ P.W. Janes, E. Nievergall, M. Lackmann. Concepts and consequences of Eph receptor clustering. *Seminars in Cell & Developmental Biology.* **2012**, 23, 43– 50.
- ⁵ N. W. Gale, G. D. Yancopoulos. Ephrins and their receptors: a repulsive topic?. *Cell. Tissue Res.* **1997**, 290, 227-241.
- ⁶ J. P. Himanen, D. B. Nikolov. Eph signaling: a structural view. *TRENDS in Neurosciences.* **2003**, 26(1), 46-51.
- ⁷ E. B. Pasquale. Eph-Ephrin bidirectional signaling in physiology and disease. *Cell.* **2008**, 133, 38-52.
- ⁸ A. Palmer, R. Klein. Multiple roles of ephrins in morphogenesis, neuronal networking, and brain function. *Genes & Development.* **2003**, 17, 1429-1450.
- ⁹ H. Miao, B. Wang. Eph/ephrin signaling in epithelial development and homeostasis. *Int. J. Biochem. Cell. Biol.* **2009**, 41, 762-770.
- ¹⁰ R. Klein. Bidirectional modulation of synaptic functions by Eph/ephrin signaling. *Nat. Neurosci.* **2009**, 12, 15-20.
- ¹¹ R. H. Adams, R. Klein. Eph receptors and ephrin ligands: essential mediator of vascular development. *Trends Cardiovasc Med.* **2000**, 10(5), 183-188.
- ¹² B. Mosch, B. Reissenweber, C. Neuber, J. Pietzsch. Eph receptors and ephrin ligands: important players in angiogenesis and tumor angiogenesis. *J. Oncol.* **2010**, 2010, 135285.
- ¹³ H. Surawska, P. C. Ma, R. Salgia. The role of ephrins and Eph receptors in cancer. *Cytokine & Growth Factor Reviews.* **2004**, 15, 419-433.

-
- ¹⁴ D. P. Zelinski, N. D. Zantek, J. C. Stewart, A. R. Irizarry, M. S. Kinch. EphA2 overexpression causes tumorigenesis of mammary epithelial cells. *Cancer Research*. **2001**, 61, 2301-23016.
- ¹⁵ M. S. Kinch, M. B. Moore, D. H. Harpole Jr. Predictive value of the EphA2 receptor tyrosine kinase in lung cancer recurrence and survival. *Clinical Cancer Research*. **2003**, 9, 613-618.
- ¹⁶ C. J. Herrem, T. Tatsumi, K. S. Olson, K. Shirai, J. H. Finke, R. M. Bukowski, M. Zhou, A. L. Richmond, I. Derweesh, M. S. Kinch, W. J. Storkus. Expression of EphA2 is prognostic of disease-free interval and overall survival in surgically treated patients with renal cell carcinoma. *Clinical Cancer Research*. **2005**, 11, 226-231.
- ¹⁷ T. Miyazaki, H. Kato, M. Fukuchi, M. Nakajima, H. Kuwano. EphA2 overexpression correlates with poor prognosis in esophageal squamous cell carcinoma. *Int. J. Cancer*. **2003**, 103, 657–663.
- ¹⁸ Z. Nikolova, V. Djonov, G. Zuercher, A.-C. Andres, A. Ziemiecki. Cell-type specific and estrogen dependent expression of the receptor tyrosine kinase EphB4 and its ligand ephrin-B2 during mammary gland morphogenesis. *Journal of Cell Science*. **1998**, 111(18), 2741–2751.
- ¹⁹ K. Ogawa, R. Pasqualini, R. A. Lindberg, R. Kain, A. L. Freeman, E. B. Pasquale. The ephrin-A1 ligand and its receptor, EphA2, are expressed during tumor neovascularization. *Oncogene*. **2000**, 19(52), 6043–6052.
- ²⁰ E. B. Pasquale. *Nat. Rev. Cancer*. Eph receptors and ephrins in cancer: bidirectional signaling and beyond. **2010**, 10, 165-180.
- ²¹ G. Martiny-Baron, P. Holzer, E. Billy, C. Schnell, J. Brueggen, M. Ferretti, N. Schmiedeberg, J. M. Wood, P. Furet, P. Imbach. The small molecule specific EphB4 kinase inhibitor NVP-BHG712 inhibits VEGF driven angiogenesis. *Angiogenesis*. **2010**, 13(3), 259-267.
- ²² M. Tandon, S. V. Vemula, S. K. Mittal. Emerging strategies for EphA2 receptor targeting for cancer therapeutics. *Expert Opin Ther Targets*. **2011**, 15(1), 31-51.
- ²³ R. Noberini, I. Lamberto, E. B. Pasquale. Targeting Eph receptors with peptides and small molecules: progress and challenges. *Semin Cell Dev Biol*. **2012**, 23(1), 51-57.

-
- ²⁴ J. Jehle, I. Staudacher, F. Wiedmann, P. A. Schweizer, R. Becker, H. A. Katus, D. Thomas. Regulation of HL-1 cardiomyocyte apoptosis by EphA2 receptor tyrosine kinase phosphorylation and protection by lithocholic acid. *Br J Pharmacol.* **2012**, 167(7), 1563-1572.
- ²⁵ C. Giorgio, I. Hassan Mohamed, L. Flammini, E. Barocelli, M. Incerti, A. Lodola, M. Tognolini. Lithocholic acid is an Eph-ephrin ligand interfering with Eph-kinase activation. *PLoS One.* **2011**, 6(3), e18128.
- ²⁶ M. Tognolini, M. Incerti, I. Hassan-Mohamed, C. Giorgio, S. Russo, R. Bruni, B. Lelli, L. Bracci, R. Noberini, E. B. Pasquale, E. Barocelli, P. Vicini, M. Mor, A. Lodola. Structure-activity relationships and mechanism of action of Eph-ephrin antagonists: interaction of cholanic acid with the EphA2 receptor. *Chem Med Chem.* **2012**, 7(6), 1071-1083.
- ²⁷ R. Noberini, S. K. De, Z. Zhang, B. Wu, D. Raveendra-Panickar, V. Chen, J. Vazquez, H. Qin, J. Song, N. D. Cosford, M. Pellecchia, E. B. Pasquale. A disalicylic acid-furanyl derivative inhibits ephrin binding to a subset of Eph receptors. *Chem Biol Drug Des.* **2011**, 78(4), 667-678.
- ²⁸ R. Noberini, M. Koolpe, S. Peddibhotla, R. Dahl, Y. Su, N. D. Cosford, G. P. Roth, E. B. Pasquale. Small molecules can selectively inhibit ephrin binding to the EphA4 and EphA2 receptors. *J Biol Chem.* **2008**, 283(43), 29461-29472.
- ²⁹ A. Petty, E. Myshkin, H. Qin, H. Guo, H. Miao, G. P. Tochtrop, J. T. Hsieh, P. Page, L. Liu, D. J. Lindner, C. Acharya, A. D. Mackerell, Jr., E. Ficker, J. Song, B. Wang. Small molecule agonist of EphA2 receptor tyrosine kinase inhibits tumor cell migration in vitro and prostate cancer metastasis in vivo. *PLoS One.* **2012**, 7(8), e42120.
- ³⁰ M. Tognolini, C. Giorgio, I. Hassan Mohamed, E. Barocelli, L. Calani, E. Reynaud, O. Dangles, G. Borges, A. Crozier, F. Brighenti, D. Del Rio. Perturbation of the EphA2-EphrinA1 System in Human Prostate Cancer Cells by Colonic (Poly)phenol Catabolites. *J Agric Food Chem.* **2012**, 60(36), 8877-8884.
- ³¹ R. Noberini, M. Koolpe, I. Lamberto, E. B. Pasquale. Inhibition of Eph receptor-ephrin ligand interaction by tea polyphenols. *Pharmacol Res.* **2012**, 66(4), 363-373.
- ³² I. H. Mohamed, C. Giorgio, R. Bruni, L. Flammini, E. Barocelli, D. Rossi, G. Domenichini, F. Poli, M. Tognolini. Polyphenol rich botanicals used as food supplements interfere with EphA2-ephrinA1 system. *Pharmacol Res.* **2011**, 64(5), 464-470.

-
- ³³ J. P. Himanen, Y. Goldgur, H. Miao, E. Myshkin, H. Guo, M. Buck, M. Nguyen, K. R. Rajashankar, B. Wang, D. B. Nikolov. Ligand recognition by A-class Eph receptors: crystal structures of the EphA2 ligand-binding domain and the EphA2/ephrin-A1 complex. *EMBO Rep.* **2009**, *10*, 722-728.
- ³⁴ A. M. Giannetti, B. D. Koch, M. F. Browner. Surface plasmon resonance based assay for the detection and characterization of promiscuous inhibitors. *J Med Chem.* **2008**, *51*(3), 574-580.
- ³⁵ A. Pini, A. Giuliani, C. Falciani, M. Fabbrini, S. Pileri, B. Lelli, L. Bracci. Characterization of the branched antimicrobial peptide M6 by analyzing its mechanism of action and in vivo toxicity. *J Pept Sci.* **2007**, *13*(6), 393-399.
- ³⁶ M. o. e. (MOE), *Molecular operating environment (MOE)*, CCG Inc, 1255 University St, Montreal, Quebec, Canada, **2008**.
- ³⁷ C. M. Lema Tome, E. Palma, S. Ferluga, W. T. Lowther, R. Hantgan, J. Wykosky, W. Debinski. Structural and functional characterization of monomeric EphrinA1 binding site to EphA2 receptor. *J Biol Chem.* **2012**, *287*(17), 14012-14022.
- ³⁸ M. Koolpe, M. Dail, E. B. Pasquale. An ephrin mimetic peptide that selectively targets the EphA2 receptor. *J Biol Chem.* **2002**, *277*(49), 46974-46979.
- ³⁹ J. B. Baell, G. A. Holloway. New substructure filters for removal of pan assay interference compounds (PAINS) from screening libraries and for their exclusion in bioassays. *J Med Chem.* **2010**, *53*(7), 2719-2740.
- ⁴⁰ F. M. Pfeffer, R. A. Russel. Strategies and methods for the attachment of amino acids and peptides to chiral [n]polynorbornane templates. *Org. Biomol. Chem.* **2003**, *1*, 1845-1851.
- ⁴¹ K. H. Chang, L. Lee, J. Chen, W. S. Li. Lithocholic acid analogues, new and potent alpha-2,3-sialyltransferase inhibitors. *Chem. Commun.* **2006**, *6*, 629-631.
- ⁴² A. N. Hulme, K. S. Curley. Approaches to the synthesis of (2R,3S)-2-hydroxymethylpyrrolidin-3-ol (CYB-3) and its C(3) epimer: a cautionary tale. *J. R. Soc. Chem. Perkin Trans.* **2002**, *1*, 1083-1091.
- ⁴³ F. Borcard, M. Baud, C. Bello, P. Vogel, G. Dal Bello, G. Grossi., P. Pronzato, M. Cea., A. Nencioni. Synthesis of new oxathiazinane dioxides and their in vitro cancer cell growth inhibitory activity. *Bioorg & Med Chem Letters.* **2010**, *20*, 5353-5356.

-
- ⁴⁴ R. Bernardini, A. Bernareggi, P. G. Cassara, G. D'Arasmo, E. Menta, A. Oliva. Preparation of peptide boronic acids as proteasome inhibitors. (Cephalon, Inc., Frazer, PA), US2006189806; **2006**.
- ⁴⁵ J. Wu, C. Li, M. Zhao, W. Wang, Y. Wang, S. A class of novel carboline intercalators: Their synthesis, in vitro anti-proliferation, in vivo anti-tumor action, and 3D QSAR analysis. Peng, *Bioorg. Med. Chem.* **2010**, 18, 6220-6229.
- ⁴⁶ C. Liang, S. Gao, Z. Li. Preparation of indolydenemethylpyrrolicarboxamides as inhibitors of VEGFR, PDEGFR, KIT, Flt-1, Flt-3, Flt-4, and RET kinase with reduced inhibition of AMPK. (XCOVERY, INC.), WO2008/33562; **2008**.
- ⁴⁷ A. Puschl, S. Sforza, G. Haaima, O. Dahl, P. E. Nielsen. Peptide nucleic acids (PNAs) with a functional backbone. *Tetrahedron Letters.* **1998**, 39, 4707-4710.
- ⁴⁸ W. J. Moran, K. M. Goodenough, P. Raubo, J. P. A. Harrity. A concise asymmetric route to Nuphar alkaloids: a formal synthesis of (-)-deoxynupharidine. *Org. Lett.* **2003**, 5, 3427-3430.
- ⁴⁹ V. Noponen, Nonappa, M. Lahtinen, A. Valkonen, H. Salo, E. Kolehmainen, E. Sievanen. Bile acid-amino acid ester conjugates: gelation, structural properties, and thermoreversible solid to solid phase transition. *Soft Matter.* **2010**, 6, 3789-3796.
- ⁵⁰ R. K. Jain, M. F. Gordeev, J. G. Lewis, C. Preparation of pyrrolidinecarboxamide derivatives as antibacterial agents. Francavilla, (Vicuron Pharmaceuticals, Inc.), US2010/22605; **2010**.
- ⁵¹ A. N. Hulme, E. M. Rosser. An indol-based approach to the synthesis of the antibiotic anisomycin. *Org. Lett.* **2002**, 4, 265-268.
- ⁵² A. R. Jacobson, D. G. Gabler, J. Oleksyszyn. Bile acid inhibitors of metalloproteinase enzymes. (OsteoArthritis Sciences, Inc., Cambridge, Mass), US005646316A; **1997**.
- ⁵³ A. H Abadi., B. D. Gary, H. N. Tinsley, G. A Piazza, M. Abdel-Halim. Synthesis, molecular modelling and biological evaluation of novel tadalafil analogues as phosphodiesterase 5 and colon tumor cell growth inhibitors, new stereochemical perspective. *Eur. J. Med. Chem.* **2010**, 45, 1278-1286.